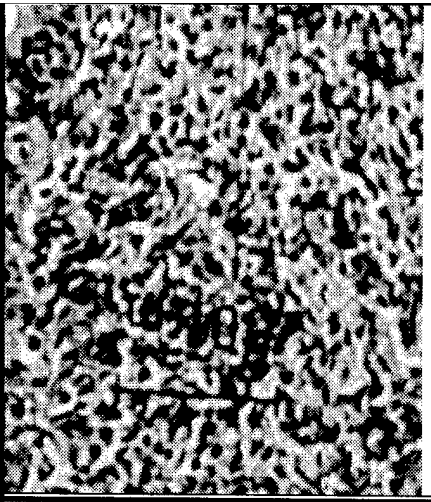

AFRRI Reports

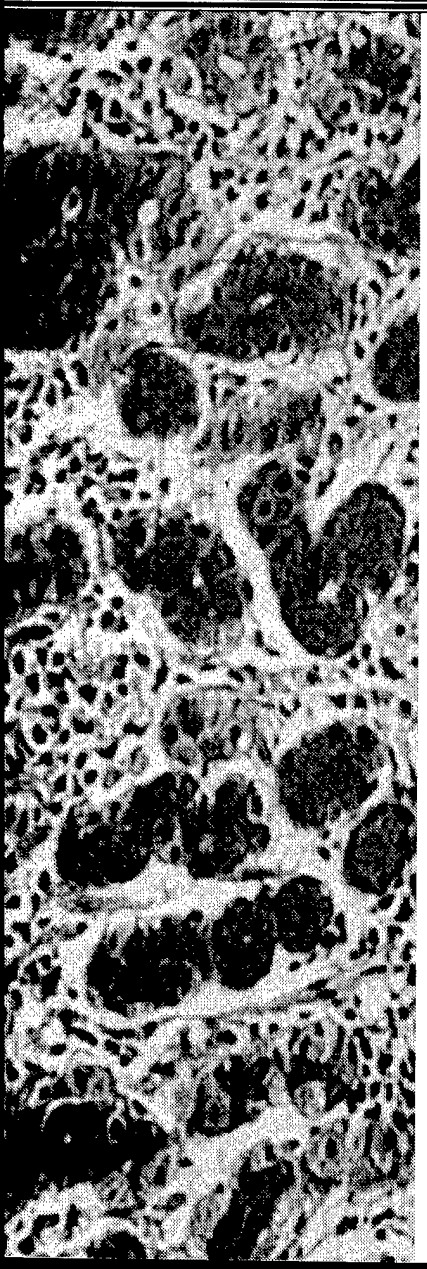

Third - Fourth Quarters

1996

Armed Forces Radiobiology Research Institute
8901 Wisconsin Avenue
Bethesda, Maryland 20889-5603

CONTENTS

This and other AFRRI publications are available to qualified users from the Defense Technical Information Center, Attention: OCP, 8725 John J. Kingman Road, Suite 0944, Fort Belvoir, VA 22060-6218; telephone (703) 767-8274. Others may contact the National Technical Information Service, 5285 Port Royal Road, Springfield, VA 22161; telephone (703) 487-4650. AFRRI publications are also available from university libraries and other libraries associated with the U.S. Government's Depository Library System.

Neurochemical Research, Vol. 21, No. 6, 1996, pp. 695–700

Effect of Chloral Hydrate on in Vivo KCl-Induced Striatal Dopamine Release in the Rat

Han-Tong Chen[1,2] and Sathasiva B. Kandasamy[1]

(Accepted March 13, 1996)

The release of striatal dopamine (DA) and its metabolites in response to locally-induced K^+ depolarization was investigated in vivo in chloral hydrate-anesthetized and freely moving rats. KCl at concentrations of 30, 50, and 100 mM induced significant dose-dependent increases in extracellular DA overflow in both chloral hydrate-anesthetized and freely moving rats ($P < 0.05$). Extracellular levels of dihydroxyphenylacetic acid (DOPAC), homovanillic acid (HVA), and 5-hydroxyindoleacetic acid (5-HIAA) were decreased. The DA overflow in response to 30 mM KCl stimulation in anesthetized rats was significantly greater than that in freely moving rats ($P < 0.05$). In addition, chloral hydrate anesthesia resulted in a significant decrease in extracellular levels of DOPAC and significant increases in extracellular levels of HVA and 5-HIAA in comparison with freely moving rats ($P < 0.05$). Furthermore, the basal level of extracellular HVA in chloral hydrate-anesthetized rats was significantly higher than that in freely moving rats. These results suggest that chloral hydrate anesthesia could have significant effects on the pharmacological response of the striatal dopaminergic neurons.

KEY WORDS: Microdialysis; anesthesia; dopamine; chloral hydrate; striatum.

INTRODUCTION

Studies using in vivo microdialysis to measure the extracellular concentrations of various endogenous neurotransmitters have been conducted in both free-moving and anesthetized rats. The possible effect of general anesthetics alone on the pharmacological response of the central nervous system is an important concern. Most investigations have been electrophysiological studies (1–5), and the results were inconsistent.

Administration of general anesthetics such as chloral hydrate, pentobarbital, or halothane resulted in an increase in the basal firing rate of substantia nigra dopaminergic neurons (2,3), and no significant difference in dopaminergic cell responses to L-dopa, d-amphetamine, and apomorphine was found between chloral hydrate-anesthetized and gallamine-paralyzed rats (1). In gallamine-paralyzed rats (4) and in freely moving rats (6), general anesthesia has been shown, on the contrary, to reduce the number of spontaneously active dopaminergic neurons that exhibit burst-firing. General anesthesia was also shown to enhance the potency of dopamine (DA) agonists to inhibit the dopaminergic cell firing rate, whereas local anesthesia and paralysis by gallamine did not (4).

Increases in the extracellular concentration of DA and its metabolites in the rat striatum have been reported recently following halothane anesthesia (7) and isoflurane anesthesia (8). In addition, Opacka-Juffry et al. (8) found that isoflurane anesthesia enhanced nomifensine-induced increases in striatal DA concentration. In contrast, however, chloral hydrate anesthesia was shown

[1] Department of Radiation, Pathophysiology, and Toxicology, Armed Forces Radiobiology Research Institute, Bethesda, Maryland 20889-5603.

[2] To whom to address reprint requests. Mailing address: Dept. of RPT, AFRRI 8901 Wisconsin Avenue Bethesda, Maryland 20889-5603 Tel: (301)295-9224; Fax: (301)295-0313.

0364-3190/96/0600-0695$09.50/0

Table I. Basal Levels of DA and Metabolites (Pmol/Sample) in the Striata of Freely Moving and Chloral Hydrate-Anesthetized Rats

Rats	N	DA	DOPAC	HVA	5-HIAA
Freely moving	7	0.048 ± 0.008[a]	8.9 ± 2.1	13.6 ± 1.0	3.8 ± 0.4
Anesthetized	9	0.060 ± 0.016	4.6 ± 0.9	22.3 ± 0.5*	4.3 ± 0.3

[a]Mean ± SEM.
*$P < 0.05$ vs freely moving rats.
The mean neurotransmitter concentrations of the initial three baseline samples were taken as basal levels.

recently to decrease the basal level of striatal DA overflow (9). The present study examined the basal as well as KCl-stimulated striatal DA overflow and the extracellular concentration of its metabolites in both freely moving and chloral hydrate-anesthetized rats.

EXPERIMENTAL PROCEDURE

Animal. Male Sprague-Dawley Crl:CD(SD)BRD rats (Charles River Breeding Laboratories, Kingston, NY) weighing 330-490 g were randomly selected for these experiments. Rats were quarantined on arrival and were screened for evidence of disease by serology and histopathology. Rats were housed in an AAALAC-accredited animal facility with a 12-h light:dark cycle and were allowed access to commercial rodent chow (Wayne Rodent Blok, Continental Grain Co., Chicago, IL) and water ad libitum.

Implantation and Perfusion. In rats under chloral hydrate anesthesia (400 mg/kg, i.p.), the CMA 12 microdialysis probe (Carnegie Medicin, Stockholm) with a 2-mm tip was stereotaxically inserted through a small burr hole in the skull into the right striatum (A:+ 9.7, L:+2.8, and V:+3.5 mm relative to interaural zero) according to the atlas of Paxinos and Watson (10). The probe was inserted with a David Kopf stereotaxic instrument with the incisor bar at −3.5 mm. The body temperature of anesthetized rats was maintained by means of a rectal probe coupled to a heating pad (CMA 150; Carnegie Medicin). Small supplements of chloral hydrate maintained the depth of anesthesia at a level where corneal reflexes were abolished. In free-moving rats, the CMA 12 microdialysis probe was inserted in the striatum on the day of experiments through a CMA 12 guide cannula (Carnegie Medicin, Stockholm) that was surgically implanted under chloral hydrate anesthesia at least 3 days prior to experimentation. The guide cannula terminated approximately 2 mm dorsal to the projected tip of the dialysis probe in the striatum. The microdialysis probe was carefully inserted into the guide cannula and secured in place in the handheld conscious rat. The inlet tubing of the probe was inserted through a stainless steel coil and attached to a liquid swivel (Instech Lab., Plymouth Meeting, PA) to allow maximum freedom of movement. The rat was placed in a rectangular activity chamber and was permitted to move freely during the experiment. Artificial cerebrospinal fluid (aCSF) containing 147.3 mM NaCl, 2.3 mM $CaCl_2$, and 4.0 mM KCl was perfused through the microdialysis probe at a flow rate of 2 µl/min. Sample collection was started 1 h after probe insertion (time 0) when the basal level of extracellular DA was stabilized, and was collected every 12.5 min in vials containing 2.5 µl of 0.05 M perchloric acid. KCl (20 µl) at the concentrations of 30, 50, and 100 mM was perfused for 10 min at 37.5, 112.5, and 187.5 min, respectively, to stimulate DA release. Administration of KCl was facilitated by a CMA 110 liquid switch. Increase in KCl concentration in the dialysate buffer is accompanied by a corresponding reduction in NaCl concentration to maintain osmolarity. The location of probes was confirmed by visual examination of frozen brain sections at the end of each experiment.

Neurotransmitter Analysis. Microdialysis samples were injected immediately after collection into a high pressure liquid chromatography system with electrochemical detection (BAS 200, Bioanalytical System, West Lafayette, IN). Mobile phase was prepared according to Chiueh et al. (11) and was delivered through a 25-cm Beckman Ultrasphere IP 5-µm reverse-phase column (Thomson Instrument Co., Springfield, VA) at 1.0 ml/min. The glassy carbon electrode was maintained at +0.72 V relative to an Ag/AgCl reference electrode.

Data Analysis. All results are presented as means ± SEM of 7 or 9 rats. The mean neurotransmitter concentrations of the initial three baseline samples were taken as basal release, and the results were expressed as a percentage of basal release. Comparisons of mean differences between groups were made by Student's *t*-test. Comparisons of percent-change response after KCl perfusion in each group were made by one-way analysis of variance. Significant differences were determined using the Student-Newman-Keuls multiple range test. Data on the percent-change response of DA after KCl perfusion were subjected to log transformation before statistical analysis to normalize the data. The significance level was chosen at $P < 0.05$.

RESULTS

Table I shows the basal levels of striatal DA and monoamine metabolites in freely moving and chloral hydrate-anesthetized rats. There were no significant differences in the basal levels of DA, DOPAC, or 5-HIAA between freely moving and anesthetized rats. Significant differences ($P < 0.05$), however, were observed in the extracellular level of HVA in the striata in these two groups.

Fig. 1 shows the effect of chloral hydrate anesthesia on KCl-induced increases in striatal DA overflow. KCl at the concentrations of 50 and 100 mM stimulated DA overflow dose-dependently and significantly ($P < 0.05$) in both freely moving (1548 ± 352% and 9666 ± 2531%, respectively) and anesthetized rats (2493 ± 546% and 9476 ± 2574%, respectively). The DA overflows in response to 30 mM KCl stimulation in anesthetized rats was significantly greater than in freely moving rats (597 ± 95% vs 328 ± 53%; $P < 0.05$).

Fig. 2 shows changes (%) in extracellular DOPAC in response to KCl stimulation in freely moving and anesthetized rats. In freely moving rats, the basal level of extracellular DOPAC remained relatively constant. There were brief but significant decreases in DOPAC levels following 50 and 100 mM KCl stimulation ($P < 0.05$). In chloral hydrate-anesthetized rats, the basal level

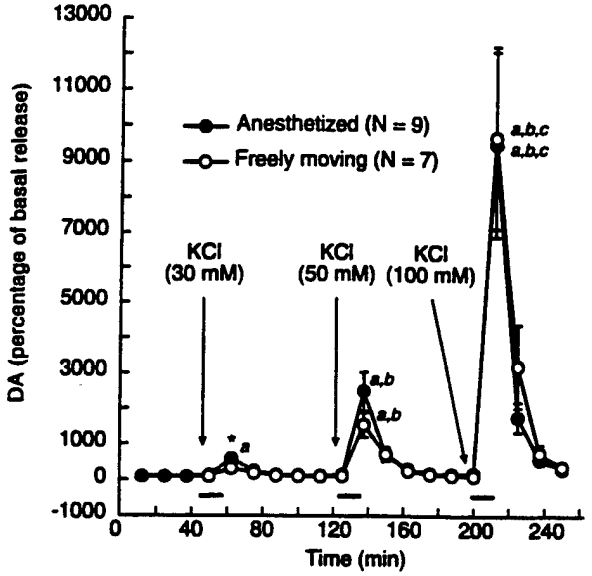

Fig. 1. The effect of chloral hydrate anesthesia on striatal DA release in response to KCl stimulation. Administration of KCl (20 µl) is indicated by an arrow, and the duration of KCl administration is indicated by a horizontal bar. Data shown are mean ± S.E.M. of 7 and 9 rats, and are expressed as a percentage of the basal release calculated from three samples prior to the administration of 30 mM KCl. *P < 0.05 vs freely moving rats; [a]P < 0.05 vs basal release; [b]P < 0.05 vs peak of DA release in response to 30 mM KCl stimulation: [c]P < 0.05 vs peak of DA release in response to 50 mM KCl stimulation.

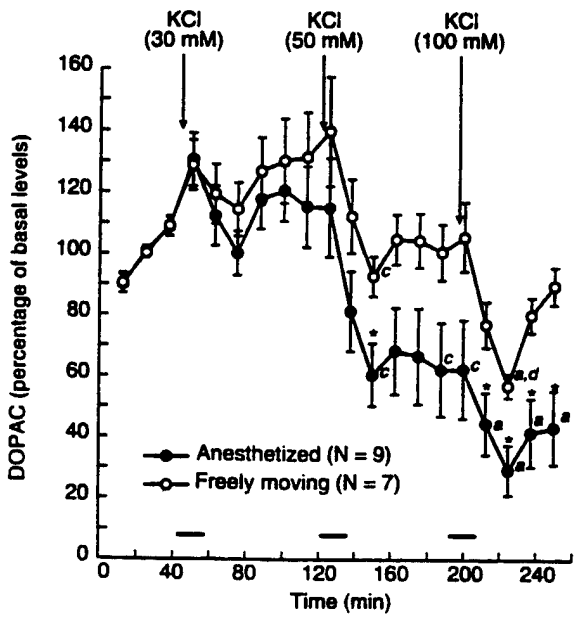

Fig. 2. The effect of chloral hydrate anesthesia on extracellular DOPAC levels in the striatum. Administration of KCl (20 µl) is indicated by an arrow, and the duration of KCl administration is indicated by a horizontal bar. Data shown are mean ± S.E.M. of 7 and 9 rats, and are expressed as a percentage of the basal level calculated from three samples prior to the administration of 30 mM KCl. *P < 0.05 vs freely moving rats; [a]P < 0.05 vs basal levels; [c]P < 0.05 vs extracellular DOPAC levels prior to the administration of 50 mM KCl; [d]P < 0.05 vs extracellular DOPAC levels prior to the administration of 100 mM KCl.

of extracellular DOPAC remained steady through the first 125 min of sample collection and then decreased sharply to a much lower level; the decrease in extracellular DOPAC levels was significant ($P < 0.05$) at 212.5 min and thereafter. Administration of KCl at all three concentrations resulted in a decrease in DOPAC levels; however, only the decrease in DOPAC levels following 50 mM KCl stimulation was statistically significant ($P < 0.05$). There were significant differences in the extracellular DOPAC level in the two groups at 150, 212.5 min, and thereafter.

Fig. 3 shows changes (%) in extracellular HVA in response to KCl stimulation in freely moving and anesthetized rats. The basal level of extracellular HVA in freely moving rats remained steady throughout the first 125 min of the experiment, then decreased sharply and significantly, and remained low throughout the rest of the experiment. The decrease in extracellular levels of HVA was significant at 137.5 min and thereafter ($P < 0.05$). In chloral hydrate-anesthetized rats, the basal level of extracellular HVA remained steady throughout the first 200 min of the experiment, and then decreased significantly thereafter. There were significant ($P < 0.05$) differences in extracellular HVA levels in the two groups at 100 and 150 min of sample collection and thereafter. Significant decreases in the basal levels of HVA were observed in anesthetized rats following the perfusion of 30 and 50 mM KCl, and in both groups following the perfusion of 100 mM KCl.

Fig. 4 shows changes (%) in extracellular 5-HIAA in response to KCl stimulation in freely moving and anesthetized rats. In freely moving rats, the basal level of extracellular 5-HIAA remained steady through the first 125 min of the experiment, decreased significantly ($P < 0.05$) at 150 min, and remained low throughout the rest of the experiment. Perfusion of 100 mM KCl resulted in a significant decrease in the 5-HIAA level. In anesthetized rats, the extracellular level of 5-HIAA increased slowly with time and reached the levels significantly above baseline ($P < 0.05$) at 125, 175, 187.5, 200, and 250 min of sample collection. Perfusion of 100 mM KCl resulted in a significant decrease in the 5-HIAA level ($P < 0.05$). There were significant differences in extracellular 5-HIAA levels in the two groups at 87.5, 112.5 min, and thereafter.

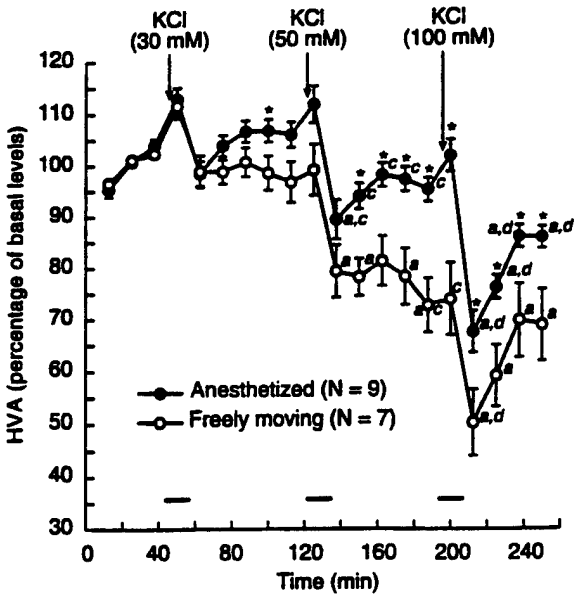

Fig. 3. The effect of chloral hydrate anesthesia on extracellular HVA levels in the striatum. See fig. 2 for additional explanation. *P < 0.05 vs freely moving rats; [a]P < 0.05 vs basal levels; [c]P < 0.05 vs extracellular HVA levels prior to the administration of 50 mM KCl; [d]P < 0.05 vs extracellular HVA levels prior to the administration of 100 mM KCl.

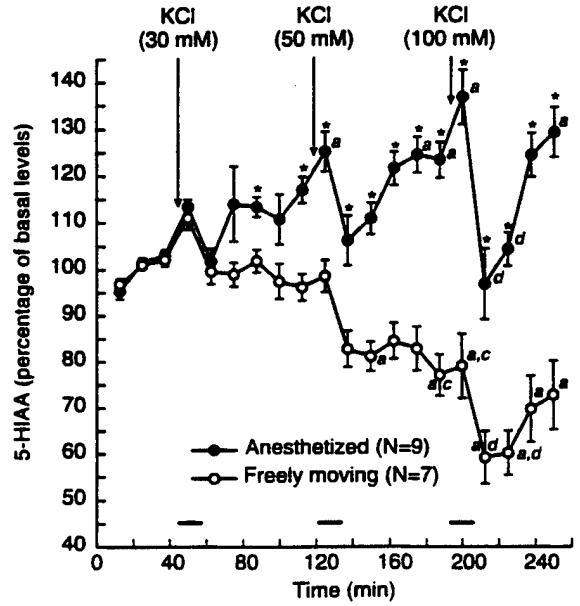

Fig. 4. The effect of chloral hydrate anesthesia on extracellular 5-HIAA levels in the striatum. See fig. 2 for additional explanation. *P < 0.05 vs freely moving rats; [a]P < 0.05 vs basal levels; [c]P < 0.05 vs extracellular 5-HIAA levels prior to the administration of 50 mM KCl; [d]P < 0.05 vs extracellular 5-HIAA levels prior to the administration of 100 mM KCl.

DISCUSSION

Our results demonstrate that chloral hydrate anesthesia can influence the pharmacological response of the striatal dopaminergic system. Increased basal levels of extracellular HVA and increased DA response to 30 and 50 mM KCl-stimulation in anesthetized rats as compared to freely moving rats are consistent with results reported earlier by other researcher (7, 8). Stahle et al. (7) demonstrated that halothane anesthesia increased basal levels of DA and HVA in the rat striatum, and Opacka-Juffry et al. (8) showed that isoflurane anesthesia increased the extracellular concentration of DA and its metabolites and enhanced the nomifensine-induced increase in striatal DA concentration. On the contrary, chloral hydrate anesthesia was shown recently to decrease the basal release of DA in the striatum (9). Our study does not confirm their finding, and we have no good explanation for this discrepancy. However, Hamilton et al. (9) did show that increases in striatal DA overflow in response to d-amphetamine and morphine, two drugs with different mechanisms of action, were significantly greater in anesthetized rats than in conscious rats. Although these authors provided their data with different interpretations, their results did suggest an increased DA response to different stimuli following chloral hydrate anesthesia.

The mechanism involved in increased DA metabolism and increased DA response to KCl-stimulation in chloral hydrate-anesthetized rats is unclear. It is possible that chloral hydrate anesthesia interferes with presynaptic DA autoreceptors in the rat striatum as suggested for isoflurane anesthesia by Opacka-Juffry et al. (8). However, the electrophysiological study of Mereu et al. (12) suggested that general anesthetics did not seem to modify the sensitivity of DA autoreceptors to agonists and antagonists. Alternatively, chloral hydrate may interfere with the presynaptic DA reuptake mechanism. Microdialysis studies by Hurd and Ungerstedt (13) have shown that most DA uptake inhibitors induce a gradual accumulation of extracellular DA with very little influence on extracellular DOPAC, HVA, and 5-HIAA. Our results, showing significant increase in extracellular HVA and 5-HIAA in chloral hydrate-anesthetized rats in contrast to free-moving rats, argue against this hypothesis and suggest that the influence of chloral hydrate anesthesia is not limited to the dopaminergic system. The third possibility is that chloral hydrate anesthesia interferes with the inhibitory neuronal mechanisms that regulate striatal DA release, as suggested by Stahle et al. (7) for halothane anesthesia. It has been shown that γ-aminobutyric acid (GABA) inhibited striatal DA release (14, 15) and synthesis (16) by acting on $GABA_B$ recep-

tors at the dopaminergic terminal. Therefore, the reduction of GABAergic cell firing and subsequent depression of basal GABA levels following general anesthesia (17) could at least partially explain the increased dopaminergic activity in the striatum.

Administering high concentrations of KCl resulted in decreases in extracellular levels of DOPAC, HVA, and 5-HIAA, which confirms an earlier study reported by Fairbrother et al. (18). The decrease in basal DOPAC levels in chloral hydrate-anesthetized rats confirms a report by Ford and Marsden (19). It is interesting to note that the decreased DOPAC levels in chloral hydrate-anesthetized rats, compared with freely moving rats, was not seen until 3.5 h after the initiation of chloral hydrate anesthesia.

In freely moving rats, the basal level of extracellular HVA reduced sharply at 137.5 min of sample collection, and remained depressed throughout the rest the experiment. The decrease in extracellular HVA coincided with the decreased HVA in response to 50 mM KCl stimulation. At present, it is unclear whether or not KCl challenge had anything to do with the depressed basal level of HVA. In any event, chloral hydrate anesthesia increased the basal level of HVA and prevented the decrease in extracellular HVA observed in freely moving rats. Westerink and Kikkert (20) reported that chloral hydrate inhibited the efflux of DOPAC and HVA from the brain, with HVA being more sensitive to inhibition. This inhibitory effect of chloral hydrate on the transport of HVA from the brain may also explain the observed difference in basal HVA between freely moving and chloral hydrate-anesthetized rats.

In this study, surgical implantation of microdialysis probes in chloral hydrate-anesthetized rats was performed approximately 1.5 h before sample collection instead of inserting probes through guide cannulas implanted 3 days before experimentation, as was done in freely moving rats. The rationale for this acute implantation was to reproduce the experimental design used frequently in microdialysis studies with chloral hydrate-anesthetized rats. Therefore, the possible contribution of acute surgery to the changes in striatal DA and its metabolites following chloral hydrate anesthesia cannot be ruled out.

In summary, our results demonstrate that chloral hydrate can interfere with the pharmacological response of the striatal dopaminergic system, and imply that caution should be taken in extrapolating results from anesthetized rats to conscious rats. Additional studies involving the use of various agents, such as nomifensine (a DA uptake inhibitor), spiperone (a D_2 antagonist) and/or 2-hydroxysaclofen (a $GABA_B$ antagonist) to stimulate DA release through different mechanisms, are needed to further characterize the effect of chloral hydrate on striatal dopaminergic transmission.

ACKNOWLEDGMENT

Supported by the Armed Forces Radiobiology Research Institute under research work unit 00157. Research was conducted according to the principles enunciated in the *Guide for the Care and Use of Laboratory Animals* prepared by the Institute of Laboratory Animal Resources, National Research Council.

REFERENCES

1. Bunney, B. S., Aghajanian, G. K., and Roth, R. H. 1973. Comparison of effects of L-DOPA, amphetamine and apomorphine on firing rate of dopaminergic neurons. Nature: New Biol. 245:123-125.
2. Bunney, B. S., Walters, J. R., Roth, R. H., and Aghajanian, C. K. 1973. Dopaminergic neurons: Effects of antipsychotic drug and amphetamine on single cell activity. J. Pharmacol. Exp. Ther. 185: 560-571.
3. Mereu, G., Fadda, F., and Gessa, G. L. 1984. Ethanol stimulates the firing rate of nigral dopaminergic neurons in unanesthetized rats. Brain Res. 292:63-69.
4. Kelland, M. D., Freeman, A. S., and Chiodo, L. A. 1989. Chloral hydrate anesthesia alters the responsiveness of identified midbrain dopamine neurons to dopamine agonist administration. Synapse 3: 30-37.
5. Kelland, M. D., Chiodo, L. A., and Freeman, A. S. 1990. Anesthetic influences on the basal activity and pharmacological responsiveness of nigrostriatal dopamine neurons. Synapse 6:207-209.
6. Freeman, A. S., and Bunney, B. S. 1987. Activity of A_9 and A_{10} dopaminergic neurons in unrestrained rats: Further characterization and effects of apomorphine and cholecystokinin. Brain Res. 405:46-55.
7. Stahle, L., Collin, A. K., and Ungerstedt, U. 1990. Effects of halothane anesthesia on extracellular levels of dopamine, dihydroxyphenylacetic acid, homovanillic acid and 5- hydroxyindoleacetic acid in rat striatum: A microdialysis study. Naunyn-Schmiedebergs Arch. Pharmacol. 342:136-140.
8. Opacka-Juffry, J., Ahier, R. G., and Cremer, J. E. 1991. Nomifensine-induced increase in extracellular striatal dopamine is enhanced by isoflurane anaesthesia. Synapse 7:169-171.
9. Hamilton, M. E., Mele, A. and Pert, A. 1992. Striatal extracellular dopamine in conscious vs. anesthetized rats: effects of chloral hydrate anesthetic on responses to drugs of different classes. Brain Res. 597:1-7.
10. Paxinos, G., and Watson, C. 1986. The rat brain in stereotaxic coordinates, Academic Press, New York.
11. Chiueh, C. C., Zukowska-Grojec, Z., Kiek, K. L., and Kopin, I. J. 1983. 6-Fluorocatecholamines as false adrenergic neurotransmitters. J. Pharmacol. Exp. Ther. 225:529–533.
12. Mereu, G., Casu, M., and Gessa, G. L. 1983. (−)-Sulpiride activates the firing rate and tyrosine hydroxylase activity of dopaminergic neurons in unanesthetized rats. Brain Res. 264:105–110.
13. Hurd, Y. L., and Ungerstedt, U. 1989. In vivo neurochemical profile of dopamine uptake inhibitors and releasers in rat caudate-putamen. Eur. J. Pharmacol. 166:251–260.
14. Bowery, N. G., Hill, D. R., Hudson, A. L., Doble, A., Middlemiss, D. N., Shaw, J., and Turnbull, M. 1980. (−)Baclofen decreases

neurotransmitter release in the mammalian CNS by an action at a novel GABA receptor. Nature 283:92–94.
15. Reimann, W. 1983. Inhibition by GABA, Baclofen, and GABA-pentin of dopamine release from rabbit caudate nucleus: Are there common or different sites of action? Eur. J. Pharmacol. 94:341–344.
16. Arias-Montano, J. H., Martinez-Fong, D. and Aceves, J. 1991. γ-Aminobutyric acid ($GABA_B$) receptor-mediated inhibition of tyrosine hydroxylase activity in the striatum of rat. Neuropharmacology 30:1047–1051.
17. Osborne, P. G., O'Connor, W. T., Drew, K. L., and Ungerstedt, U. 1990. An in vivo microdialysis characterization of extracellular dopamine and GABA in dorsolateral striatum of awake freely moving and halothane anaesthetised rats. J. Neurosci. Methods 34: 99–105.
18. Fairbrother, I. S., Arbuthnott, G. W., Kelly, J. S., and Butcher, S. P. 1990. In vivo mechanisms underlying dopamine release from rat nigrostriatal terminals: II. Studies using potassium and tyramine. J. Neurochem. 54:1844–1851.
19. Ford, A. P. D. W., and Marsden, C. A. 1986. Influence of anaesthetics on rat striatal dopamine metabolism in vivo. Brain Res. 379:162–166.
20. Westerink, B. H. C., and Kikkert, R. J. 1986. Effect of various centrally acting drugs on the efflux of dopamine metabolites from the rat brain. J. Neurochem. 46:1145–1152.

RADIATION RESEARCH **146**, 111–115 (1996)
0033-7587/96 $5.00

ARMED FORCES RADIOBIOLOGY RESEARCH INSTITUTE
SCIENTIFIC REPORT
SR96-6

SHORT COMMUNICATION

Effect of Ionizing Radiation on *In Vivo* Striatal Release of Dopamine in the Rat

Han-Tong Chen and Sathasiva B. Kandasamy

Department of Radiation, Pathophysiology, and Toxicology, Armed Forces Radiobiology Research Institute, Bethesda, Maryland 20889-5603

Chen, H-T. and Kandasamy, S. B. Effect of Ionizing Radiation on *In Vivo* Striatal Release of Dopamine in the Rat. *Radiat. Res.* 146, 111–115 (1996).

The time-course effect of ionizing radiation on the levels of basal and KCl-stimulated striatal release of dopamine (DA) was examined *in vivo* using microdialysis techniques. The basal level of extracellular DA in sham-irradiated controls was 0.172 ± 0.042 pmol/sample (n = 9), and it increased 7.1-fold after the stimulation by 30 m*M* KCl (20 μl). However, the release of dihydroxyphenylacetic acid (DOPAC) and homovanillic acid (HVA), two metabolites of DA, was reduced significantly by 30 m*M* KCl (P < 0.05). In the presence of 10 μ*M* forskolin, an activator of adenylate cyclase, a second stimulation by 30 m*M* KCl increased the release of DA 6.9-fold. Radiation exposure, at a dose of 10 Gy at 10 Gy/min, had no significant effect on the levels of either basal or KCl-stimulated release of DA or on the release of DOPAC and HVA. Striatal DA release increased in response to two consecutive challenges of KCl. However, the release of DA in response to the second challenge of KCl was significantly smaller than that after the first challenge (543 ± 110% compared to 794 ± 164%, P < 0.05; Student's paired t test). Pretreatment with 10 μ*M* forskolin, which by itself had no significant effect on the level of basal release of DA, prevented the decreased response of DA to the second challenge of KCl. Our results suggest that radiation exposure at the dose we used has no significant effect on the level of the basal release of DA or the release of DA stimulated by 30 m*M* KCl in the rat striatum, and that a reduced release of DA in response to repeated KCl stimulation might involve the cAMP effector system.

INTRODUCTION

Studies with animals including non-human primates have suggested that exposure to high doses of ionizing radiation resulted in deficits in psychomotor performance (*1*, *2*). The mechanisms involved in these radiation-induced behavioral changes are not well understood. Electrophysiological studies have revealed significant neurophysiological changes after acute radiation exposure. Within hours whole-body exposure to 10 Gy or less of γ radiation resulted in a modified synaptic efficacy and spike generation ability in guinea pig hippocampus (*3*). Electrophysiological changes in hippocampal neurons were also observed after *in vitro* exposure to γ or X radiations (*4*, *5*). Since a number of behavioral and neurological abnormalities have been associated with functional changes in synaptic transmission in the brain, it is possible that radiation might disturb the synaptic transmission of specific neurotransmitters in discrete areas of the brain.

Exposure to ionizing radiation reduces voltage-dependent calcium influx in rat brain synaptosomes *in vitro* (*6*). Because calcium influx is essential during voltage-dependent neurotransmitter release (*7*), radiation exposure could affect neurotransmitter release adversely. In fact, exposure of rats to high-energy iron particles at doses in the range of 0.1–5.0 Gy has been shown to result in a profound decrement in the oxotremorine-enhanced, KCl-evoked *in vitro* release of dopamine (DA) from perfused striatal slices (*8*) and in the concentrations of 3-methoxytyramine (3-MT), a metabolite of DA, in the caudate nucleus (*9*) dissected from these animals. In the present study, we examined the time-course effect of ionizing radiation on the levels of the basal and KCl-stimulated striatal release of DA *in vivo* using microdialysis techniques. Since Westfall *et al.* (*10*) and Lee *et al.*[1] have reported that cyclic AMP (cAMP) may play a role in regulating release of DA in rat neostriatal slices *in vitro*, we also examined striatal release of DA in the absence and presence of forskolin, an activator of adenylate cyclase (*11*).

METHODS

Drugs. Chloral hydrate and standards for DA, dihydroxyphenylacetic acid (DOPAC) and homovanillic acid (HVA), were purchased from Sigma Chemical Co. (St. Louis, MO). All other reagents were analytical grade. Forskolin (Research Biochemicals, Inc., Natick, MA) was initially dissolved in dimethyl sulfoxide and diluted in artificial cerebrospinal fluid (aCSF) to the final concentration.

[1]H. Lee, V. Reid and M. H. Weiler, Effects of forskolin on dopamine and acetycholine release in rat neostriatal slices. Abstract, 20th Neuroscience Meeting, St. Louis, MO, 1990.

TABLE I
Levels of Basal Release of DA and Metabolites (pmol/sample) in the Striatum of Control Rats and of Rats on Days 1, 2, 4 and 6 after Radiation Exposure at a Dose of 10 Gy and a Dose Rate of 10 Gy/min

Group	*n*	DA	DOPAC	HVA
Controls	9	0.172 ± 0.042	26.8 ± 2.1	21.0 ± 1.1
Irradiated rats				
Day 1	4	0.186 ± 0.088	21.7 ± 2.2	17.8 ± 1.0
Day 2	7	0.071 ± 0.021[a]	27.7 ± 1.2	20.5 ± 0.7
Day 4	5	0.096 ± 0.028	23.8 ± 3.2	17.1 ± 2.3
Day 6	4	0.148 ± 0.044	24.7 ± 2.3	20.8 ± 1.2

Note. Values are mean ± SEM.
[a] $n = 6$.

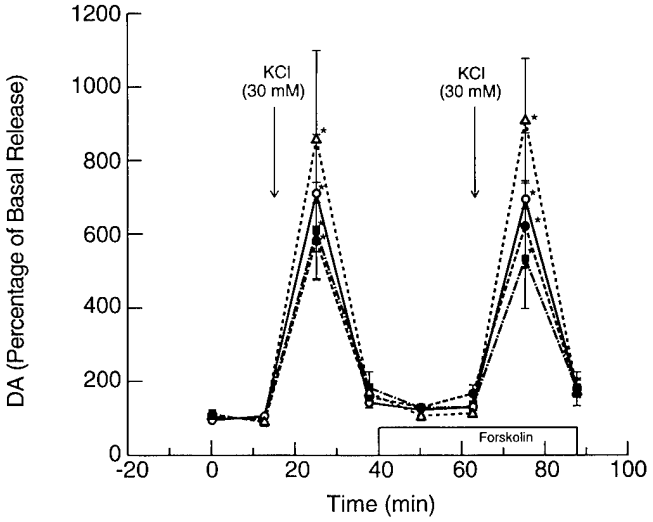

FIG. 1. Time-course effects of ionizing radiation on the levels of basal and KCl-stimulated release of DA in rat striatum in the absence and presence of 10 μ*M* forskolin. (○) Controls, (△) day 2, (●) day 4, (■) day 6. Data shown are mean ± SEM of four to nine rats. *$P < 0.05$ compared to basal release in all groups.

Animals. Male Sprague-Dawley Crl:CD(SD)BRD rats (Charles River Breeding Laboratories, Kingston, NY) weighing 250–450 g were used in these experiments. The rats were housed in an AAALAC-accredited animal facility with a 12-h light:dark cycle and were allowed access to commercial rodent chow (Wayne Rodent Blok, Continental Grain Co., Chicago, IL) and water *ad libitum*.

Radiation exposure. Rats were exposed bilaterally to ^{60}Co γ radiation as described previously (*12*), except that a dose of 10 Gy at a dose rate of 10 Gy/min was used. Sham-irradiated rats served as controls. The dose rate was established using an acrylic rat phantom. Dosimetry was performed in accordance with the AAPM protocol (*13*) using a 0.5-ml tissue-equivalent ion chamber whose calibration was traceable to the National Institute of Standards and Technology.

Implantation and perfusion. Microdialysis was performed according to Glue *et al.* (*14*) with a CMA 10 microdialysis probe (2-mm tip, Carnegie Medicin, Stockholm) in rats under chloral hydrate anesthesia (400 mg/kg, ip). Small supplements of chloral hydrate maintained the depth of anesthesia at a level where corneal reflexes were abolished. The probe was inserted stereotaxically through a small burr hole in the skull into the right striatum (A: +9.9, L: +3.0, and V: +3.0 mm relative to interaural zero) according to the atlas of Paxinos and Watson (*15*) and perfused with aCSF at a flow rate of 2 μl/min. The aCSF contained 147.3 m*M* NaCl, 2.3 m*M* $CaCl_2$ and 4.0 m*M* KCl. Sample collection was started 1 h after probe insertion (time 0) when the basal level of extracellular DA was stabilized, and was collected every 12.5 min in vials containing 2.5 μl of 0.05 *M* perchloric acid. The location of probes was confirmed by visual examination of frozen brain sections at the end of each experiment.

Experimental protocols. In the first study, the time-course effect of ionizing radiation on striatal release of DA was examined in rats on days 1, 2, 4 and 6 after radiation exposure. Sham-irradiated rats served as controls. The striatal tissue was perfused with aCSF during the first half of the experiment. After four samples were collected, 10 μ*M* forskolin was then administered locally through the microdialysis probe, and four additional samples were collected. The KCl (30 m*M* for 10 min) was also perfused locally through the same probe at 15 min and again at 65 min to stimulate release of DA. Administration of drugs was facilitated by a CMA 110 liquid switch. The effect of forskolin on KCl-stimulated release of DA was examined further in the second study. Rats were divided randomly into two groups. The striatal tissue of rats in the first group was perfused with aCSF throughout the whole experiment. In the second group, rats were perfused with aCSF during the first half of the experiment and then perfused with aCSF containing 10 μ*M* forskolin in the second half of the experiment as described previously. The KCl was perfused at 15 min and again at 65 min.

Neurotransmitter analysis. Microdialysis samples (20 μl) were injected immediately after collection into a high-pressure liquid chromatography system with electrochemical detection (BAS 200, Bioanalytical System, West Lafayette, IN). Mobile phase was prepared according to Chiueh *et al.* (*16*) and was delivered through a 15-cm C-18 3-μm reverse-phase column (Varian Associates, Sunnyvale, CA) at 1.0 ml/min. Samples from the second study were analyzed with a 25-cm Beckman Ultrasphere IP 5-μm reverse-phase column (Thomson Instrument Co., Springfield, VA). The glassy carbon electrode was maintained at +0.72 V relative to an Ag/AgCl reference electrode.

Data analysis. All results are presented as mean ± SEM. The mean neurotransmitter concentrations of the initial two baseline samples were taken as basal release. Releases of monoamines and metabolites after administration of KCl and/or forskolin were expressed as percentage of basal release. Comparisons of the level of the basal release among different groups and the percentage change after treatment with KCl and/or forskolin in each group were made by one-way analysis of variance. Significant differences were determined by using Bonferroni simultaneous confidence intervals for all comparisons. In the second study, the differences between the first and second KCl-stimulated releases of DA were analyzed using Student's paired *t* test. The second KCl-stimulated DA peaks were also expressed as the percentage of the first DA peaks, and the differences between groups were determined using Student's *t* test. The significance level was set at $P < 0.05$.

RESULTS

Table I shows the levels of basal release of striatal DA and the extracellular levels of metabolites in controls and in rats after exposure to ionizing irradiation. Radiation exposure had no significant effect on the levels of basal release of either DA or its metabolites in the striatum.

Figure 1 shows the time-course effects of ionizing radiation on the levels of basal and KCl-stimulated release of DA in the absence and presence of 10 μ*M* forskolin. For clarity of viewing, data from rats on day 1 after irradiation are not shown in this figure or in Figs. 2 and 3. In controls, there was a significant increase (7.1-fold) in release of DA ($P < 0.05$) after the first administration of 30 m*M* KCl. In

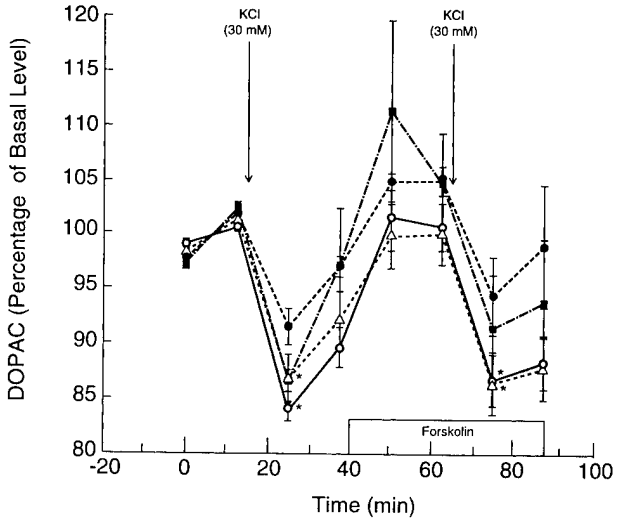

FIG. 2. Time-course effects of ionizing radiation on basal and KCl-reduced extracellular DOPAC levels in rat striatum in the absence and presence of 10 μ*M* forskolin. (○) Controls, (△) day 2, (●) day 4, (■) day 6. Data shown are mean ± SEM of 4–9 rats. **P* < 0.05 compared to basal levels in controls and in rats 2 days after irradiation.

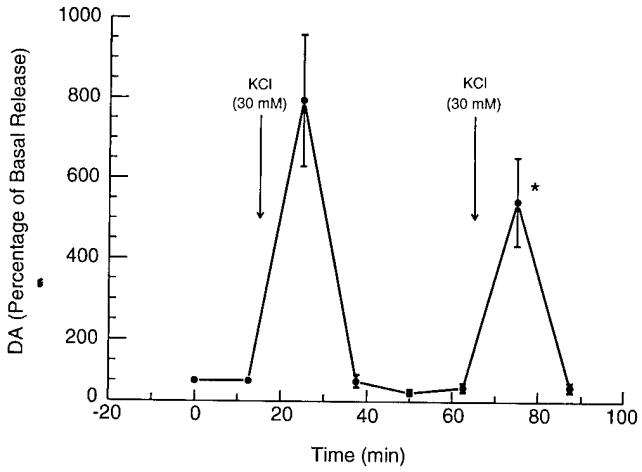

FIG. 4. Striatal release of DA in response to two consecutive challenges of 30 m*M* KCl in male rats. Data shown are mean ± SEM of 13 rats. **P* < 0.05 compared to the first DA peak (Student's paired *t* test).

the presence of 10 μ*M* forskolin, the second challenge of 30 m*M* KCl increased release of DA 6.9-fold ($P < 0.05$). There was no significant difference in the levels of either the basal or KCl-stimulated release of DA in the absence or presence of forskolin between controls and irradiated rats.

The time-course effects of ionizing radiation on extracellular levels of DOPAC and HVA in the absence and presence of 10 μ*M* forskolin are shown in Figs. 2 and 3, respectively. The basal levels of DOPAC and HVA, two metabolites of DA, were reduced by 30 m*M* KCl in all groups studied; however, decreases in DOPAC and HVA were statistically significant ($P < 0.05$) only in controls and in rats on day 2 after irradiation. Forskolin had no significant effect on extracellular levels of DOPAC and HVA. Radiation exposure also had no significant effect on the level of either the basal or KCl-induced decrease in extracellular levels of DOPAC and HVA.

Striatal releases of DA in normal rats increased in response to two consecutive challenges with KCl (Fig. 4). However, the release of DA in response to the second challenge with KCl was significantly smaller than after the first challenge (543 ± 110% compared to 794 ± 164%; $P < 0.05$). In the control group, the second DA peak in response to KCl stimulation was only 66 ± 7% ($n = 5$) of the first DA

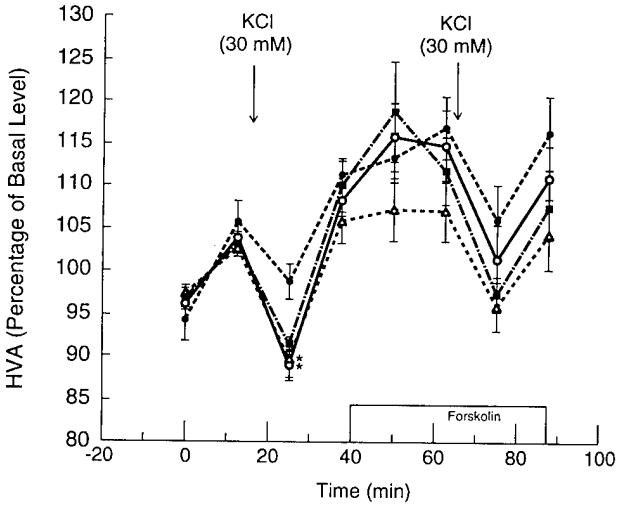

FIG. 3. Time-course effects of ionizing radiation on basal and KCl-reduced extracellular HVA levels in rat striatum in the absence and presence of 10 μ*M* forskolin. (○) Controls, (△) day 2, (●) day 4, (■) day 6. Data shown are mean ± SEM of 4–9 rats. **P* < 0.05 compared to basal levels in controls and in rats 2 days after irradiation.

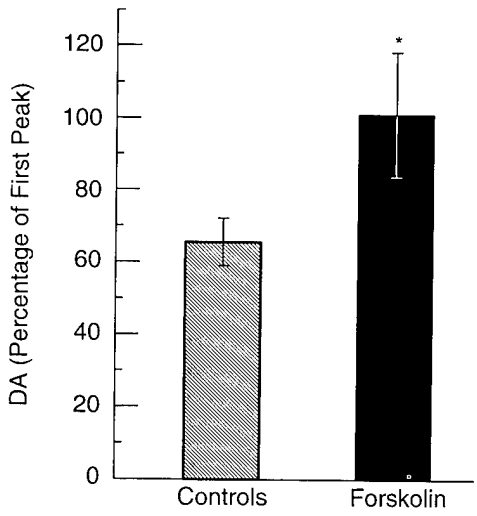

FIG. 5. Effects of 10 μ*M* forskolin on release of DA in response to the second challenge of 30 m*M* KCl in male rats. Data shown are mean ± SEM of 5–13 rats and are expressed as the percentage of the first DA peak. **P* < 0.05 compared to controls.

peak (Fig. 5). Pretreatment with forskolin, which by itself had no significant effect on release of DA (data not shown), prevented the decreased response of DA to the second challenge with KCl ($P < 0.05$ compared to controls).

DISCUSSION

To our knowledge, this is the first study to examine the time-course effects of γ radiation on striatal DA efflux *in vivo*. Our results suggest that exposure of rats to γ radiation at the dose we used has no significant effect on the level of the basal or the KCl-stimulated release of DA and its metabolites in the rat striatum. However, it has been reported that striatal tissue from rats irradiated with 150 Gy of γ-ray photons released significantly more DA *in vitro* in response to 30 m*M* KCl stimulation than that from sham-irradiated controls in the presence of various concentrations of haloperidol (*17*). Furthermore, exposure of rats to a single dose of 100 Gy of high-energy electrons was shown to induce an immediate and transient increase in KCl-stimulated release of DA *in vitro* in rat caudate nucleus (*18*). Reports from this laboratory also suggest that high-energy iron particles are more effective than high-energy electrons or γ-ray photons in inducing neural changes in rats (*8, 9*). The discrepancy between our results and those reported earlier could have been due to the use of different techniques, different radiation sources and/or different doses of γ radiation. However, our results do not rule out the possibility that the release of DA stimulated by other agents through a receptor-mediated event can be affected by the radiation.

Administering a high concentration of KCl resulted in a decrease in extracellular levels of DOPAC and HVA in all groups, which was in agreement with an earlier study reported by Fairbrother *et al.* (*19*). The mechanism involved in this KCl-induced decrease in extracellular metabolite levels is unclear. It is possible that depletion of newly synthesized intracellular DA due to increased release by a high concentration of KCl leads to the decrease in extracellular levels of its metabolites because extracellular DOPAC is believed to be derived predominantly from newly synthesized DA (*20*).

A reduced DA efflux in response to the second KCl stimulation observed in this study confirmed an early study reported by Ng Cheong Ton *et al.* (*21*). However, the mechanism involved in this reduced response by DA to repeated KCl challenge is not known. Lee *et al.*[1] reported that forskolin, which induced a dose-dependent increase in cAMP, increased KCl-stimulated release of DA in a dose-dependent manner *in vitro* in rat neostriatal slices. In this study we found that forskolin (10 μ*M*), which had no significant effect on the levels of basal release of DA, prevented the reduced DA response to the second challenge with KCl in rat striatum. It is possible that increased efflux of DA in response to the first KCl stimulation acts on the presynaptic D_2 autoreceptor that is negatively coupled to adenylate cyclase through the guanyl nucleotide regulatory protein G_i (*22*). Since cAMP has been suggested to be involved in mechanisms that increase striatal release of DA, decreased cAMP by activation of D_2 receptors could explain the reduced response in DA efflux to the second challenge of KCl. Forskolin has been known to activate adenylate cyclase (*11*). Therefore, prior to the second stimulation of KCl, perfusion of forskolin restored the striatal DA response to the second challenge of KCl. It would be interesting to see whether or not pretreatment with specific D_2 blockers can also prevent the degraded DA response to repeated stimulation with KCl.

In summary, our study shows that radiation exposure at the dose we used has no significant effect on the level of basal release of DA or release of DA stimulated by 30 m*M* KCl in the striatum. Our data suggest that a reduced release of DA in response to repeated KCl stimulation might involve the cAMP effector system.

ACKNOWLEDGMENT

This work was supported by the Armed Forces Radiobiology Research Institute under work unit 00157. Research was conducted according to the principles enunciated in the *Guide for the Care and Use of Laboratory Animals* prepared by the Institute of Laboratory Animal Resources, National Research Council.

Received: September 5, 1995; accepted: February 9, 1996

REFERENCES

1. W. F. Burghardt, Jr. and W. A. Hunt, Characterization of radiation-induced performance decrement using a two-lever shock-avoidance task. *Radiat. Res.* **103**, 149–157 (1985).
2. C. G. Franz, Effects of mixed neutron–γ total-body irradiation on physical activity performance of rhesus monkeys. *Radiat. Res.* **101**, 434–441 (1985).
3. T. C. Pellmar and D. L. Lepinski, Gamma radiation (5–10 Gy) impairs neuronal function in the guinea pig hippocampus. *Radiat. Res.* **136**, 255–261 (1993).
4. J. M. Tolliver and T. C. Pellmar, Ionizing radiation alters neuronal excitability in hippocampal slices of the guinea pig. *Radiat. Res.* **112**, 555–563 (1987).
5. T. C. Pellmar, D. A. Schauer and G. H. Zeman, Time- and dose-dependent changes in neuronal activity produced by X radiation in brain slices. *Radiat. Res.* **122**, 209–214 (1990).
6. S. B. Kandasamy, T. C. Howerton and W. A. Hunt, Reductions in calcium uptake induced in rat brain synaptosomes by ionizing radiation. *Radiat. Res.* **125**, 158–162 (1991).
7. G. J. Augustine, M. P. Charlton and J. S. Smith, Calcium entry and transmitter release at voltage-clamped nerve terminals of squid. *J. Physiol.* **367**, 163–181 (1985).
8. J. A. Joseph, W. A. Hunt, B. M. Rabin and T. K. Dalton, Possible "accelerated striatal aging" induced by ^{56}Fe heavy-particle irradiation: Implications for manned space flights. *Radiat. Res.* **130**, 88–93 (1992).
9. W. A. Hunt, T. K. Dalton, J. A. Joseph and B. M. Rabin, Reduction of 3-methoxytyramine concentrations in the caudate nucleus of rats after exposure to high-energy iron particles: Evidence for deficits in dopaminergic neurons. *Radiat. Res.* **121**, 169–174 (1990).
10. T. C. Westfall, D. Kitay and G. Wahl, The effect of cyclic nucleotides on the release of ^{3}H-dopamine from rat striatal slices. *J. Pharmacol. Exp. Ther.* **199**, 149–157 (1976).

11. K. B. Seamon, W. Padgett and J. W. Daly, Forskolin: unique diterpene activator of adenylate cyclase in membrane and intact cells. *Proc. Natl. Acad. Sci. USA* **78**, 3363–3367 (1981).
12. S. B. Kandasamy, W. A. Hunt and A. H. Harris, Role of neurotensin in radiation-induced hypothermia in rats. *Radiat. Res.* **126**, 218–222 (1991).
13. American Association of Physicists in Medicine, AAPM Task Group 21: A protocol for the determination of absorbed dose from high-energy photon and electron beams. *Med. Phys.* **10**, 741–771 (1983).
14. P. Glue, M. J. Costello, A. Pert, A. Mele and D. J. Nutt, Regional neurotransmitter responses after acute and chronic electroconvulsive shock. *Psychopharmacology* **100**, 60–65 (1990).
15. G. Paxinos and C. Watson, In *The Rat Brain in Stereotaxic Coordinates*. Academic Press, New York, 1986.
16. C. C. Chiueh, Z. Zukowska-Grojec, K. L. Kirk and I. J. Kopin, 6-Fluorocatecholamines as false adrenergic neurotransmitters. *J. Pharmacol. Exp. Ther.* **225**, 529–533 (1983).
17. J. A. Joseph, S. B. Kandasamy, W. A. Hunt, T. K. Dalton and S. Stevens, Radiation-induced increases in sensitivity of cataleptic behavior to haloperidol: possible involvement of prostaglandins. *Pharmacol. Biochem. Behav.* **29**, 335–341 (1988).
18. W. A. Hunt, T. K. Dalton and J. H. Darden, Transient alterations in neurotransmitter activity in the caudate nucleus of rat brain after a high dose of ionizing radiation. *Radiat. Res.* **80**, 556–562 (1979).
19. I. S. Fairbrother, G. W. Arbuthnott, J. S. Kelly and S. P. Butcher, *In vivo* mechanisms underlying dopamine release from rat nigrostriatal terminals: II. Studies using potassium and tyramine. *J. Neurochem.* **54**, 1844–1851 (1990).
20. T. Zetterstrom, T. Sharp, A. K. Collin and U. Ungerstedt, *In vivo* measurement of extracellular dopamine and DOPAC in rat striatum after various dopamine-releasing drugs; implications for the origin of extracellular DOPAC. *Eur. J. Pharmacol.* **148**, 327–334 (1988).
21. J. M. Ng Cheong Ton, G. Gerhardt, M. Friedemann, A. M. Etgen, G. M. Rose, N. S. Sharpless and E. L. Gardner, The effects of Δ^9-tetrahydrocannabinol on potassium-evoked release of dopamine in the rat caudate nucleus: an *in vivo* electrochemical and *in vivo* microdialysis study. *Brain Res.* **451**, 59–68 (1988).
22. J. C. Stoof and J. W. Kebabian, Opposing roles for D1 and D2 dopamine receptors in efflux of cyclic AMP from rat neostriatum. *Nature* **294**, 366–368 (1981).

INFECTION AND IMMUNITY, Aug. 1996, p. 2885–2891
0019-9567/96/$04.00+0

Vol. 64, No. 8

Transient and Persistent Experimental Infection of Nonhuman Primates with *Helicobacter pylori*: Implications for Human Disease

ANDRE DUBOIS,[1,2]* DOUGLAS E. BERG,[3] ENGIN T. INCECIK,[3] NANCY FIALA,[1,2] LILLIE M. HEMAN-ACKAH,[4] GUILLERMO I. PEREZ-PEREZ,[5] AND MARTIN J. BLASER[5]

Laboratory of Gastrointestinal and Liver Studies, Digestive Diseases Division, Department of Medicine, Uniformed Services University of the Health Sciences,[1] and Departments of Physiology[2] and Veterinary Science,[4] Armed Forces Radiobiology Research Institute, Bethesda, Maryland; Department of Molecular Microbiology, Washington University Medical School, St. Louis, Missouri[3]; and Division of Infectious Diseases, Department of Medicine, Vanderbilt University School of Medicine and Department of Veterans Affairs Medical Center, Nashville, Tennessee[5]

Received 25 March 1996/Returned for modification 19 April 1996/Accepted 1 May 1996

***Helicobacter pylori* can establish chronic infection in the human gastric mucosa, and it is a major cause of peptic ulcer disease and a principal risk factor for gastric cancer. This creates a need for *H. pylori* infection models that mimic the human condition. To test the suitability of rhesus monkeys as infection models, *H. pylori*-free animals were inoculated intragastrically with mixtures of *H. pylori* strains, bacteria recovered from colonized animals were typed by arbitrarily primed PCR, and host inflammatory and immunologic responses were monitored. Among five *H. pylori*-free animals inoculated with a mixture of two human strains plus one monkey strain, one became persistently infected and one became only transiently infected. The recovered bacteria matched the monkey input strain in DNA fingerprint. A subsequent trial using two new human isolates and three animals that had resisted colonization by the monkey strain resulted in persistent infection in one animal and transient infection in two others. Antral gastritis, anti-*H. pylori* serum immunoglobulin G, and atrophy all increased, but with patterns that differed among animals. We conclude that (i) rhesus monkeys can be infected experimentally with *H. pylori*, (ii) individuals differ in susceptibility to particular bacterial strains, (iii) infections may be transient, and (iv) the fitness of a particular strain for a given host helps determine the consequences of exposure to that strain.**

Helicobacter pylori, a common bacterial pathogen of humans, is the principal cause of chronic active gastritis and peptic ulcer disease and a risk factor for gastric cancer, even though most infections are asymptomatic (3, 4, 41). Once established, most infections last for years and rarely cure spontaneously, although they usually can be cured by antimicrobial therapy. Infection also increases the risk of other diseases, such as cholera (8) and persistent diarrhea (44). *H. pylori* is a very diverse species, and it is possible that the range of outcomes following infection reflects differences in bacterial genotypes, as well as human host genotypes and environmental factors.

Much of our understanding of *H. pylori*-host interactions has come from hundreds of studies of humans with well-established infections, often identified during population screens or because of persistent gastroduodenal disease symptoms. Fragmentary data indicate major differences between such chronic (established) infections and the early (acute) phase when a person is just being colonized (3, 17, 27, 29, 32–34). Acute infections are particularly difficult to analyze in people, however, because experimental human infection is unethical and early stages of natural infections do not usually receive medical attention. This emphasizes the special need for human-like *H. pylori* infection models.

The importance of *H. pylori* has spurred development of several animal models for studies of *Helicobacter* infection. Of particular interest are (i) gnotobiotic newborn piglets, which are easily infected by *H. pylori* of human origin (2, 23) but are best suited for short-term studies; (ii) mice and ferrets, which can be colonized for months and years, respectively, although most easily by *Helicobacter* species other than *H. pylori* (16, 24); (iii) certain domestic cats, which can carry *H. pylori* (20); and (iv) particular strains of mice, which can be colonized by selected *H. pylori* strains (26, 30). Each of these models, although useful, is also limited by major differences from humans in gastric anatomy, physiology, diet, immune or inflammatory responses, technical difficulty of endoscopy, and/or short-term life span. It is in this context that nonhuman primates are of particular interest, especially for studies of subtle bacterial and host-specific factors that affect colonization or the emergence and progression of gastroduodenal disease.

Of the several primate species studied (6, 7, 15, 18, 21, 42, 43), rhesus monkeys appeared most promising because of their worldwide availability, moderate size, and large repertoire of useful immunological reagents, and the knowledge base gained through years of study. *H. pylori* is enzootic in at least some rhesus monkey colonies, including that from which the animals used in this study come (10, 12, 14). More than half of such animals become colonized by 2 years of age, although some remain uninfected for many years (13). This high incidence of infant infection resembles epidemiologic patterns among the very poor in developing countries and even in the United States and Western Europe (19, 31, 38). It is also noteworthy that *H. pylori*-infected rhesus monkeys exhibit atrophy, microerosions, and loss of mucus reminiscent of those seen in hu-

* Corresponding author. Mailing address: Department of Medicine, Uniformed Services University of the Health Sciences, 4301 Jones Bridge Road, Bethesda, MD 20814-4799. Fax: (301) 295-3676 or -3557. Electronic mail address: DUBOIS@USUHSB.USUHS.MIL.

TABLE 1. Characteristics of *H. pylori* strains used in the study

Strain no. [other name] (reference)	Source	Phenotype[a]	Trial(s) in which used
H_1 [92-26][b]	Patient with non-ulcer dyspepsia	$CagA^+$ Tox^+	1 and 2
H_2 [88-23 or ATCC-49503] (9)	Patient with non-ulcer dyspepsia	$CagA^+$ Tox^+	1 and 2
H_3 [U-1][c]	Patient with duodenal ulcer	Unknown	3
H_4 [U-2][c]	Patient with gastric ulcer	$CagA^+$ Tox^-	3
M_1 [788-2][c]	Monkey with gastritis	$CagA^+$ Tox^+	1 and 2

[a] Production of the *cagA*-encoded high-molecular-weight protein and of the vacuolating cytotoxin (9, 45).
[b] Isolated at Vanderbilt University School of Medicine, Nashville, Tenn.
[c] Isolated at the Uniformed Services University of the Health Sciences, Bethesda, Md.

mans (12, 14) and that peptic ulcers and gastric cancer also have been reported in them (36, 37).

Experimental infection of rhesus monkeys has been tried several times. In one trial, one of five animals inoculated with a strain of human origin was reported to have become infected, but the recovered strain did not match the input strain in its DNA fingerprint (15). In another trial, each of five monkeys inoculated with a strain of monkey origin became infected, and the recovered strains were said to match the input strain in DNA fingerprint, but no data supporting this interpretation were presented (15). Experimental infection of Japanese monkeys and chimpanzees have been reported, but without DNA fingerprinting data to show whether the recovered strains matched those used for inoculation (21, 42).

Here we report experimental infection of colony-raised *H. pylori*-free rhesus monkeys, with DNA fingerprinting that identifies input and recovered strains, and describe immediate and long-term inflammatory and immune responses to infection.

MATERIALS AND METHODS

Inocula. Five different *H. pylori* strains were used in these experiments (Table 1). Primary isolates were stored at −70°C in saline or brucella broth with 20% glycerol. Two days before inoculation of monkeys, the strains were transferred to flasks containing 25 ml of brain heart infusion broth plus 4% fetal calf serum, which were then incubated with shaking for 2 days in an atmosphere of 90% N_2, 5% O_2, and 5% CO_2. On the day of inoculation, the cultures were centrifuged at 4°C and resuspended in brucella broth at 10^8 to 10^9 *H. pylori* CFU/ml and mixed when indicated.

Animals. The experiments reported herein were conducted according to the principles set forth in *Guide for the Care and Use of Laboratory Animals* (21a). All experiments were approved by the Armed Forces Radiobiology Research Institute Institutional Animal Care and Use Committee and monitored and reapproved yearly. Eight domestic male rhesus monkeys (*Macaca mulatta*) that were 2 to 5 years old, weighed 2 to 5 kg, had not been in previous research protocols, and were free of *H. pylori* by culture and histology were used. They had been bred, reared, and socially housed either in indoor gang cages, in outdoor corrals, or in a large free-ranging colony on a sea island (Laboratory Animals Breeders and Services, Yemassee, S.C.).

Upon arrival at our facility in Bethesda, Md., monkeys were quarantined for 90 days in individual stainless steel cages in conventional holding rooms of an animal facility approved by the American Association for Accreditation of Laboratory Animal Care and were provided with tap water ad libitum, commercial primate chow, and fruits. They were tested by three intradermal tuberculin injections at 2-week intervals; all were negative. After release from quarantine, they were kept in equivalent individual housing. Endoscopies were performed between 8:00 and 12:00 a.m. after overnight fasts (see below).

Endoscopic procedures and biopsies. Monkeys underwent gastroduodenal endoscopic examination under general anesthesia (atropine sulfate, 0.02 mg/kg intramuscularly followed by ketamine HCl, 10 mg/kg intramuscularly), using an EG2700 Pentax (Orangeburg, N.Y.) videogastroscope with an outer diameter of 9.0 mm. After each endoscopy, the equipment was rinsed with water and then disinfected by soaking for 10 min in an activated dialdehyde solution of a 2% glutaraldehyde solution (Cidex: Johnson & Johnson Medical, Inc., Arlington, Tex.); the instruments were then rinsed sequentially with sterile water and 70% alcohol and air dried. Six pinch mucosal biopsies each of the gastric corpus and antrum were taken from each animal.

Histologic examination. Two biopsies each from the corpus and antrum were fixed in neutral 10% buffered formalin and embedded in paraffin. Five-micrometer-thick sections were stained with hematoxylin and eosin (H&E) and viewed under ×100 to ×1,000 magnification. Antral gastritis was scored on coded slides, using a scale of 0 to 3 as modified from reference 28 (0, intact mucosal lining and essentially no infiltration of the lamina propria with lymphocytes and plasma cells; 1, mild increase of mononuclear infiltration, localized in the upper half of the mucosa; 2, mononuclear infiltration extending from the surface into the lamina propria; 3, marked mononuclear infiltration extending from the surface into the lamina propria and disrupting the structure of the glands and leading to atrophy, and/or polymorphonuclear leukocytes in glands and surface erosions). Slides also were scored for the presence of *H. pylori* infection after Warthin-Starry or H&E plus Gram staining.

Microbiological methods. Two other biopsies each from the corpus and antrum were immediately placed in 0.1 ml of sterile 0.9% NaCl on ice, coded, and homogenized with a sterile ground-glass cone-shaped pestle fitting a tapered 1.5-ml Eppendorf tube. An aliquot (1 to 2 μl) was streaked on *Campylobacter* chocolate agar plates supplemented with trimethoprim, vancomycin, amphotericin B, and polymyxin B (Remel, Lenexa, Kans.) and incubated at 37°C in an atmosphere of 90% N_2, 5% O_2, and 5% CO_2. *H. pylori* isolates were identified as forming pinhead-sized colonies that grew within 7 to 10 days and had urease, oxidase (Becton Dickinson, Cockeysville, Md.), and catalase activities and by microscopy as gram-negative and curved or "gull-wing" rods. The two remaining biopsies from each region of the stomach were immediately placed in sterile 20% glycerol in 0.9% NaCl and frozen at −70°C for further analyses.

DNA fingerprinting. To distinguish among *H. pylori* strains, the arbitrarily primed PCR or random amplified polymorphic DNA (RAPD) fingerprinting method was used as described previously (1, 5) with DNAs purified by phenol extraction from cultures of individual single colony isolates. Four arbitrary primers were used: 1247 (5′-AAGAGCCCGT), 1254 (5′-CCGCAGCCAA), 1281 (5′-AACGCGCAAC), and 1283 (5′-GCGATCCCCA) (1). After PCR, 8-μl aliquots were electrophoresed in 2% agarose gels in 1× Tris acetate running buffer containing 0.5 μg of ethidium bromide per ml and photographed under UV light. The 1-kb DNA ladder (Gibco-BRL, Gaithersburg, Md.) was used as a size marker in all gels.

Measurement of *H. pylori*-specific plasma IgG. Five milliliters of blood was drawn from each monkey at the time of each endoscopy into 7-ml tubes containing 10.5 mg of EDTA and centrifuged, and the supernatant plasma was frozen at −70°C. Anti-*H. pylori* immunoglobulin G (IgG) levels in the plasma were determined blindly, using a modification of a previously described enzyme-linked immunosorbent assay (ELISA) with >95% sensitivity and specificity for human infection (11, 39). This modified ELISA used anti-monkey antibody conjugates, and established thresholds provided 92% specificity and 85% sensitivity for infection in monkeys (12). Results were corrected for day-to-day variation of the ELISA and expressed as optical density ratios. All assays were done at least in duplicate.

Inoculation protocol. Monkeys were treated with famotidine (Pepcid; Merck, Inc., West Point, Pa.; 2 mg/kg, given intramuscularly 14 and 1 h before inoculation) to suppress acid output. After an overnight fast, the animals were endoscoped as described above, phenol red was sprayed to estimate the pH of the gastric mucosa (generally a pH of between 2 and 7), and 5 ml of 0.25 M $NaHCO_3$ was introduced onto the antrum to neutralize gastric acid. A suspension of 10^8 to 10^9 CFU of *H. pylori* (1 ml of each strain) was then sprayed onto the gastric antrum. The monkeys were reendoscoped 5 to 7 days after inoculation, and generally at 3- to 5-week intervals thereafter, at which time biopsies were collected and plasma was also obtained for measurement of IgG levels. To use these animals most efficiently, some that had been inoculated, but in which *H. pylori* had not become established, were enrolled in a subsequent trial.

RESULTS

Colonization. We tested whether rhesus monkeys that had somehow evaded natural infection despite 2 to 3 years in a high-risk environment could be experimentally infected with *H. pylori* strains of rhesus monkey (M_1) or human (H_1, H_2, H_3, and H_4) origin in three trials (Table 2). Eight monkeys that had

TABLE 2. Results of *H. pylori* inoculation

Monkey no.[a]	Colonization		Gastritis score >2	Serum IgG >cutoff	RAPD fingerprint
	By culture	By histology			
Trial 1					
7N1	None	None	None	None	
7MG	None	None	None	None	
8R1	None	None	None	None	
8RC	None	None	None	None	
8V5	None	None	None	None	
9A5	None	None	None	2 mo only	
Trial 2[b]					
8RC	1–12 mo	1–12 mo	1.5–12 mo[c]	2.5–12 mo	M_1
8V5	None	None	1 wk–3 mo	1 wk–6.5 mo	
9A5	1 wk only	1–7 wk	2–3 mo only	1–4 mo only	M_1
E0E	None	None	3 mo only	3–4 mo only	
KJ2	None	None	None	None	
Trial 3[d]					
8V5	1 wk only	None	1 wk only	1–2 mo only	H_4
9A5	1 wk only	None	None	1–2 mo only	H_4
KJ2	1 wk–9 mo	2 and 9 mo	8–9 mo only	3.5–9 mo	H_4

[a] Ages of monkeys in years: E0E, 2; E5V, 2 to 3; 8R1, 3; 9A5, 8V5, and KJ2, 3 to 4; 7N1 and 7MG, 4; 8RC, 4 to 5.
[b] 8RC, 8V5, and 9A5 were rechallenged 3 months after the beginning of trial 1; E0E and KJ2 were used for the first time.
[c] Gastric corpus and antral atrophy starting at 9 months.
[d] KJ2 was used 7 months after the beginning of trial 2; 8V5 and 9A5 were used 14 months after the beginning of trial 2. Inoculation of an animal with a natural low-grade infection led to establishment of the inoculum strain and also emergence of new, apparently recombinant strains.

evaded natural infection were inoculated with various *H. pylori* strains in these trials, and the following results were obtained.

(i) Trial 1. Six animals were inoculated with human strain H_1. None of the animals was judged to have become colonized by it, given the failure to culture *H. pylori* from any of 32 biopsies taken at 3- to 5-week intervals from day 7 through 3 months, and also given the failure to detect *H. pylori* by microscopy in Warthin-Starry-, or H&E-, and/or Gram-stained histologic sections from 16 other biopsies taken at the same times. In consequence, this trial was discontinued.

(ii) Trial 2. To more efficiently assess whether any *H. pylori* strain could colonize a monkey after experimental challenge, we decided to use a mixture of several strains, each of which was readily distinguishable by DNA fingerprinting. Five animals were each inoculated with a mixture of H_1 (used in trial 1), H_2 (another human isolate), and M_1 (an isolate from a monkey). Three animals (8RC, 8V5, and 9A5) were from trial 1, which had started 3 months earlier, and the other two (E0E and KJ2) had not been used previously.

We recovered *H. pylori* from biopsies taken a week after inoculation from two of the three animals that had resisted infection in the first trial. One of them (8RC) remained infected throughout the 12 months that he was studied. The other (9A5) was judged to have spontaneously cured his infection by 3 months after inoculation, as judged from the inability to detect *H. pylori* organisms histologically in four biopsies or to culture them from any of eight other biopsies. However, light infection was still evident in him by histologic examination, but not by culture, at 4 and 7 weeks. In contrast, neither the third animal (8V5) nor either of the two new animals (E0E and KJ2) showed any sign of having been colonized during the 3 months of observation.

Since each input strain was readily distinguishable from the others by RAPD fingerprinting (Fig. 1), eight representative isolates taken at 1 month from each colonized animal were fingerprinted. Each isolate tested matched the input strain of monkey origin; none matched either input human strain (Fig. 1). These results indicate that while some monkeys could be infected experimentally with an enzootic, monkey-adapted *H. pylori* strain, other animals were resistant to this same strain. Left unsettled, however, was the issue of whether colonization of monkeys by *H. pylori* strains of human origin is possible or is blocked by lack of appropriate host specificity determinants.

(iii) Trial 3. Two of the monkeys that had resisted infection in the second trial (KJ2 and 8V5), plus the monkey that had sustained a transient infection (9A5), were again challenged with *H. pylori*, this time using a mixture of two other human strains (H_3 and H_4). *H. pylori* was recovered from all three animals at 1 week. Histology and culture tests indicated that two of the animals had spontaneously cleared their infections within a month of inoculation, whereas the other one remained colonized for the duration of the study. By RAPD fingerprinting, all 62 isolates from both the transiently and persistently infected animals matched input strain H_4 (Fig. 2). This trial establishes that an *H. pylori* strain of human origin can colonize

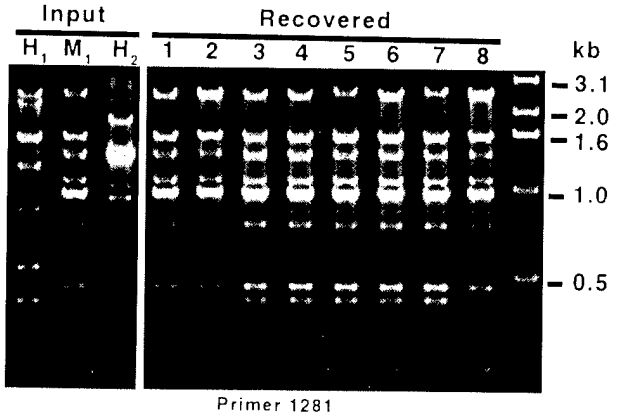

FIG. 1. RAPD fingerprinting with primer 1281 of representative isolates recovered after inoculation of monkey 8RC with a mixture of two human strains, H_1 (=92-26) and H_2 (=88-23), and one monkey strain (M_1). Data showing that all eight recovered isolates matched the monkey input strain M_1 also were obtained with primers 1254 and 1283.

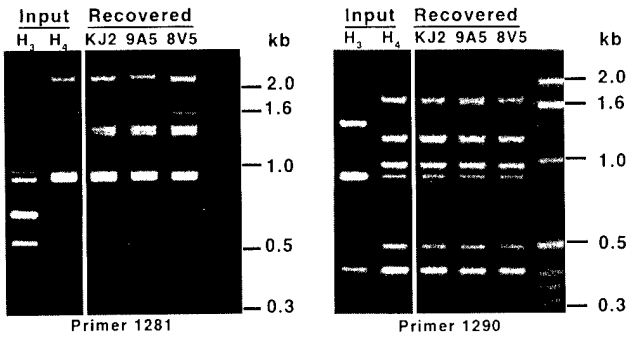

FIG. 2. RAPD fingerprinting of representative isolates recovered after inoculation of monkeys KJ2, 9A5, and 8V5 with a mixture of two human strains (H_3 and H_4). All recovered isolates matched strain H_4, which was obtained from a patient with a gastric ulcer.

rhesus monkeys either persistently or transiently and can infect animals resistant to an *H. pylori* strain of monkey origin that is enzootic in their colony.

Histological findings. The two animals with persistent infection (8RC in trial 2; KJ2 in trial 3) had normal gastric mucosae just prior to infection but developed chronic-active antral gastritis within a month of inoculation. The gastritis increased progressively to grade >2 by 1.5 months in monkey 8RC and by 8 months in monkey KJ2 and then persisted for the duration of observations (9 to 12 months). In addition, each monkey developed marked atrophy of the previously normal stomach mucosae and microerosions and loss of mucus from superficial epithelial cells beginning 6 to 8 months after inoculation (Fig. 3 and 4). Interestingly, each animal also had developed transient gastritis in the earlier trial that had not led to their becoming colonized (Fig. 4). In animals with either no colonization or only transient colonization, a gastritis score of >2 either was not observed or lasted only 1 to 3 months (Fig. 5 and data not shown).

Serological immune responses. The two animals with long-term infection (8RC and KJ2) exhibited increased anti-*H. pylori* plasma IgG, beginning 2.5 to 3.5 months postinoculation. The levels peaked at 4 to 5 months and then declined, but remained greater than the cutoff for positivity for the remaining 2 to 6 months of the study (Fig. 4). In contrast, the two transiently colonized monkeys (8V5 and 9A5) exhibited rapid increases in levels of anti-*H. pylori* IgG within 1 week of inoculation and then gradual decreases following elimination of the bacteria (Fig. 5). The four monkeys that were not colonized in trial 1 or 2 (7MG, 8R1, 7N1, and E0E) did not exhibit any consistent change in anti-*H. pylori* IgG levels (Table 2 and Fig. 5).

DISCUSSION

The experiments presented here (i) establish conditions for experimental infection of rhesus monkeys by *H. pylori*; (ii) help develop monkeys as human-like infection models; (iii) exploit mixtures of bacterial strains that are readily distinguished by DNA fingerprinting to assess whether a given host can be colonized; and (iv) lead to three major conclusions that are particularly relevant to human infection.

First, individuals differ in susceptibility to particular *H. pylori* strains. This conclusion emerges from the finding that two of six monkeys tested in trial 2 were susceptible, and four were resistant, to an *H. pylori* strain that had been circulating in their colony. This large fraction of animals apparently resistant to *H. pylori* infection may be related to the fact that these animals had been selected as being *H. pylori* free despite several years in group housing with infected animals. The spontaneous cure of infection in some colonized animals, but not others, in trials 2 and 3 also indicates diversity among individual hosts in factors important for maintaining a given strain.

Second, *H. pylori* strains differ in the ability to grow in different hosts. This conclusion is based on findings in trial 3 that three animals that had been resistant to a monkey strain were colonized by a human isolate, H_4.

Third, *H. pylori* infection can be of short duration, as demonstrated by the observation that two monkeys that seemed to be well colonized by *H. pylori* when examined 1 to 7 weeks after

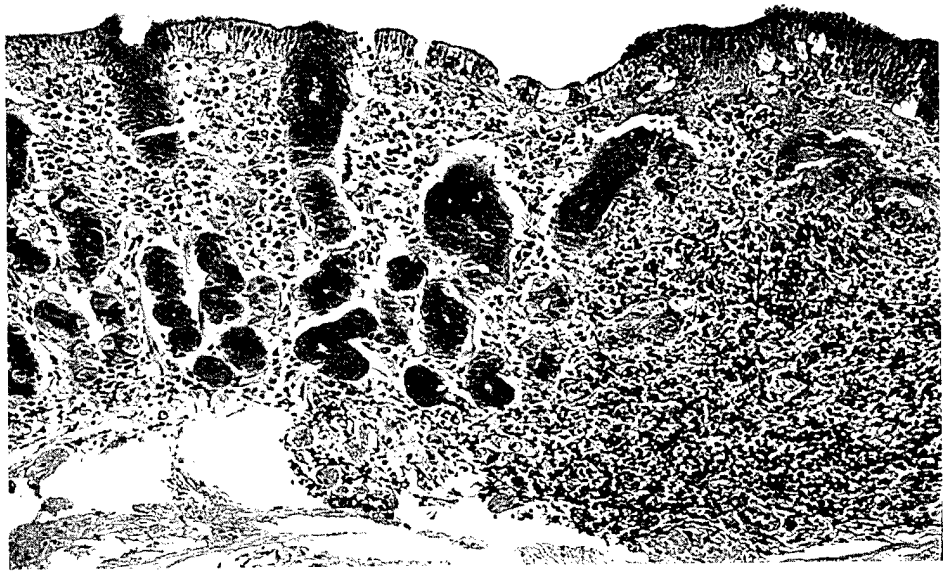

FIG. 3. Illustration of chronic-active (grade 3) antral gastritis in animal 8RC at 10 months postinoculation, demonstrating marked atrophy, microerosions, and loss of mucus (H&E stain). *H. pylori* was isolated from this animal throughout a 12-month period.

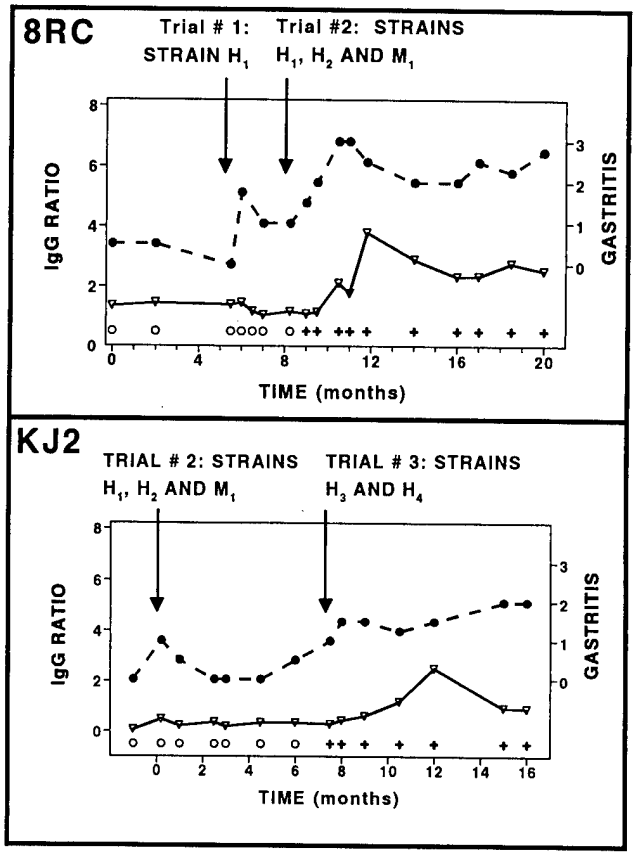

FIG. 4. Time course of antral gastritis score (●) and plasma IgG ratio (▽) before and after successful colonization. Absence of infection is indicated by ○, and positivity for infection by culture and/or histology is illustrated by +. Animal 8RC, also illustrated in Fig. 1 and 3, became persistently infected in trial 2, and plasma IgG and gastritis score increased after a 3-month delay. Animal KJ2 was not included in trial 1, did not become infected in trial 2, but was colonized by one of the strains isolated from a patient with gastric ulcer used in trial 3, as illustrated in Fig. 2.

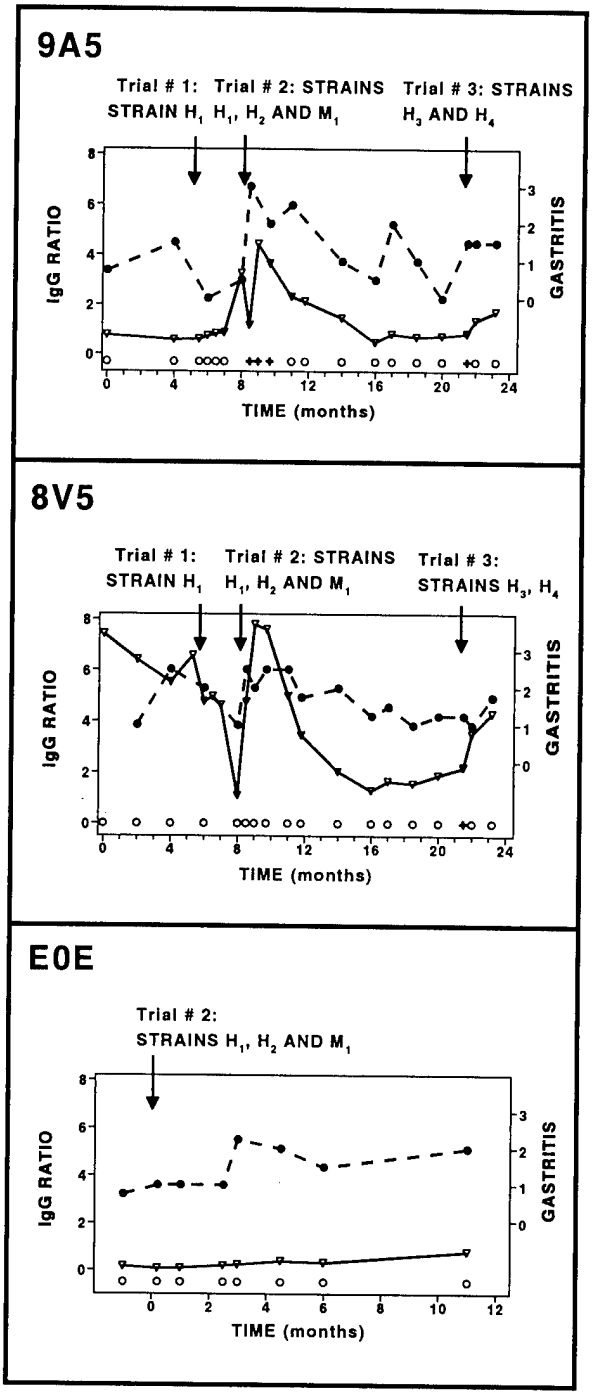

FIG. 5. Time course of antral gastritis score (●) and plasma IgG ratio (▽) before and after transient or unsuccessful colonization. Absence and presence of infection are indicated by ○ and +, respectively, as in Fig. 4. Animal 9A5 was not colonized in trial 1 but developed transient infection during trials 2 and 3. Animal 8V5 was not colonized during trials 1 and 2 but developed transient infection during trial 3. Animal E0E was included only in trial 2 and did not become colonized by *H. pylori*.

inoculation had eliminated these bacteria by 3 months postinoculation. This observation contrasts with the traditional view that *H. pylori* infections persist for years, which is based primarily on patients with infections that were established long before diagnosis and that the bacteria, therefore, must have been well adapted to their hosts. There are, however, at least three reports of studies of human *H. pylori* infection in which the patients also were monitored closely from the time of exposure, and two of these infections were also transient (27, 34), whereas the third persisted until it was cured with antibiotic therapy (35). Interestingly, transient infection might also underlie the reported "spontaneous" clearance of *H. pylori* in a patient receiving placebo (46). Further evidence comes from recent studies of infants in Peru and in The Gambia, using urea breath tests, which demonstrated dramatic fluctuations over time in gastric urease levels (high, low, and then high again) in many children in the study group (22, 44). If the urea breath test is an accurate indicator of *H. pylori* infection in this population, as it is in adults in other societies (40), these results would support the hypothesis that cycles of transient infection are common in humans when first exposed to *H. pylori*.

Cases of spontaneous clearance have been ascribed to the patient immune response, which may reflect host genotype or physiology (27, 34). Consistent with this view are correlations of particular genotypes in humans and apparent resistance to infection (25). This explanation is also compatible with our finding that the three animals that were only transiently infected had rapid immune responses, whereas the two animals

(8RC and KJ2) that became persistently infected did not develop peak IgG levels until 3 to 4 months after inoculation (Fig. 4). This delay in antibody response is similar to that in the only reported human case of persistent infection after experimental inoculation (35). Thus, this rapid response may reflect protective immunity (although the serum antibodies measured here only approximate the more relevant gastric mucosal immune responses). Since gastritis appeared more rapidly after inoculation in animals that did not develop long-term infection than in those that did, we propose that a strong early tissue response can help the host eventually repel the infecting strain. Taken together, these considerations support the prospect for development of effective anti-*H. pylori* vaccines (26).

We propose that there is a link between the phenomenon of transient infection and differences among strains in the ability to colonize a given host and in susceptibility of potential hosts. Differences in susceptibility in a potential host population are, of course, a familiar theme in infectious disease. In the case of *H. pylori*, it probably reflects genetically determined traits, in combination with environmental cofactors and age of acquisition. In this context, the extensive genetic diversity among *H. pylori* strains may be adaptive, reflecting continuous selection for variants that are increasingly fit for a given infected host, even as it may change over time. A strain with such a history might often be imperfectly suited to the next host to ingest it and, in the extreme, either fail to colonize that host or result in only transient infection, much as has been seen here.

In conclusion, our results show that rhesus monkeys can be experimentally infected with strains of *H. pylori* of human or of monkey origin and suggest that monkeys may serve as particularly important models for studies of gastric physiology and immune responses. Our analysis also shows that rhesus monkeys vary in susceptibility to infection by a given *H. pylori* strain, that *H. pylori* strains also vary in traits that may be important in colonization of individual hosts, and that some infections are very short-lived. We propose that much of the remarkable diversity among *H. pylori* strains reflects selection by the different genotypes, physiologic states, and immunologic experience of billions of different human hosts. Thus, future inoculation of rhesus monkeys with sets of strains that are genetically well characterized, and DNA level analysis of recovered strains as here, should provide new insights into the mechanisms by which *H. pylori* causes gastroduodenal disease and into host-specific adaptation of the pathogen during years of chronic infection.

ACKNOWLEDGMENTS

This work was supported by NIH grants AI38166, DK48029, and DK50837 and American Cancer Society grant VM-121. Engin T. Incecik is enrolled at the Universität Regensburg, Regensburg, Germany, and was supported by the Deutscher Akademischer Austauschdienst exchange in molecular biology between Washington University and the Universität Regensburg.

We thank Natalia S. Akopyants for initial strain typing; E. Susan Drazek and Richard I. Walker (MicroCarb, Inc.) for growing strains for the present experiments; and N. S. Akopyants, E. S. Drazek, and R. I. Walker for many stimulating discussions.

REFERENCES

1. **Akopyanz, N., N. O. Bukanov, T. U. Westblom, S. Kresovich, and D. E. Berg.** 1992. DNA diversity among clinical isolates of *Helicobacter pylori* detected by PCR-based rapid fingerprinting. Nucleic Acids Res. **20:**5137–5142.
2. **Akopyants, N. S., K. A. Eaton, and D. E. Berg.** 1995. Adaptive mutation and cocolonization during *Helicobacter pylori* infection of gnotobiotic piglets. Infect. Immun. **63:**116–121.
3. **Anonymous.** 1994. *Helicobacter pylori* in peptic ulcer disease. NIH Consensus Conference. JAMA **272:**65–69.
4. **Anonymous.** 1994. IARC monograph on the evaluation of carcinogenic risks to humans, vol. 61. Schistosomes, liver flukes and *Helicobacter pylori*. International Agency for Research on Cancer, Lyon, France.
5. **Berg, D. E., N. S. Akopyants, and D. Kersulyte.** 1994. Fingerprinting microbial genomes using the RAPD or AP-PCR method. Methods Mol. Cell. Biol. **5:**13–24.
6. **Bronsdon, M. A., C. S. Goodwin, L. I. Sly, T. Chilvers, and F. D. Schoenknecht.** 1991. *Helicobacter nemestrinae* sp. nov., a spiral bacterium found in the stomach of a pigtailed macaque (*Macaca nemestrina*). Int. J. Syst. Bacteriol. **41:**148–153.
7. **Brondson, M. A., and F. D. Schoenknecht.** 1988. *Campylobacter pylori* isolated from the stomach of the monkey *Macaca nemestrina*. J. Clin. Microbiol. **26:**1725–1728.
8. **Clements, J., J. Albert, M. Rao, F. Quadri, S. Huda, B. Kay, F. P. L. van Loon, D. Sack, B. A. Pradhan, and R. B. Sack.** 1995. Impact of infection by *Helicobacter pylori* on the risk and severity of endemic cholera. J. Infect. Dis. **171:**1653–1656.
9. **Cover, T. L., and M. J. Blaser.** 1994. Purification and characterization of the vacuolating toxin from *Helicobacter pylori*. J. Biol. Chem. **267:**10570–10575.
10. **Drazek, E. S., A. Dubois, and R. K. Holmes.** 1994. Characterization and presumptive identification of *Helicobacter pylori* isolates from rhesus monkeys. J. Clin. Microbiol. **32:**1799–1804.
11. **Drumm, B., G. I. Perez-Perez, M. J. Blaser, and P. M. Sherman.** 1990. Intrafamilial clustering of *Helicobacter pylori* infection. N. Engl. J. Med. **322:**359–363.
12. **Dubois, A., N. Fiala, L. M. Heman-Ackah, E. S. Drazek, A. Tarnawski, W. N. Fishbein, G. I. Perez-Perez, and M. J. Blaser.** 1994. Natural gastric infection with *Helicobacter pylori* in monkeys. A model for human infection with spiral bacteria. Gastroenterology **106:**1405–1417.
13. **Dubois, A., N. Fiala, R. H. Weichbrod, G. S. Ward, M. Nix, P. T. Mehlman, D. M. Taub, G. I. Perez-Perez, and M. J. Blaser.** 1995. Seroepizootiology of *H. pylori* gastric infection in socially housed rhesus monkeys. J. Clin. Microbiol. **33:**1492–1495.
14. **Dubois, A., A. Tarnawski, D. G. Newell, N. Fiala, W. Dabros, J. Stachura, H. Krivan, and L. M. Heman-Ackah.** 1991. Gastric injury and invasion of parietal cells by spiral bacteria in rhesus monkeys. Are gastritis and hyperchlorhydria infectious diseases? Gastroenterology **100:**884–891.
15. **Euler, A. R., G. E. Zurenko, J. B. Moe, R. G. Ulrich, and Y. Yagi.** 1990. Evaluation of two monkey species (*Macaca mulatta* and *Macaca fascicularis*) as possible model for human *Helicobacter pylori* disease. J. Clin. Microbiol. **28:**2285–2290.
16. **Fox, J. G., G. Otto, N. S. Taylor, W. Rosenblad, and J. C. Murphy.** 1991. *Helicobacter mustelae*-induced gastritis and elevated gastric pH in the ferret (*Mustela putorius furo*). Infect. Immun. **59:**1875–1880.
17. **Frommer, D. J., J. Carrick, A. Lee, and S. L. Hazell.** 1988. Acute presentation of *Campylobacter pylori* gastritis. Am. J. Gastroenterol. **83:**1168–1171.
18. **Fujioka, T., T. Kubota, R. Shuto, R. Kodama, K. Murakami, K. Perparim, and M. Nasu.** 1994. Establishment of an animal model for chronic gastritis with *Helicobacter pylori*: potential model for long term observation. Eur. J. Gastroenterol. Hepatol. **6**(Suppl. 1):S73–S78.
19. **Gilman, R.** Personal communication.
20. **Handt, L. K., J. O. Fox, F. E. Dewhirst, G. J. Fraser, B. J. Paster, L. L. Yan, H. Rozmiarek, R. Rufo, and I. H. Stalis.** 1994. *Helicobacter pylori* isolated from the domestic cat: public health implications. Infect. Immun. **62:**2367–2374.
21. **Hazell, S. L., J. W. Eichberg, D. R. Lee, L. Alpert, D. G. Evans, D. J. Evans, Jr., and D. Y. Graham.** 1992. Selection of the chimpanzee over the baboon as a model for *Helicobacter pylori* infection. Gastroenterology **103:**848–854.

21a. **Institute of Laboratory Animal Resources, National Research Council.** 1985. Guide for the care and use of laboratory animals. HHS/NIH publication no. 85-23. Department of Health and Human Services, Washington, D.C.

22. **Klein, P. D., R. H. Gilman, R. Leon-Barua, F. Diaz, E. O. Smith, and D. Y. Graham.** 1994. The epidemiology of *Helicobacter pylori* in Peruvian children between 6 and 30 months of age. Am. J. Gastroenterol. **89:**2196–2200.
23. **Krakowka, S., D. R. Morgan, W. G. Kraft, and R. D. Leunk.** 1987. Establishment of gastric *Campylobacter pylori* infection in the neonatal gnotobiotic piglet. Infect. Immun. **55:**2789–2796.
24. **Lee, A., J. G. Fox, G. Otto, and J. Murphy.** 1990. A small animal model of human *Helicobacter pylori* active chronic gastritis. Gastroenterology **99:**1315–1323.
25. **Malaty, H. M., L. Engstrand, N. L. Pedersen, and D. Y. Graham.** 1994. *Helicobacter pylori* infection: genetic and environmental influences. Ann. Intern. Med. **120:**982–986.
26. **Marchetti, M., B. Arico, D. Burroni, N. Figura, R. Rappuoli, and P. Ghiara.** 1995. Development of a mouse model of *Helicobacter pylori* infection that mimics human disease. Science **267:**1655–1658.
27. **Marshall, B. J., J. A. Armstrong, D. B. McGechie, and R. J. Glancy.** 1985. Attempt to fulfill Koch's postulate for pyloric campylobacter. Med. J. Aust. **142:**436–439.
28. **Marshall, B. J., and J. R. Warren.** 1984. Unidentified curved bacilli in the stomach of patients with gastritis and peptic ulceration. Lancet **i:**1311–1315.
29. **Matysiak-Budnik, T., F. Briet, M. Heyman, and F. Mégraud.** 1995. Laboratory-acquired *Helicobacter pylori* infection. Lancet **346:**1489–1490.

30. **McColm, A. A., J. Bagshaw, C. O'Malley, and A. McLaren.** 1995. Development of a mouse model of gastric colonisation with *Helicobacter pylori*. Gut **37**(Suppl. 1):198. (Abstract.)
31. **Mégraud, F., M. P. Brassens-Rabbé, F. Denis, A. Belbuori, and D. Q. Hoa.** 1989. Seroepidemiology of *Campylobacter pylori* infection in various populations. J. Clin. Microbiol. **27:**1870–1873.
32. **Mitchell, H. M., S. L. Hazell, T. Kolesnikow, J. Mitchell, and D. Frommer.** 1996. Antigen recognition during progression from acute to chronic infection with a *cagA*-positive strain of *Helicobacter pylori*. Infect. Immun. **64:**1166–1172.
33. **Mitchell, J. D., H. M. Mitchell, and V. Tobias.** 1992. Acute *Helicobacter pylori* infection in an infant, associated with gastric ulceration and serological evidence of intra-familial transmission. Am. J. Gastroenterol. **87:**382–386.
34. **Miyaji, H., Y. Kohli, T. Azuma, S. Ito, M. Hirai, Y. Ito, T. Kato, and M. Kuriyama.** 1995. Endoscopic cross-infection with *Helicobacter pylori*. Lancet **345:**464.
35. **Morris, A. J., M. R. Ali, G. I. Nicholson, G. I. Perez-Perez, and M. J. Blaser.** 1991. Long term follow-up of voluntary ingestion of *Helicobacter pylori*. Ann. Intern. Med. **114:**662–663.
36. **Natelson, B. J., A. Dubois, and F. J. Sodetz.** 1977. Effect of multiple stress procedures on monkey gastroduodenal mucosa, serum gastrin and hydrogen ion kinetics. Am. J. Digest. Dis. **22:**888–897.
37. **O'Gara, R. W., and R. H. Adamson.** 1972. Spontaneous and induced neoplasms in nonhuman primates, p. 190–238. *In* R. L. Fiennes (ed.), Pathology of human primates, part I. Karger, Basel.
38. **Perez-Perez, G. I., L. Bodhidatta, J. Wongsrichanalai, W. B. Baze, B. E. Dunn, P. D. Etcheverria, and M. J. Blaser.** 1990. Seroprevalence of *Helicobacter pylori* infection in Thailand. J. Infect. Dis. **161:**1237–1241.
39. **Perez-Perez, G. I., B. M. Dworkin, J. E. Chodos, and M. J. Blaser.** 1988. *Campylobacter pylori* antibodies in humans. Ann. Intern. Med. **109:**11–17.
40. **Phillips, M.** 1995. Breathtaking technology for the detection of *Helicobacter pylori*. Am. J. Gastroenterol. **90:**2089–2090.
41. **Riegg, S. J., B. E. Dunn, and M. J. Blaser.** 1995. Microbiology and pathogenesis of *Helicobacter pylori*, p. 535–550. *In* M. J. Blaser, P. D. Smith, J. I. Ravdin, H. B. Greenberg, and R. L. Guerrant (ed.), Infections of the gastrointestinal tract. Raven Press, Ltd., New York.
42. **Shuto, R., T. Fujioka, T. Kubota, and M. Nasu.** 1993. Experimental gastritis induced by *Helicobacter pylori* in Japanese monkeys. Infect. Immun. **61:**933–939.
43. **Takahashi, S., H. Igarashi, N. Ishiyama, M. Nakano, M. Ozaki, M. Ito, N. Masubuchi, S. Saito, T. Aoyagi, I. Yamagishi, et al.** 1993. Serial change of gastric mucosa after challenging with *Helicobacter pylori* in the cynomolgus monkey. Int. J. Med. Microbiol. Virol. Parasitol. Infect. Dis. **280:**51–57.
44. **Thomas, J.** Personal communication.
45. **Tummuru, M. K., T. L. Cover, and M. J. Blaser.** 1993. Cloning and expression of a high-molecular-mass major antigen of *Helicobacter pylori*: evidence of linkage to cytotoxin production. Infect. Immun. **61:**799–809.
46. **Veldhuyzen van Zanten, S., D. Malatjalian, R. Tanton, D. Leddin, R. H. Hunt, W. Blanchard, et al.** 1995. The effect of eradication of *Helicobacter pylori* (HP) on symptoms of non-ulcer dyspepsia (NUD): a randomized double-blind placebo controlled trial. Gastroenterology **108:**A250.

Editor: B. I. Eisenstein

J. RADIAT. RES., 37, 209–215 (1996)

Indomethacin Attenuation of Radiation-Induced Hyperthermia Does Not Modify Radiation-Induced Motor Hypoactivity

JOHN L. FERGUSON, SATHASIVA B. KANDASAMY, ALAN H. HARRIS, HIRSCH D. DAVIS[1] and MICHAEL R. LANDAUER

Armed Forces Radiobiology Research Institute
8901 Wisconsin Avenue, Bethesda, MD 20889–5603, USA

(Received, May 16, 1996)
(Revision received, August 19, 1996)
(Accepted, August 20, 1996)

Ionizing radiation/thermoregulation/prostaglandins/locomotion/rats

Exposure of rats to 5–10 Gy of ionizing radiation produces hyperthermia and reduces motor activity. Previous studies suggested that radiation-induced hyperthermia results from a relatively direct action on the brain and is mediated by prostaglandins. To test the hypothesis that hypoactivity may be, in part, a thermoregulatory response to this elevation in body temperature, adult male rats were given indomethacin (0.0, 0.5, 1.0, and 3.0 mg/kg, intraperitoneally), a blocker of prostaglandin synthesis, and were either irradiated (LINAC 18.6 MeV (nominal) high-energy electrons, 10 Gy at 10 Gy/min, 2.8 μsec pulses at 2 Hz) or sham-irradiated. The locomotor activity of all rats was then measured for 30 min in a photocell monitor for distance traveled and number of vertical movements. Rectal temperatures of irradiated rats administered vehicle only were elevated by 0.9 ± 0.2°C at the beginning and the end of the activity session. Although indomethacin, at the two higher doses tested, attenuated the hyperthermia in irradiated rats by 52–75%, it did not attenuate radiation-induced reductions in motor activity. These results indicate that motor hypoactivity after exposure to 10 Gy of high-energy electrons is not due to elevated body temperature or to the increased synthesis of prostaglandins.

INTRODUCTION

Effects of ionizing radiation over a wide range of doses include lethargy, hypokinesia and impairment of performance on tasks requiring rapid movement[1–6]. Exposures to 5 to 15 Gy from a ^{60}Co gamma-ray source produce hyperthermia in rats[7,8]. There is evidence that this hyperthermia requires head exposure and is mediated by an increased synthesis of prostaglandin E-2 (PGE-2)[7,8]. Also, it was shown that rats reduce their activity level following the induction of deep hyperthermia produced by heat exposure, exertion, or the

Send correspondence to:
Michael R. Landauer, Ph.D.
AFRRI/RPT
8901 Wisconsin Avenue, Bethesda, MD 20889–5603 USA
Telephone: (301) 295–5606; 295–9120; Fax: (301) 295–6552
E-mail address: landauer@vax.afrri.usuhs.mil

[1] Current address is Food and Drug Administration, Division of Antiviral Drug Products, HFD-530 5600 Fishers Lane, Rockville, MD 20857, USA

stress of a novel environment[9,10]. It has been speculated that some behavioral effects induced by drugs (e.g., interleukin-1) could be secondary to the treatment's pyrogenic effects[11]. Our study tested the hypothesis that the reduced motor activity after exposure to ionizing radiation is a thermoregulatory response. Rats were given indomethacin, a prostaglandin synthesis inhibitor, to antagonize the radiation-induced increase in core body temperature.

MATERIALS AND METHODS

Subjects. Adult male Sprague-Dawley Crl:CD(SD)BRD rats weighing 200–300 g (Charles River Breeding Laboratories, Kingston, NY) were used in this experiment. The rats were maintained in our facility, which is approved by the American Association for Accreditation of Laboratory Animal Care. The care, treatment, and use of the rats were approved by our Institutional Animal Care and Use Committee in accordance with the National Research Council's *Guide for the Care and Use of Laboratory Animals.* The rats were quarantined on arrival and screened for evidence of disease. Rats were housed individually in Micro Isolator cages on autoclaved hardwood contact bedding and were given Wayne Rodent Blox and water *ad libitum.* Animal holding rooms were kept at 21 ± 1°C with 50 ± 10% relative humidity on a 12-h light:dark cycle with lights off at 1800. Irradiation, temperature measurement and behavioral testing took place between 1000 and 1400 according to the schedule in Table 1.

Table 1. Time Line for Treatments and Measurements

Minutes preirradiation (–) or postirradiation (+)	Procedure
– 45	Rats placed into holding tubes
– 35	Rectal temperatures recorded
– 30	Indomethacin/vehicle given
– 10	Rectal temperatures recorded
0	Rats irradiated (10 Gy) / sham-irradiated
+ 10	Rectal temperatures recorded
+30 to + 60	Locomotor activity tested
+ 100	Rectal temperatures recorded

Drug administration. Rats were randomly assigned to eight treatment groups. Each group consisted of rats that were irradiated or sham-irradiated and had received an intraperitoneal (i.p.) injection either of the saline vehicle (n = 16) or 0.5, 1.0, or 3.0 mg/kg indomethacin (n = 8). All rats were placed in well-ventilated Plexiglas holding tubes and, 15 min later, were administered vehicle or indomethacin.

Irradiation. Thirty minutes after injection, rats were either whole-body irradiated with high-energy electrons from the AFRRI linear accelerator (LINAC)[12] or sham-irradiated. Irradiated animals received a dose of 10 Gy (nominal 18.6 MeV, 10 Gy/min, 2.8 μ sec pulses at 2 Hz). The 10-Gy dose was chosen because it is in

the midrange for maximal induction of hyperthermia[7]. The indomethacin doses were selected because they reduce, by 50–70%, hyperthermia after a 10-Gy exposure[7].

Temperature measurement. Rectal temperatures were measured 35 and 10 min preirradiation as well as 10 and 100 min postirradiation. Temperatures were measured with thermistor probes (YSI series 700, Yellow Springs Instrument Co., Inc., Yellow Springs, OH) inserted approximately 6 cm into the rectum.

Behavioral testing. Locomotor behavior of each rat was recorded for 30 min beginning 30 min after irradiation or sham-irradiation. A computerized Digiscan Animal Activity Monitor (Model RXYZCM-16, Omnitech Electronics, Columbus, OH) was used to quantify the locomotor activity. The apparatus used an array of infrared photo detectors spaced 2.5 cm apart to determine ambulation expressed as the total distance traveled (cm) and the number of vertical movements. The photocells used to record ambulation and vertical activity were positioned 4.5 cm and 12.5 cm, respectively, above the floor of the Plexiglas activity monitor (40 cm $\times$ 40 cm $\times$ 30 cm).

Statistical Analysis. Temperature, distance-traveled and vertical-activity data were each analyzed with two-way analysis of variance. Where appropriate these were followed by Dunnett's multiple comparison tests. A two-tailed alpha level of at least 0.05 was used.

RESULTS

Rats exposed to 10 Gy of high-energy electrons showed an overall increase in rectal temperatures (0.25 to 0.9°C) when measured 10 and 100 min postirradiation (Fig. 1). Analysis of variance indicated an increase at 10 min ($F(1, 72) = 12.4$, $p < 0.05$) and at 100 min ($F(1, 72) = 14.8$, $p < 0.05$) relative to 10 min preirradiation. Also compared to sham-irradiated controls, irradiated rats showed an overall temperature increase at 10 min ($F(1, 72) = 33.0$, $p < 0.05$) and at 100 min ($F(1, 72) = 37.3$, $p < 0.05$). The Dunnett's multicomparison test indicated that relative to the sham-irradiated group there was a significant increase in rectal temperature in the irradiated group only when given saline or the lowest dose of indomethacin, 0.5 mg/kg (10 min postirradiation: critical value = 2.52, observed statistics = 5.76, 2.96; 100 min postirradiation: critical value = 2.51, observed statistics = 5.77, 2.84).

The prostaglandin synthesis inhibitor indomethacin produced the general effect of reducing radiation-induced hyperthermia at both 10 and 100 min postirradiation ($F(1, 36) = 5.12$, $p < 0.05$; $F(1, 36) = 3.05$, $p < 0.05$, respectively). At 10 min postirradiation, the temperature reductions were significant at 1.0 and 3.0 mg/kg doses of indomethacin (with vehicle-treated, irradiated group as control, critical value = 2.45, observed statistics = 2.97, 3.37) and at 100 min at 3.0 mg/kg indomethacin (observed statistic = 2.64).

Rats exposed to 10 Gy of high-energy electrons showed an overall statistically significant decrease in the number of vertical ($F(1, 72) = 12.32$, $p < 0.001$, Fig. 2) movements and the total distance travelled ($F(1, 72) = 5.36$, $p < 0.05$, Fig. 3) over the 30-min test period.

Analysis of variance indicated no overall effect of drug treatment (indomethacin) on vertical activity (F(3,

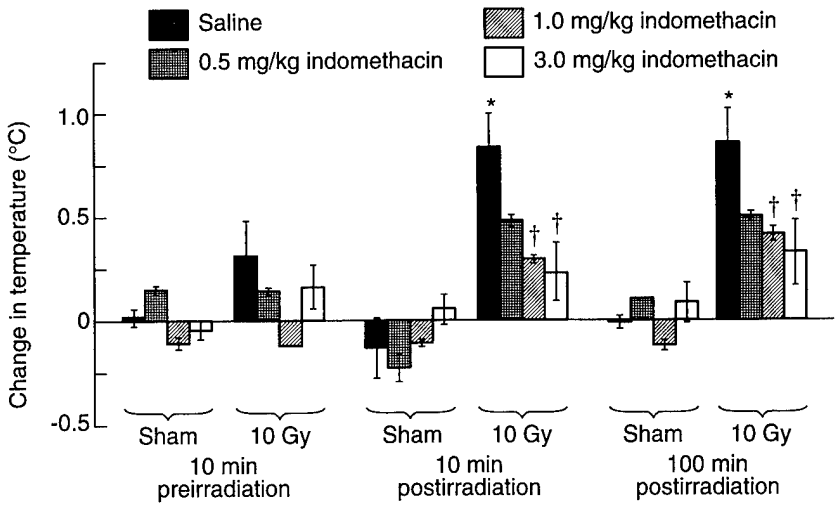

Fig. 1. Change in rectal temperature from pretreatment baseline (–35 min). For sham-irradiated group, n = 8 rats for each dose of indomethacin, n = 16 for saline control. For irradiated group, n = 8 rats for each dose, n = 16 for saline control. * indicates significant difference ($p < 0.05$) from saline-treated, sham-irradiated group (Dunnett's test). † indicates significant difference ($p < .05$) from saline-treated, irradiated group (Dunnett's test).

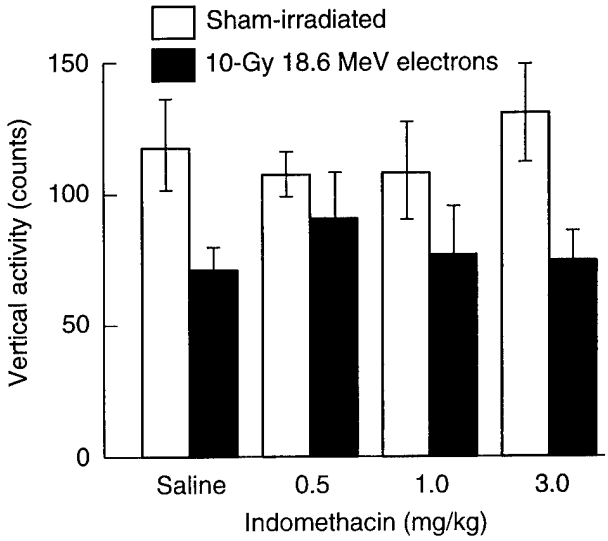

Fig. 2. Number of vertical movements in the 30-min observation period versus dose of indomethacin. Although analysis of variance indicated an overall radiation effect on vertical activity, indomethacin had no effect on this activity measure.

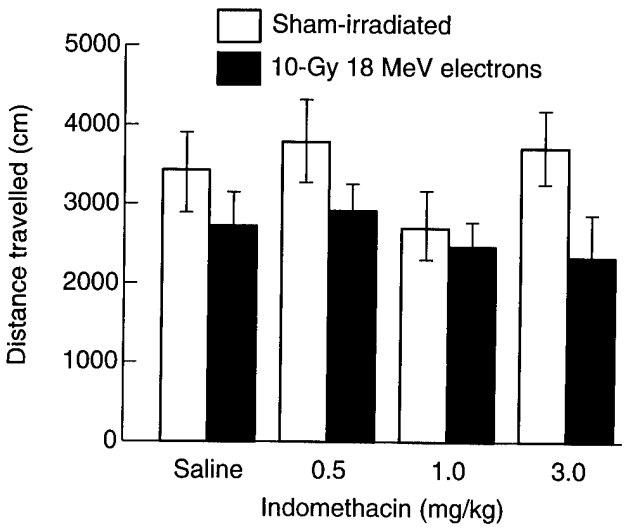

Fig. 3. Total distance travelled in the 30-min observation period versus dose of indomethacin. Although analysis of variance indicated an overall radiation effect on distance travelled, indomethacin had no effect on this activity measure.

72) = 0.175, $P = 0.91$) and distance traveled ($F(3, 72) = 0.76$, $P = 0.52$).

DISCUSSION

Exposure of rats to 10 Gy of high-energy electrons increased postirradiation rectal temperature by 0.9 ± 0.2°C. In addition, postirradiation spontaneous motor activity was reduced by 18–40% in the 30-min observation period. Although indomethacin (1.0 or 3.0 mg/kg) attenuated the radiation-induced increase in body temperature by 52–75%, the depression of motor activity was unaffected by indomethacin. These results do not support the hypothesis that reduced motor activity after irradiation is a behavioral thermoregulatory response to the radiation-induced hyperthermia.

Ionizing radiation (5–10 Gy from a ^{60}Co gamma-ray source) has been reported to increase levels of E-series prostaglandins (PGEs) in the brain[8,13]. We did not measure PGE levels because it has previously been shown that indomethacin at the highest dose given in this study (3 mg/kg) gives nearly maximal (80–90%) inhibition of brain PG synthesis[14]. PGEs have been found to reduce open-field spontaneous motor activity in rodents[15,16]. Our finding that the prostaglandin synthesis inhibitor indomethacin has no effect on the radiation-induced hypoactivity, indicates that prostaglandin synthesis does not play a role in this hypoactivity. This result parallels the report that lipopolysaccharide-induced depression of motor activity is also prostaglandin independent[17].

It is well established that ionizing radiation induces cytokines including IL-1 and INF-α[18–21]. Both these cytokines elevate body temperature and these elevations are reduced by indomethacin[22,23]. Although both cytokines also reduce open field locomotion, the IL-1-induced decrease is attenuated by indomethacin[11]

while the INF-α-induced decrease is not attenuated by even high doses of indomethacin[18,24,25]. It is therefore possible that INF-α may play a role in the failure of indomethacin to block decreases in motor activity following exposure to ionizing radiation. Further support for this possibility is that INF-α shows specific opiate-like activities[26,27], and central opioid functions have already been found to mediate opioid-like behavioral changes following radiation exposure[28,29]. Work is in progress to further determine the mechanism of radiation-induced motor hypoactivity.

ACKNOWLEDGEMENTS

The authors thank Mr. Tom Dalton and Ms Sherrie Stevens-Blakely for technical assistance, Mr. William Jackson for statistical advice and Ms Donna K. Solyan for editorial advice. This research was supported by the Armed Forces Radiobiology Research Institute.

REFERENCES

1. Kimeldorf, D. J. and Hunt, E. L. (1965) In "Ionizing Radiation: Neural Function and Behavior", Eds. D. J. Kimeldorf and E. L. Hunt, p 185, Academic Press, New York.
2. Jones, D. C., Kimeldorf, D. J., Rubadeau, D. O., Osborn, G. K. and Castanera, T. J. (1954) Effect of x-irradiation on performance of volitional activity by the adult male rat. Am. J. Physiol. **177**: 243–250.
3. Mickley, G. A. and Teitelbaum, H. (1978) Persistence of lateral hypothalamic-mediated behaviors after a supralethal dose of ionizing radiation. Aviat. Space Environ. **4**: 868–873.
4. Landauer, M. R., Davis, H. D., Dominitz, J. A. and Weiss, J. F. (1988) Long-term effects of radioprotector WR-2721 on locomotor activity and body weight of mice following exposure to ionizing radiation. Toxicol. **49**: 315–323.
5. Bogo, V., Franz, C. B., Jacobs, A. J., Weiss, J. F. and Young, R. W. (1988) Effects of ethiofos (WR-2721) and radiation on monkey visual discrimination performance. Pharmacol. Therap. **39**: 93–95.
6. Minamisawa, T. and Hirokaga, K. (1995) Long term effects of prenatal exposure to low level gamma rays on spontaneous circadian motor activity of male mice. J. Radiat. Res. **36**: 179–184.
7. Kandasamy, S. B. and Hunt, W. A. (1990) Involvement of prostaglandins and histamine in radiation-induced temperature responses in rats. Radiat. Res. **121**: 84–90.
8. Kandasamy, S. B., Dalton, T. K. and Hunt, W. A. (1990) Ionizing radiation-induced hyperthermia: Implication of a protein mediator. Transact Am. Soc. Neurochem. **21**: 106.
9. Roberts, W. W. (1988) Differential thermosensor control of thermoregulatory grooming, locomotion, and relaxed postural extension. Ann. N. Y. Acad. Sci. **525**: 363–374.
10. Long, N. C., Vander, A. J., Kunkel, S. L. and Kluger, M. J. (1990) Antiserum against tumor necrosis factor increases stress hyperthermia in rats. Am. J. Physiol. **258**: R591–R595.
11. Crestani, F., Seguy, F., and Dantzer, R. (1991) Behavioral effects of peripherally injected interleukin-1: role of prostaglandins. Brain Res. **542**: 330–335.
12. Gee, M. T. (1984) LINAC facility at Armed Forces Radiobiology Research Institute. Technical Report TR84-3, Armed Forces Radiobiology Research Institute, Bethesda, Maryland.
13. Pausecu, E., Chirvasie, R., Teodosiu, T. and Paun, C. (1976) Effects of ^{60}Co gamma-radiation on the hepatic and cerebral levels of some prostaglandins. Rad. Res. **65**: 163–171.
14. Abdel-Halim, M. S., Sjoquist, B. and Anggard, E. (1978) Inhibition of prostaglandin synthesis in rat brain. Acta Pharmacol. et Toxicol. **43**: 266–272.

15. Landauer, M. R., Davis, H. D., Kumar, K. S. and Weiss, J. F. (1992) Behavioral toxicity of selected radioprotectors. Adv. Space Res. **12**: 273–283.
16. Weiner, M., and Olson, J. W. (1975) Comparative behavioral effects of dibutryl cyclic AMP and prostaglandin E1 in mice. Prostaglandins **9**: 927–943.
17. Kozak, W., Conn, C. A. and Kluger, M. J. (1994) Lipopolysaccharide induces fever and depresses locomotor activity in unrestrained mice. Am. J. Physiol. **266**: R125–R135.
18. Crnic, L. S., and Segall, M. A. (1992) Prostaglandins do not mediate interferon-α effects on mouse behavior. Physiol. Behav. **51**: 349–352.
19. Woloschak, G. E., Chang-Liu, C. M., Jones, P. S. and Jones, C. A. (1990) Modulation of gene expression in Syrian hamster embryo cells following ionizing radiation. Cancer Res. **50**: 339–344.
20. Weichselbaum, R. R., Hallahan, D. E., Sukhatme, V., Dritschilo, A., Sherman, M. L., and Kufe, D. W. (1991) Biological consequences of gene regulation after ionizing radiation exposure. J. Nat. Cancer Inst. **83**: 480–484.
21. Ishihara, H., Tsuneoka, K., Dimchev, A. B. and Shikita, M. (1993) Induction of the expression of the interleukin-1β gene in mouse spleen by ionizing radiation. Radiat. Res. **133**: 321–326.
22. Clark, W. G. and Cumby, H. R. (1975) The antipyretic effect of indomethacin. J. Physiol. **248**: 625–638.
23. Blatteis, C. M., Xin, L. and Quan, N. (1991) Neuromodulation of fever: Apparent involvement of opioids. Br. Res. Bull. **26**: 219–223.
24. Miller R. L., Steis, R. G., Clark, J. W., Smith J. W., II, Crum, E., McKnight, J. E., Hawkins, M. J., Jones, J. D., Longo, J. D. and Urba, W. J. (1989) Randomized trial of recombinant α2b-interferon with or without indomethacin in patients with metastatic malignant melanoma. Cancer Res. **49**: 1871–1876.
25. Quesada, J. R., Talpaz, M., Rios, A., Kurzrock, R. and Gutterman, J. U. (1986) Clinical toxicity of interferons in cancer patients: A review. J.Clin. Oncol. **4**: 234–243.
26. Mannering, G. J. and Deloria, L. B. (1986) The pharmacology and toxicology of the interferons: An overview. Ann. Rev. Pharmacol. Toxicol. **26**: 455–515.
27. Dafny, N., Lee, J. R. and Dougherty, P. M. (1988) Immune response products alter CNS activity: Interferon modulates central opioid functions. J. Neurosci. Res. **19**: 130–139.
28. Mickley, G. A., Stevens, K. E., White, G. A. and Gibbs, G. L. (1983) Endogenous opiates mediate radiogenic behavioral change. Science **220**: 1185–1186.
29. Teskey, G. C. and Kavaliers, M. (1984) Ionizing radiation induces opioid-mediated analgesia in male mice. Life Sci. **35**: 1547–1552.

In: Proceedings of the 1995 ERDEC Scientific Conference on Chemical and Biological Defense Research. Berg DA (ed). Research and Technology Directorate, U.S. Army Chemical and Biological Defense Command, ERDEC-SP-043, July 1996

ARMED FORCES RADIOBIOLOGY RESEARCH INSTITUTE
SCIENTIFIC REPORT
SR96-9

BEHAVIORAL TOXICITY AND RADIOPROTECTIVE EFFICACY OF WR-151327 IN COMBINATION WITH ADENOSINE RECEPTOR ANTAGONISTS

Michael R. Landauer, John B. Hogan, Carl A. Castro,
Kimberly A. Benson, Christina W. Shehata, and Joseph F. Weiss

Armed Forces Radiobiology Research Institute
Bethesda, MD 20889-5603

ABSTRACT

Caffeine has been demonstrated to mitigate the locomotor decrement produced by aminothiol radioprotective compounds. A possible mechanism of action is caffeine's antagonism through the adenosine system. This study compared the behavioral effects of xanthine adenosine antagonists that either are nonselective (theophylline, caffeine), exhibit very weak antagonism (enprofylline), are selective for A_1 receptors (8-cyclopentyl-1,3-dimethylxanthine, CPT), or are selective for A_2 receptors (3,7-dimethyl-1-propylargylxanthine, DMPX). Locomotor activity was significantly reduced after injection of the phosphorothioate radioprotector WR-151327 (200 mg/kg, i.p.). Activity returned to control levels when caffeine (20 mg/kg), theophylline (20 mg/kg), or DMPX (20 mg/kg) were administered 30 min before WR-151327. Enprofylline (20 and 40 mg/kg) and CPT (20 and 40 mg/kg) did not mitigate the WR-151327 induced locomotor decrement. These results suggest that antagonism of the A_2 adenosine receptors is important in the mitigation of motor decrement. There was a trend for the adenosine antagonists to enhance the radioprotective effect (30-day survival) of WR-151327. The best protection from ^{60}Co (1 Gy/min) radiation was obtained by the theophylline plus WR-151327 combination, which significantly enhanced the dose reduction factor (DRF). The combination produced a DRF of 1.64 compared with 1.51 for WR-151327 alone.

INTRODUCTION

A number of phosphorothioate compounds such as WR-151327 (*S*-3-[3-methylaminopropylamino]propylphosphorothioic) can protect normal tissue from damage due to chemotherapy or radiation therapy. WR-151327 has been shown to protect against acute[1] and late[2,3] effects of both gamma and neutron radiation as well as toxic effects of nitrogen

mustard.[4] One of the principal problems associated with the use of phosphorothioate protectors in humans is their adverse side effects such as hypotension, vomiting, and somnolence, which lead to performance degradation.[5]

One approach to this problem is to develop combinations of drugs that maximize radioprotection and minimize side effects.[6] Using this paradigm, we found that caffeine was effective in mitigating the motor performance decrement produced by the phosphorothioate WR-3689.[7] The mechanism by which caffeine reduced this behavioral deficit may be mediated through the adenosine system.

Among the xanthines, caffeine and theophylline are nonspecific A_1 and A_2 antagonists of the adenosine system.[8] Enprofylline has very low affinity to both of the adenosine receptors. CPT (8-cyclopentyl-1,3-dimethylxanthine) is a selective A_1 adenosine receptor antagonist[9] while DMPX (3,7-dimethyl-1-propargylxanthine) is an adenosine antagonist selective for the A_2 receptor.[10] In the present study, WR-151327 was combined with the above xanthines to characterize any effects on radioprotection as well as the contributions of the A_1 and A_2 adenosine receptor subtypes in the mitigation of locomotor deficits produced by this phosphorothioate compound.

METHOD

Subjects

Locomotor activity and survival were measured in 24- to 31-g male CD2F1 mice (BALB/c x DBA/2)F1, provided by Charles River Breeding Laboratory, Raleigh, NC. All mice were quarantined on arrival and representative animals were screened for evidence of disease. Mice were housed in groups of 10 in Microisolator cages (Lab Products, Maywood, NJ) on hardwood chip contact bedding in a facility approved by the American Association for Accreditation of Laboratory Animal Care. Animal rooms were maintained at 21 ± 2 °C with 50% ± 10% humidity on a 12-hr light/dark cycle. Commercial rodent chow was freely available as was acidified (pH 2.5) water to control opportunistic infections.[11]

Behavioral Testing

Computerized Digiscan activity monitors (Omnitech Electronics, Columbus, OH) were used to quantify locomotor activity. Each monitor used an array of infrared photodetectors spaced 2.5 cm apart to determine horizontal locomotor activity, which was expressed as the total distance traveled. Immediately following all injections, mice were placed into individual Plexiglas activity chambers (20 x 20 x 30 cm). Activity was monitored for 3 hr. All testing took place during the dark portion of the light/dark cycle. Each animal was tested only once. Food and water were available throughout the testing period.

Radioprotection Experiments

Survival was assessed after irradiation in the bilateral gamma-radiation field of the AFRRI ^{60}Co facility.[12] The mice were confined in a Plexiglas restrainer to limit movement. The midline tissue dose to the animals ranged from 7 to 16 Gy and was delivered at a dose rate of 1 Gy/min. The dose rate was established in an acrylic mouse phantom using a 0.5-cc tissue-equivalent ionization chamber (calibration factor traceable to the National Institute of Standards and Technology). The tissue-air ratio was 0.96 and the field was uniform to within ±3%. Dosimetric measurements were made in accordance with the American Association of Physicists in Medicine protocol for the determination of absorbed dose from high-energy photon and electron beams.[13]

Mice were injected with either saline or adenosine antagonists 60 min before irradiation. WR-151327 was injected 30 min before irradiation. Following irradiation, mice were returned to their home cages where survival was monitored for 30 days. For each treatment at any given dose of radiation, the number of mice per group averaged 24. A dose reduction factor (DRF) was determined for each drug regimen by dividing the $LD_{50/30}$ following drug treatment by the $LD_{50/30}$ for saline-treated animals.

Drugs

All drugs were administered i.p. Caffeine (20 mg/kg), theophylline (20 mg/kg), enprofylline (20 mg/kg), DMPX (20 mg/kg) and CPT (20 and 40 mg/kg) were each administered 30-min prior to the radioprotector WR-151327 (200 mg/kg; U.S. Bioscience, West Conshohocken, PA). Enprofylline and CPT (20 mg/kg) were not evaluated in the radioprotection experiments because they did not mitigate WR-151327 induced locomotor decrement in the behavioral experiments.

Statistical Analysis

Locomotor activity data were log transformed to stabilize the variances. An analysis of variance and the Newman-Keuls multiple range test was used to statistically analyze the data. Thirty-day survival was analyzed by probit analysis.

RESULTS AND CONCLUSIONS

WR-151327 (200 mg/kg) produced significant locomotor decrements throughout the 3-hr testing period. A single administration of nonspecific adenosine antagonists (caffeine or theophylline) returned WR-151327 induced locomotor decrements to control levels for 2 hr and 1 hr, respectively. A very weak adenosine antagonist (enprofylline) did not mitigate WR-151327 induced locomotor decrement, indicating that methylxanthines with strong

adenosine antagonism are important for the reversal of WR-151327 induced locomotor activity. A specific A_2 adenosine receptor antagonist (DMPX) returned WR-151327 induced locomotor deficits to control levels for 1 hr. In contrast, an A_1 adenosine receptor antagonist (CPT) failed to mitigate this motor decrement. These results indicate that A_2 adenosine receptor antagonism plays an important role in reversing locomotor deficits produced by the radioprotector WR-151327. In addition, all adenosine receptor antagonists enhanced 30-day survival when combined with WR-151327 (Table 1). The best protection was obtained when theophylline was combined with WR-151327. The combination yielded a significantly higher DRF (1.64) compared to the DRF (1.51) produced by WR-151327 alone.

TABLE 1

Radioprotection by WR-151327 Alone and in Combination with Xanthines[1]

Treatment[2]	$LD_{50/30}$ (Gy^3) (95% Confidence Limits)	DRF
Saline	8.30 (8.16, 8.56)	–
Saline + WR-151327[4]	12.57 (12.44, 12.71)	1.51
Caffeine + WR-151327	12.75 (12.57, 12.97)	1.54
DMPX + WR-151327	13.12* (12.80, 13.67)	1.58
CPT + WR-151327	13.26** (12.94, 14.03)	1.60
Theophylline + WR-151327	13.62** (13.18, 14.77)	1.64

[1] Xanthines were given i.p. 60 min before radiation; WR-151327 was given i.p. 30 min before radiation.

[2] WR-151327 (200 mg/kg); caffeine (20 mg/kg); DMPX = 3,7 dimethyl-1-propargylxantine (20 mg/kg), CPT = 8-cyclopentyl-theophylline (40 mg/kg), theophylline (20 mg/kg).

[3] ^{60}Co @ 1 Gy/min.

[4] All WR-151327 groups significantly different ($p < 0.001$) from saline control.

* Significantly different ($p < 0.01$ from saline/WR-151327.

** Significantly different ($p < 0.001$) from saline/WR-151327.

ACKNOWLEDGEMENTS

We thank William E. Jackson III for statistical advice, Donna K. Solyan for editorial assistance, and Carolyn Wooden for layout support. The research was supported in part by a grant administered through the Department of Defense/Department of Veterans Affairs Cooperative Research Program. Research was conducted according to the principles enunciated in the Guide for the Care and Use of Laboratory Animal Resources, National Research Council.

REFERENCES

1. Ledney, G.D., Elliott, T.B., Landauer, M.R., Henderson, P.L., Harding, R.A. and Tom, S.P. (1994) Survival of irradiated mice treated with WR-151327, synthetic trehalose dicorynomycolate, or ofloxacin. Adv. Space Research, 14:583-586.

2. Grdina, D.J., Wright, B.J. and Carnes, B.A. (1991) Protection of WR-151327 against late-effects damage from fission-spectrum neutrons. Radiat. Res., 128:S124-S127.

3. Matsushita, S., Ando, K., Koike, S., Grdina, D.J. and Furukawa, S. (1994) Radioprotection by WR-151327 against late normal tissue damage in mouse hind legs from gamma ray radiation. Int. J. Radiat. Oncol. Biol. Phys., 30:867-872.

4. Green, D., Bensely, D. and Schien, P. (1994) Preclinical evaluation of WR-151327: An orally active chemotherapy protector. Cancer Res., 54:738-741.

5. Kligerman, M.M., Turrisi, A.T., Urtasun, R.C., Norfleet, A.L., Phillips, T.L., Barkley, T. and Rubin, T. (1988) Final report on phase I trial of WR-2721 before protracted radiation therapy. Int. J. Radiat. Oncol. Biol. Phys., 14:1119-1122.

6. Weiss, J. F., Kumar, K. S., Walden, T. L., Neta, R., Landauer, M. R. and Clark, E.P. (1990). Advances in radioprotection through the use of combined agent regimens. Int. J. Radiat. Biol., 57:709-722.

7. Landauer, M.R., Davis, H.D., Kumar, K.S. and Weiss, J.F. (1992) Behavioral toxicity of selected radioprotectors. Adv. Space Research, 12:273-283.

8. Rall, T.W. (1990) Drugs used in the treatment of asthma. In: *The Pharmacological Basis of Therapeutics.* A.F. Gilman, T.W. Rall, A.S. Nies and P. Taylor (eds). New York: Pergamon Press, pp. 618-637.

9. Nikodijevic, O., Daly, J. W. and Jacobson, K. A. (1990) Characterization of the locomotor depression produced by an A2-selective adenosine agonist. FEBS Lett., 261:67-70.

10. Seale, T. W., Abla, K. A., Shamin, M. T., Carney, J. M. and Daly, J. W. (1988). 3,7-dimethyl-1-propargylxanthine: A potent and selective *in vivo* antagonist of adenosine analogs. Life Sci., 43:1671-1684.

11. McPherson, C.W. (1963) Reduction of *Pseudomonas aeruginosa* and coliform bacteria in mouse drinking water following treatment with hydrochloric acid or chlorine. Lab Animal Care, 13:737-744.

12. Carter, R.E. and Verrelli, D.M. (1973) AFRRI cobalt whole-body irradiation. Technical Report 73-3, Armed Forces Radiobiology Research Institute, Bethesda, MD.

13. American Association of Physicists in Medicine (AAPM Task Group 21) (1983) Protocol for the determination of absorbed dose from high-energy photon electron beams. Med. Phys., 10:741-771.

ELSEVIER

Journal of Pharmaceutical and Biomedical Analysis
14 (1996) 317–324

JOURNAL OF
PHARMACEUTICAL
AND BIOMEDICAL
ANALYSIS

Chromatographic and mass spectral analysis of the radioprotector and chemoprotector *S*-3-(3-methylaminopropylamino)propanethiol (WR-151326) and its symmetrical disulfide (WR-25595501)

Yashesh N. Vaishnav *, James A. Pendergrass, Jr., Edward P. Clark, Charles E. Swenberg

Radiation Biochemistry Department, Armed Forces Radiobiology Research Institute, 8901 Wisconsin Avenue, Bethesda, MD 20889-5603, USA

Received for review 21 March 1995

Abstract

Metabolically active forms of the radioprotective and chemoprotective drug *S*-3-(3-methylaminopropylamino)propylphosphorothioic acid (WR-151327) are *S*-3-(3-methylaminopropylamino)propanethiol (WR-151326) and its symmetrical disulfide (WR-25595501). This paper describes applications of sensitive and specific procedures such as capillary column gas chromatography with flame ionization detection, electron impact mass spectrometry and liquid chromatography with electrochemical detection for structural characterization and analysis of the active forms of WR-151327. These chromatographic procedures provide reproducible linear calibration graphs for a relatively wide range of concentrations of the active forms of WR-151327. The described procedures will further facilitate in vivo and in vitro investigations of chemoprotective and radioprotective properties of WR-151327 and its active metabolites.

Keywords: Radioprotector; Chemoprotector; Aminothiols; Symmetrical disulfides; Mass spectral analysis; Electrochemical detection

1. Introduction

The use of chemical agents such as cysteine for protection against acute effects of irradiation was first investigated in the late 1940s by Patt et al. [1]. In 1959, the US Army initiated an antiradiation drug development program at the Walter Reed Army Institute of Research (WRAIR) [2]. In this program, phosphorylated aminothiols, or phosphorothioates, were developed.

Recently, antimutagenic and antineoplastic properties for this class of chemical agents have been observed [3,4] and the ability of these compounds to enhance the interaction of topoisomerases with DNA has been reported [5]. The active forms of the phosphorothioates are the free

* Corresponding author.

SSDI 0731-7085(95)01602-3

thiol and its symmetrical disulfide [6] (see Table 1). The dephosphorylation of the phosphorothioate compounds has been shown to occur in vivo and in vitro in the presence of the enzyme alkaline phosphatase [7,8] or mineral acids[9]. In the presence of oxygen and trace metal ions, these thiols can be further oxidized to form their corresponding symmetrical disulfides [10].

WR-2721 and its dephosphorylated form WR-1065 remain the benchmark radioprotectors; however, WR-151326, the dephosphorylated form of WR-151327 appears to be equally or more effective not only against higher linear energy transfer (LET) radiation [11] but also as a combination drug against the anti-AIDS agent AZT (3′-azido-3′-deoxythymidine) [12]. AZT is known to be mutagenic in the human hepatoma cell line designated HepG2 at the HGPRT (hypoxanthine guanine phosphoribose transferase) locus. Administration of WR-151326 with AZT reduces the mutagenic effects of AZT by approximately half [12].

To understand fully the protection mechanisms and therapeutically utilize these drugs with greater effectiveness, for in vivo or in vitro experiments, a rapid, selective and sensitive procedure for their analysis must be available. To the best of the authors' knowledge, such procedures for WR-151326 and WR-25595501 have not been documented. In this paper, we describe gas chromatography (GC), liquid chromatography with electrochemical detection (LC–EC) and mass spectrometry (MS) for the analysis and structural characterization of the active metabolites of WR-151327.

Table 1
Chemical names and structures of aminothiol compounds and their derivatives

Compound	Name and structure
WR-2721	*S*-2-(3-Aminopropylamino)ethylphosphorothioic acid $H_2NCH_2CH_2CH_2NHCH_2CH_2SPO_3H_2$
WR-1065	*N*-(2-Mercaptoethyl)-1,3-diaminopropane $H_2NCH_2CH_2CH_2NHCH_2CH_2SH$
WR-33278	Symmetrical disulfide of WR-1065 $H_2N(CH_2)_3NH(CH_2)_2SS(CH_2)_2NH(CH_2)_3NH_2$
WR-151327	*S*-3-(3-Methylaminopropylamino)propolyphosphorothioic acid $CH_3NH(CH_2)_3NH(CH_2)_3SPO_3H_2$
WR-151326	*S*-3-(3-Methylaminopropylamino)-propanethiol $CH_3NH(CH_2)_3NH(CH_2)_3SH$
WR-25595501	Symmetrical disulfide of WR-151326 $CH_3NH(CH_2)_3NH(CH_2)_3SS(CH_2)_3NH(CH_2)_3NHCH_3$

2. Experimental

2.1. Reagents and materials

All reagents were of analytical-reagent grade. Acetonitrile, methylene chloride and methanol were obtained from Fisher Scientific (Pittsburgh, PA, USA). WR-151327 (Lot #1, USBR 110) was received from the US Bioscience Laboratory (West Conshohocken, PA, USA) and authentic samples of WR-151326 (bottle #AV58457) and WR-25595501 (bottle #24307) were received from the Walter Reed Army Research Institute (Washington, DC, USA).

2.2. Synthesis, GC and MS analysis of WR-151326

In a 100 ml, two-necked, round-bottomed flask with an argon inlet and reflux condenser, 1.62 g of recrystallized WR-151327 was placed in 10 ml of 2.5 mM HCl (60°C, pH 1.5) under a constant stream of argon. To monitor the progress of the hydrolysis reaction, 10 μl aliquots from the reaction mixture were withdrawn at 30-min intervals. Each sample was quenched at room temperature in 1.8 ml of 50 mM phosphate buffer (pH 7.0) and assayed for the presence of sulfhydryl group with 5′,5′-dithiobis(2-nitrobenzoic acid) (DTNB) using the Ellman methodology [13]. The hydrolysis reaction was allowed to proceed at 65°C until no increases in the DTNB absorption assays were observed. The reaction mixture was stirred for an additional 3 h at room temperature to assure complete hydrolysis of WR-151327, after which the pH was re-adjusted to 1.5 and the mixture was lyophilized. The lyophilate was extracted three times with 10 ml of cold, degassed methylene

chloride followed by four extractions with 10 ml of chloroform. The solid residue was subsequently dissolved in a minimal quantity (<3 ml) of cold, degassed ethanol/water (9:1, v/v) and allowed to crystallize at 4°C overnight. The crystalline product was collected (1.1 g, >67% yield).

Trimethylsilyl (TMS) ether preparation was then carried out for the aliquots from the following samples: (1) lyophilate of the reaction mixture; (2) residue from the methylene chloride extract; (3) crystalline product obtained from ethanol–water recrystallization; and (4) authentic sample of WR-151326. The TMS derivatives were prepared in hypovials by first dissolving 25 μg of the material in 30 μl of warm acetonitrile and subsequently mixing this with 30 μl of bis(trimethylsilyl)trifluoroacetamide (BSTFA). The resulting mixtures were heated at 60°C for 1 h and then allowed to equilibrate at room temperature for an additional 1 h prior to GC analysis. Each TMS preparation was subsequently analyzed on a Varian 3700 gas chromatograph (Varian Associates, Sunnyvale, CA, USA) in flame ionization detection mode using a fused-silica capillary column (25 m × 0.32 mm i.d.) coated with 5% cross-linked phenylmethylsilicone gum phase in the split mode (1:10) and using helium as the carrier gas. The column oven temperature was programmed from 90 to 170°C, 5°C min^{-1}.

MS of the above-mentioned TMS samples and their corresponding underivatized samples was carried out using a Kratos 25RFA analytical mass spectrometer (Kratos Analytical, Manchester, UK) in a direct insertion probe/electron impact (DIP/EI) MS mode at 70 eV and a source temperature of 260°C.

2.3. Synthesis, GC and MS analysis of WR-25595501

WR-25595501 was synthesized from WR-151326 using both iodine-induced and metal ion-catalyzed oxidations.

2.4. Iodine-induced oxidation

In a 25 ml round-bottomed flask, a sample of WR-151326 (0.81 g) was gradually dissolved in cold 10% NaOH. To the resulting solution, 1.1 g of iodine crystals were added over a 60 min period while the reaction mixture was stirred at 4°C. The progress of the oxidation reaction was monitored by the withdrawal of 10-μl aliquots from the reaction mixture at regular intervals. Each sample was assayed for the sulfhydryl group by the DTNB method as noted above [13]. When all of the sulfhydryl groups had been consumed, the reaction mixture was lyophilized and the residue extracted twice with 20 ml of warm (37°C) acetonitrile. The acetonitrile extracts were combined and allowed to stand overnight at room temperature to crystallize the product. Crude crystalline product was collected and recrystallized in a minimal quantity of acetonitrile/water (1:1, v/v). An approximate yield of 30% was observed after further recrystallization from methanol/water (9:1, v/v).

2.5. Metal ion-catalyzed oxidation

The freshly recrystallized WR-151326 (0.81 g) was dissolved in 4.0 ml of 2 μM copper(II) sulfate and the pH of the solution was adjusted to 9.0. The solution was then saturated with oxygen gas and allowed to stand at room temperature for 48 h or until all of the free sulfhydryls were consumed. The reaction mixture was lyophilized and the residue was washed with 5 ml of cold methanol and extracted three times with 10 ml of chloroform. The chloroform extracts were combined and the chloroform evaporated under nitrogen. The residue was then recrystallized in a minimal quantity of methanol. An approximately 60% yield of the purified product was observed. The product and its authentic sample, WR-25595501, were transformed into their corresponding TMS derivatives and analyzed on a Varian GC and the observed retention times (RT) were compared. MS analysis of the derivatized and underivatized product was also performed in the DIP/EI mode to confirm the identity of the product.

2.6. GC analysis of a mixture of WR-151326 and WR-25595501

Equimolar mixtures of WR-151326 and WR-25595501 (5, 50, 100, 250, 500 and 1000 pmol)

were treated with BSTFA and transformed into their corresponding TMS derivatives. The TMS preparations were analyzed on a GC and calibration graphs for both the compounds were determined by peak integration of the corresponding GC peak area as a function of concentration.

2.7. LC–EC analysis of WR-151326 and WR-25595501

Sample purity determination and analysis of the synthesized WR-151326 and WR-25595501 compounds were performed using LC–EC on a BAS 200A chromatograph (Bioanalytical Systems, West Lafayett, IN, USA). Analysis was performed at room temperature with a 100 × 4.6 mm i.d., 5 μm, reversed-phase SynChropak^{R} SCD-100 column (SynChrom, West Lafayette, IN, USA) and a dual Hg/Au amalgam electrode. The mobile phase consisted of 100 mM monochloroacetic acid (pH 2.97) and was run at a flow rate of 1 ml min^{-1}. The downstream, working electrode potential was fixed at +150 mV while the potential of the upstream, "generator" electrode, was set at −1 V. (Disulfides are reduced at the upstream electrode, generating thiols for detection downstream.) The sensitivity of the working electrode was set at 500 nA full-scale. The helium sparge exhaust vent on the LC was fitted with a short length of PEEK^{R} microbore tubing and was used to degas all samples for at least 5 min before injection. Standards (10 mM) were prepared in 50 mM perchloric acid from the authentic samples of WR-151326 and WR-25595501 and subsequently diluted with mobile phase to achieve the desired concentrations. Calibration graphs ranging between 39 and 2500 pmol (injected) were generated. Injections (20 μl) were made using a Rheodyne Model 7725I syringe-loading injector (Rheodyne, Cotati, CA, USA) equipped with a 100 μl sample loop. Chromatographic analysis was performed using Chrom Perfect Direct (Justice Innovations, Palo Alto, CA, USA) installed on a personal computer. The analysis of each of the synthesized compound's chromatograms for their RT and redox state as compared with those of the corresponding authentic sample was used as a qualitative measure of each synthetic compound's purity. The slope and correlation coefficients were determined by linear regression analysis.

3. Results and discussion

For proper usage and pharmacological or toxicological studies, it is often necessary to assess the drug (or its metabolites) for various reasons, including stability of the drug and the presence of impurities or decomposition products. As the first step towards the methods development for the analysis of WR-151326 and WR-25595501, it was necessary to synthesize, isolate and purify these drugs. Both these active forms are known; however, neither is commercially available. To the best of the authors' knowledge, specific protocols for their preparation also have not been published. Therefore, although the primary focus of this report is at the analysis of the drugs, some necessary background details regarding the synthetic and purification procedures for these drugs are also provided.

Synthesis of WR-151326 was accomplished by acid hydrolysis of WR-151327. The product, in turn, was oxidized to WR-25595501 under relatively mild oxidation conditions. GC and LC–EC in conjunction with DIP/EI/MS methodologies were utilized to identify, characterize the chemical structures and analyze the purity of the synthesized compounds. For the GC and MS analyses, both synthetic and authentic samples of WR-151326 and WR-25595501 were transformed into their corresponding TMS derivatives [14,15] (to decrease their polarity and increase their volatility and thermal stability). In addition, aliquots from the crude lyophilate and residue from its methylene chloride extracts were individually transformed into their corresponding TMS derivatives in order to identify all products from the acid hydrolysis of WR-151327.

Fig. 1 shows the gas chromatograms of the above-mentioned TMS preparations, in which a represents the solvent front, b the TMS derivative of phosphoric acid, c the TMS derivative of WR-151326 and d the TMS derivative of WR-25595501. The identities of b, c and d were made by comparison of their GC RTs with those of the

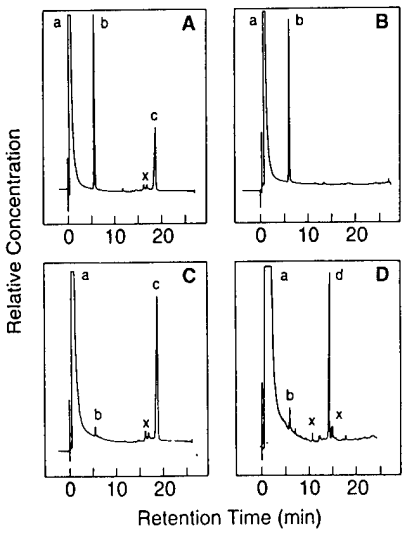

Fig. 1. Gas chromatograms of the TMS preparations: a, solvent and air; b, tri-TMS of phosphoric acid; c, tri-TMS of WR-151326; d, di-TMS of WR-2559550; x, unidentified product, perhaps partially derivatized material. (A) TMS preparation of hydrolysis products of WR-151327 prior to purification of the individual components; (B) TMS preparation of phosphoric acid after purification; (C) TMS preparation of synthetic WR-151326 after purification; (D) TMS preparation of synthetic WR-25595501 after purification.

appropriate TMS derivatives of the authentic samples and by observation of the appropriate peak enhancement when TMS derivatives of the synthesized products were mixed with those of the corresponding authentic samples and mixtures were analyzed individually. It is obvious from the GC data (Fig. 1) that acid hydrolysis of WR-151327 principally results in the formation of phosphoric acid and WR-151326 (Fig. 1A). Phosphoric acid can be isolated from the hydrolysis reaction product mixture by methylene chloride extraction (Fig. 1B). The methylene chloride-insoluble material WR-151326 can be further purified by recrystallization from ethanol–water (9:1, v/v) (Fig. 1C). WR-25595501 can be isolated from the reaction product mixture of mild oxidation of WR-151326 (Fig. 1D).

The structural identities of the synthesized compounds were confirmed by MS analysis of both their underivatized and the TMS derivatives in the DIP/EI mode. Fig. 2 shows the fragmentation pattern of the TMS derivative of WR-151326. The molecular ion, M^+, is observed at m/z 378. Other ions of significant interest are at m/z 363, 170, 143, 116 and 102, which are attributed respectively to $(M^+-{}^{\bullet}CH_3)$, $[CH_3-N(TMS)-CH_2-CH=CH-NH=CH_2]^+$, $[CH_3-NH(TMS)-CH_2-CH=CH_2]^+$, $[CH_3-N(TMS)-CH_3]^+$ and $[CH_3-NH-(TMS)]^+$. The ion at [15] m/z 73 is $[Si-(CH_3)_3]^+$. Based on the presence of the M^+ and other characteristic fragment ions, the structure of this TMS derivative was confirmed to be a tri-TMS derivative of WR-151326.

The mass spectral fragmentation pattern of the underivatized WR-151326 was consistent with the chemical structure of the compound (spectrum not shown). The observed M^+ fragmentation pattern (ion and ion relative intensity, %) was as follows; m/z at 162 (10%), 147 (90%), 131 (10%), 103 (10%) and 93 (10%).

The mass spectral identity of the TMS preparation of phosphoric acid was confirmed to be a tri-TMS derivative of phosphoric acid. The confirmation was made principally by detection of the molecular ion, M^+, at m/z 314, and its daughter ion $(M^+-{}^{\bullet}CH_3)$ at m/z 299 (spectrum not shown).

The TMS preparation of WR-25595501 under the present protocol forms the di-TMS derivative. This was confirmed by MS analysis of the TMS derivative (Fig. 3). The spectrum shows the molecular ion M^+ at m/z 466, $(M^+-{}^{\bullet}CH_3)$ at m/z 451 and $[CH_3-N(TMS)-CH_3]^+$ at m/z 116. The presence of low-intensity ions at m/z 314 and 299

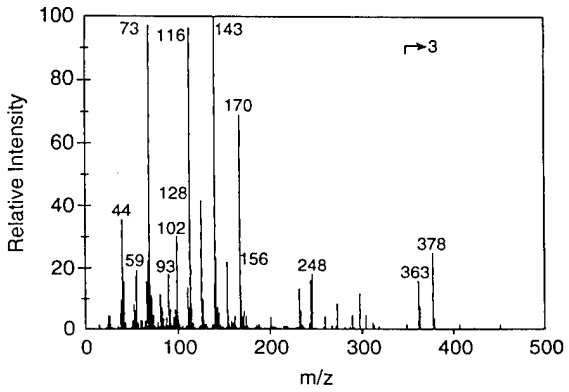

Fig. 2. DIP/EI mass spectrum of tri-TMS derivative of WR-151326.

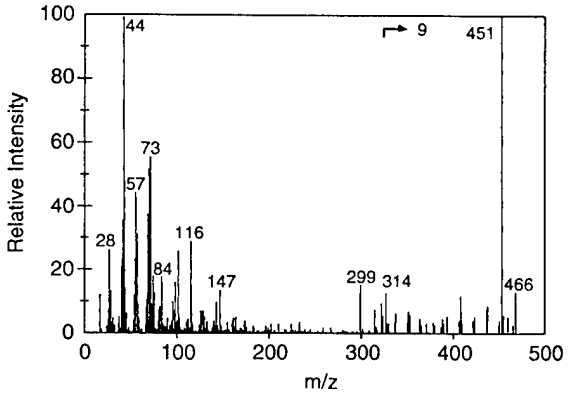

Fig. 3. DIP/EI mass spectrum of di-TMS derivative of WR-25595501.

suggests some remaining traces of phosphoric acid in the sample which were also detected in Fig. 1D as b. On the other hand, the DIP/EI mass spectrum of the underivatized WR-25595501 failed to show a molecular ion at m/z 322 but the spectrum did show other important characteristic ions: m/z at 277 (10%), 147 (100%) and 73 (30%). The degradation of WR-25595501 under mass spectral conditions cannot be ruled out, since it is a polar molecule.

To test the feasibility of simultaneous detection and analysis of mixtures of the aminothiol and its corresponding disulfide, GC calibration graphs for the TMS preparations of the equimolar mixtures of WR-151326 and WR-25595501 were analyzed on a capillary GC column, compound concentrations being plotted against peak areas from the corresponding peak integrations. The lowest concentration of each of the compounds detected was close to 5 pmol. Linear regression was used to analyze the calibration graphs. In both cases, the observed correlation coefficient R^2 was >0.997 and was reproducible, indicating an acceptable relationship for the data ranges of concentration of the compounds examined.

In addition to the GC and MS methodologies, we developed a rapid and sensitive LC–EC methodology for the simultaneous detection and analysis of WR-151326 and WR-25595501 as further confirmation of drug purity and analysis. The LC–EC procedure is similar in principle to that described by McGovern et al. [16] for WR-1065 and by Pendergrass et al. [17] for glutathione. The procedure did not require derivatization of the samples prior to analysis and took less than 15 min to complete.

Table 2
WR-151326 and WR-25595501: redox state, sensitivity and detection limit

Parameter	WR-151326 (WR-151326 [a])	WR-25595501 (WR-25595501 [a])
Redox state [b]	>29 (>16×10^8)	<4×10^{-9} (<4×10^{-9})
Slope [c]	162	70
x-Axis intercept [d]	132	23

[a] Synthesized thiol and disulfide compounds.
[b] Ratio of thiol to disulfide.
[c] Detector sensitivity (pA pmol^{-1}).
[d] Limit of detection (pmol).

External calibration graphs for WR-151326 were linear over the range 156–2500 pmol injected (slope, 162 nA pmol^{-1}; $R^2 > 0.999$). The disulfide, WR-25595501, showed a linear response from 39 to 2500 pmol injected (slope, 70.4 nA pmol^{-1}; $R^2 > 0.999$). These data are summarized in Table 2. The active forms of WR-151327, whose specific syntheses are described here, are indicated in Table 2.

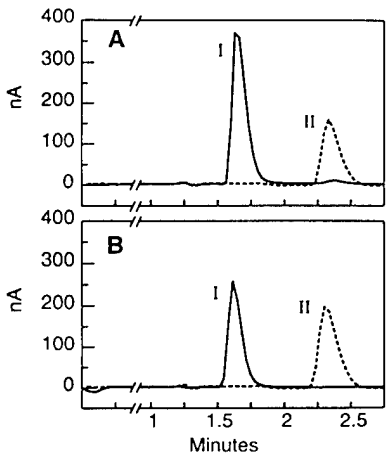

Fig. 4. LC–EC profiles of authentic samples of (A) WR-151326 and WR-25595501 and (B) newly synthesized compounds. I, WR-151326 (solid line); II, WR-25595501 (dashed line).

As can be seen in Fig. 4, the chromatograms for the synthesized compounds (B) are superimposable over the chromatograms for the authentic samples (A). The purity of each synthetic compound was confirmed by estimation of its redox state (the ratio of its thiol to disulfide content). The authentic thiol compound exhibited traces of its symmetrical disulfide, presumably due to autooxidation. However, both the newly synthesized disulfide preparation and the WRAIR (authentic) disulfide preparation were essentially free of LC–EC-detectable contaminating species. (Authentic samples of thiol and disulfide were desiccated and stored at −20°C.) The detection limit (signal-to-noise ratio >3) was 156 pmol for the thiol and 39 pmol for the disulfide.

The procedures for the conversion of WR-151327 into WR-151326 and WR-25595501 described in this paper provide overall high yields and purities of products. The mechanistic pathway for the formation of WR-151326 from WR-151327 is presumably analogous to that described by Risley et al. [9] for the formation of WR-1065 from the hydrolysis of WR-2721. Hydrolysis of the phosphorothioate compound results in the cleavage of the S–P bond to yield thiol and inorganic phosphate:

$$R\text{–}S\text{–}PO_3H_2 + H_2O \rightarrow R\text{–}S\text{–}H + H_3PO_4 \quad (1)$$

The formation of disulfide by iodine-induced oxidation of WR-151326 can best be explained as a two-electron displacement process:

$$R\text{–}S^- + I_2 \rightarrow R\text{–}S\text{–}I + I^- \quad (2)$$

$$R\text{–}S^- + R\text{–}S\text{–}I \rightarrow R\text{–}S\text{–}S\text{–}R + I^- \quad (3)$$

However, metal ion–oxygen-induced oxidation of WR-151326 is best considered as a one-electron process as described by the following sequence of reactions:

$$R\text{–}S^- + M^{+2} \rightarrow R\text{–}S^{\cdot} + M^+ \quad (4)$$

$$R\text{–}S^{\cdot} + O_2 \rightarrow R\text{–}S\text{–}O\text{–}O^{\cdot} \quad (5)$$

$$R\text{–}S\text{–}O\text{–}O^{\cdot} + R\text{–}S\text{–}H \rightarrow R\text{–}S\text{–}O\text{–}O\text{–}H + R\text{–}S^{\cdot} \quad (6)$$

$$R\text{–}S^{\cdot} \rightarrow R\text{–}S\text{–}S\text{–}R \quad (7)$$

The results indicate that both the GC and LC–EC methods described in this paper are specific and sensitive techniques for the simultaneous detection of active metabolites of WR-151327, with the estimate for the lower limis of detection in the pmol range. Although the GC method appears to be more sensitive than LC–EC, both methods are reliable and provide reproducible linear calibration graphs for a relatively wide range of concentrations of the active forms. The linearity of the calibration graphs observed from the GC and LC–EC analyses suggest that these methods may be useful for support of bulk drug studies. However, a more rigorous validation needs to be performed for use of these procedures in toxicological studies demonstrating specificity (i.e. blank plasma versus low-level spiked standards), precision and accuracy including drug stability.

4. Conclusions

The analytical procedures described herein for the active metabolities of WR-151327 will be useful to investigators working in the area of radio- or chemoprotection with in vivo and in vitro studies. Future research is essential in order to continue to evaluate chemo- and radioprotective properties of these aminothiols and symmetrical disulfide class of compounds having structural similarity to the benchmark radioprotector WR-2721 and its active metabolites. The GC, LC–EC and MS procedures described for the analysis of the active metabolites of WR-151327 may be useful in evaluating many compounds of this class.

Acknowledgments

The authors thank Dr. W.Y. Ellis of Walter Reed Army Institute of Research, Washingrton, DC, for supplying authentic samples WR-151326 and WR-25595501 and US Bioscience, West Conshohocken, PA, for WR-151327. This work was supported by the Armed Forces Radiobiology Research Institute.

References

[1] H.M. Patt, E.B. Tyree, R.L. Straube and D.E. Smith, Science, 110 (1949) 213–215.
[2] T.R. Sweeney, A Survey of Compounds from the Antiradiation Drug Development Program of the US Army Medical Research and Development Command, Walter Reed Army Institute of Research, Washington, DC, 1979.
[3] H. Marquardt, M.D. Sapozink and M.S. Zedeck, Cancer Res., 74 (1978) 415–419.
[4] C.K. Hill, B. Nagy, C. Paraino and D.J. Grdina, Carcinogenesis, 7 (1978) 665–672.
[5] E.A. Holwitt, E. Koda and C.E. Swenberg, Radiat. Res., 126 (1990) 107–110.
[6] J.F. Utley, N. Seaver, G.L. Newton and R.C. Fahey, Int. J. Radiat. Oncol. Biol. Phys., 10 (1984) 1525–1532.
[7] T. Mori, M. Watanabe, M. Horikawa, P. Nikaido, H. Kimura, T. Aoyma and T. Sugahara, Int. J. Radiat. Biol., 44 (1983) 41–45.
[8] G.D. Smoluk, R.C. Fahey, P.M. Calabro-Jones, J.A. Aguilera and J.F. Ward, Cancer Res., 48 (1988) 3641–3646.
[9] J.M. Risley, R.L. Van Etten, L.M. Shaw and H. Bonner, Biochem. Pharmacol., 35 (1986) 1453–1459.
[10] W.A. Prutz, Int. J. Radiat. Biol., 56 (1989) 21–27.
[11] D.J. Grdina, C.P. Sigdestad and B.A. Carnes, Radiat. Res., 17 (1989) 500–507.
[12] D.J. Grdina, P. Dale and B.A. Weichselbaum, Int. J. Radiat. Oncol. Biol. Phys., 22 (1992) 813–820.
[13] G.L. Ellman, Arch. Biochem. Biophys., 82 (1959) 70–77.
[14] Y.N. Vaishnav and C.E. Swenberg, Radiat. Res., 133 (1992) 12–17.
[15] Y.N. Vaishnav, E.A. Holwitt, C.E. Swenberg, H.-C. Lee and L.-S. Kan, J. Biomol. Struct. Dyn., 8 (1991) 935–951.
[16] E.P. McGovern, N.F. Swynnerton, P.D. Steele and D.J. Mangold, Int. J. Radiat. Oncol. Biol. Phys., 10 (1984) 1517–1520.
[17] J.R. Pendergrass, E.P. Clark and D.L. Palazzolo, Curr. Sep., 123 (1993) 137–140.

INT. J. RADIAT. BIOL 1996, VOL. 70, NO. 6, 735–745

Mechlorethamine-induced enhancement of radiation sensitivity of guanine

Y. N. VAISHNAV* and C. E. SWENBERG

(Received 4 March 1996; accepted 19 August 1996)

Abstract. This study describes and characterizes the interactions of nitrogen mustard mechlorethamine (HN_2) with guanine and the radiation sensitivity of guanine in the presence of HN_2. Briefly, in an equimolar solution (0·5 mmol dm^{-3}) the pH-dependence (pH 3·0–12·0) and time-dependence (0–36 h) of alkylation of guanine at room temperature were determined using a reverse-phase high-performance liquid chromatography (hplc) column. Based on the hplc peak areas of the product and intact guanine, the optimal pH for alkylation was determined to be 8·0. Similarly, the optimal time required for alkylation was 10 h. Two products, i.e. alkylated guanines, were detected (10 : 1, peak areas measured at 260 nm) and purified. Structural studies of the products were performed by direct insertion probe-electron impact mass spectrometry. These products were identified as *N*-(2-chloroethyl)-*N*-[2-(7-guanyl)-ethyl]-methylamine (product 1) and *N*-(2-hydroxyethyl)-*N*-[2-(7-guanyl)ethyl]-methylamine (product 2). At optimal conditions, samples of either guanine or an equimolar solution of guanine and HN_2 were ^{60}Co irradiated (γ-ray) at 25 Gy min^{-1} at doses up to 400 Gy. Both sets of samples were analysed by hplc. In each case, the sole radiation product observed and characterized was 8-hydroxy-guanine. Dose–yield plots were linear and showed that HN_2 enhanced the radiation sensitivity of guanine. This increase in radiation sensitivity is attributed to the differences in electrophilic properties between nitrogen mustard and guanine.

1. Introduction

Nitrogen mustard mechlorethamine [(bis-2-chloroethyl)methyl-amine; HN_2] was the first effective anticancer agent employed clinically (Mattes *et al.* 1986). Derivatives of HN_2, such as L-phenylalanine mustard, chlorambucil and cyclophosphamide are also effective therapeutic agents (Haskell 1990) even though they are highly carcinogenic. Studies of the risk of acute non-lymphocytic leukaemia in the presence of radiation, radiation and alkylating agents, and alkylating agents alone demonstrated the increased occurrence of a non-additive risk when both agents are used (Curtis *et al.* 1992). Nitrogen mustards are bifunctional alkylating agents and, due to their electrophilic nature, they may alkylate any accessible nucleophilic atoms in nucleic acids, proteins or other biomolecules (Ehrenberg 1961). However, the major site of alkylation of DNA is the N-7 position of guanine (Tomaz 1969). This particular interaction accounts for approximately 90% of the total. All bifunctional nitrogen mustards, including mechlorethamine, covalently modify DNA predominantly at the N-7 position of guanine, resulting in monoadducts as well as inter- and intrastrand cross-links (Brookes and Lawley 1961). DNA–mustard–protein cross-links have also been observed in intact cells (Ewig and Kohn 1978). The role of these lesions in cytotoxicity is not clear; however, it is generally believed that DNA alkylating agent-mediated interstrand linkage is essential for inhibition of DNA replication (Kohn *et al.* 1966). Therapeutically effective antitumour activity suggests that mustards have two functional groups involved in the formation of crosslinks between the macromolecular sites (Hartley *et al.* 1992).

The nitrogen mustards often mimic ionizing radiation in many respects (Calabresi and Welch 1968). Both mustard agents and ionizing radiation induce a number of lesions in DNA, including modified bases, base-free sites and single- and double-strand breaks (Geacintov and Swenberg 1993, Povirk and Shuker 1994). Both agents appear to be relatively unique in their actions against chromosomes and their capacity to induce genetic mutation (Calabresi and Welch 1968). However, their actions are not entirely qualitatively similar (Koller 1960). The important differences relate to the temporal course of induced cytological changes and to the combined toxicities of nitrogen mustard and ionizing radiation that are not strictly additive (Calabresi and Welch 1968), a result supported by our research.

In spite of the importance of the biological endpoints produced by nitrogen mustards alone

* Author for correspondence.
Applied Cellular Radiobiology Department, Armed Forces Radiobiology Research Institute, Bethesda, MD 20889-5603, USA.

0955-3002/96 $12.00

and in combination with radiation, relatively few studies have been undertaken to characterize and elucidate fully the chemical nature of such DNA lesions. As nitrogen mustards and ionizing radiation remain parts of the radiotherapeutic and chemotherapeutic regimen for malignant diseases, it is important to investigate their individual and combined interactions with constituents of DNA in order to understand further their biological consequences. A detailed molecular description of events involved in combined exposures of these two agents should be helpful in understanding adverse reactions and for the development of appropriate countermeasures. As guanine is known to be the base most susceptible to alkyl modifications, we used it as our model system. In this paper, the conditions used for the formation of the detected products of mechlorethamine interactions with guanine are optimized, and the radiation sensitivity and radiation chemistry of guanine in the absence and presence of nitrogen mustard (HN_2) are reported.

2. Materials and methods

2.1. *Reagents and instruments*

Guanine, mechlorethamine hydrochloride and triethanolamine hydrochloride were purchased from Sigma Chemical Co. (St Louis, MO, USA). Hplc-grade acetonitrile was obtained from Aldrich Chemical Co. (Milwaukee, WI, USA). *N-O*-bis-(trimethylsilyl)-trifluoroacetamide (BSTFA) was purchased from Supelco, Inc. (Bellefonte, PA, USA). All hplc analyses were performed using a Kratos Analytical Spectroflow 400 solvent delivery system on-line with a model SP-4100 computing integrator and an Applied Biosystems model 783 absorbance detector gradient controller (all Ramsey, NJ, USA). Mass spectral analyses were performed on the Kratos Analytical 25RFA mass spectrometer system (Manchester, UK) using a direct insertion probe/electon impact mode (DIP/EI) using perfluorokerosine (PFK) as an internal standard. Experiments using γ-irradiation were performed in our ^{60}Co facility.

2.2. *Detection and isolation of the products*

Aqueous solutions of guanine (0·5 mmol dm^{-3}) alone and an equimolar mixture of guanine and mechlorethamine (0·5 mmol dm^{-3} each) in aqueous triethanolamine hydrochloride (100 mmol dm^{-3}, pH 7·5 adjusted with 0·5 mol dm^{-3} NaOH) were allowed to stand at room temperature for 3 h. Subsequently, aliquots (10 μl) from each solution were analysed by high-performance liquid chromatography (hplc) using a reverse-phase semipreparatory column (Speris, UK; 250 × 10 mm) in an isocratic eluent mode (water-acetonitrile-acetic acid in 85:13:2, v/v/v or 0·1 mmol dm^{-3} ammonium acetate-acetonitrile in 9:1, v/v). Hplc peak profiles of both samples were recorded by optical detection at 260 nm. Products were collected and freeze-dried for subsequent mass spectral (MS) analysis.

2.3. *Mass spectrometry*

Hplc-purified products 1 and 2 (P-1 and P-2) were converted into their corresponding trimethylsilyl (TMS) derivatives. In reaction vials, approximately 100-μg samples of either P-1 or P-2 were dissolved in 25-μl mixtures of acetonitrile–BSTFA (1 : 2, v/v). The resulting mixtures were subsequently heated to 65°C for 45 min and then allowed to stand at room temperature for an additional 40 min to equilibriate the mixtures. Using the direct insertion probe (DIP), 3–4 μl of the silylated products were individually analysed in an electron impact (EI) mode (70 eV; constant source temperature 270°C), and mass spectra were recorded as previously described (Vaishnav and Swenberg 1993).

2.4. *Interaction of guanine with mechlorethamine: pH dependence*

An aqueous solution of triethanolamine hydrochloride (100 mmol dm^{-3}, 100 ml) was equally divided into 10 fractions. This pH was adjusted from 3·0 to 12·0 respectively with either 0·1 mol dm^{-3} NaOH or 0·1 mol dm^{-3} HCl. After having adjusted pH, each fraction was made to 0·5 mmol dm^{-3} (equimolar) with respect to guanine and mechlorethamine. The resulting mixtures were allowed to incubate at room temperature for 3 h, and then placed in an icebath until all samples were analysed. The progress of the reaction at each pH was monitored by a reverse-phase hplc column as described. The peak areas for each product were determined by triangulation by a digital integrator. Following initial analysis, samples were allowed to incubate at room temperature (72 h) and were subsequently reanalysed.

2.5. *Interactions of guanine with mechlorethamine: time dependence*

An equimolar mixture of guanine and mechlorethamine (0·5 mmol dm^{-3}) in 100 mmol dm^{-3} triethanolamine (pH 8) was allowed to incubate at room temperature, and aliquots (10 μl) were withdrawn periodically between 0 and 40 h from the incubating mixture and analysed on a reverse-phase hplc column as described. The peak areas for P-1, P-2 and the unreacted guanine (G) were determined.

2.6. *Irradiation of guanine with/without mechlorethamine*

Aqueous solutions of guanine and mechlorethamine (0·5 mmol dm^{-3} each) were prepared in 100 mmol dm^{-3} triethanolamine hydrochloride buffer (pH 7·5). The solutions were allowed to stand overnight at room temperature. Aliquots (200 μl) from these solutions were withdrawn and placed individually into irradiation vials (micro-polypropylene tubes [500 μl]). Marsch Biomedical Products, Rochester, NY, USA). The air-saturated samples were then exposed bilaterally to different doses of ^{60}Co (γ-rays; 0, 40, 80, 120, 160, 200, 250, 300 and 400 Gy) at a dose-rate of approximately 25 Gy min^{-1}. Irradiated samples and unirradiated controls were allowed to stand at 4°C until analysis. Both sets of samples were analysed according to the conditions for reverse-phase hplc described previously (0·1 mmol dm^{-3} ammonium acetate–acetonitrile, 9:1, v/v). Prior to sample irradiations, the desired dose-rate was established using a 0·5-cm^3 tissue-equivalent (TE) ionization chamber. The tissue–air ratio (*TAR*) was estimated to be 0·98.

3. Results

3.1. *Hplc and mass spectral analysis*

The hplc product profiles of the interaction of guanine with mechlorethamine in equimolar aqueous mixture of guanine and mechlorethamine in 100 mmol dm^{-3} triethanolamine buffer (pH 7·5) are provided in Figure 1. From the hplc product profiles it was determined that an equimolar aqueous mixture of guanine and mechlorethamine at room temperature (pH 7·5) resulted in two new products, P-1 (*RT* = 11·08 min) and P-2 (*RT* = 14·44 min), in addition to unaltered

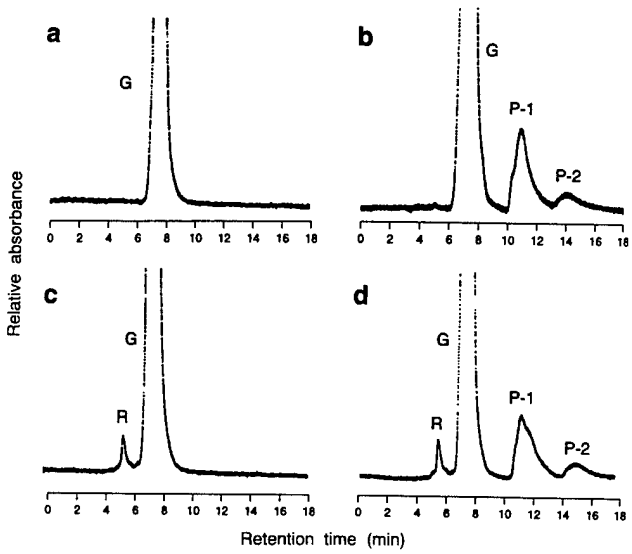

Figure 1. Representative hplc product profiles of (a) guanine standard, (b) interaction products of guanine with mechlorethamine, (c) ^{60}Co γ-irradiated guanine (100 Gy, 25 Gy/min), and (d) ^{60}Co γ-irradiated equimolar mixture of guanine and mechlorethamine at optimal conditions of adduct formation (100 Gy, 25 Gy min^{-1}), where G, P-1, P-2 and R represent guanine, product 1, product 2 and the radiation product respectively.

guanine (*RT* = 7·90 min) (Figure 1). The homgeneity of P-1, P-2 and G were confirmed by two additional analytical hplc columns (Speris and Hypersil ODS, both 250 × 4 mm) using 0·2 mmol dm^{-3} ammonium acetate–acetonitrile eluent (9:1, v/v; 260 nm) in an isocratic mode. The Speris semipreparatory hplc column (250 × 10 mm, 0·1 mmol dm^{-3} ammonium acetate-acetonitrile, 9:1, v/v) system was routinely employed to analyse R, P-1, P-2 and G simultaneously (Figure 1). The unaltered guanine peak, labelled G, P-1 and P-2, was isolated and purified on a reverse-phase hplc. The purified samples were freeze-dried and converted into their corresponding TMS derivatives. The TMS derivatives of P-1, P-2 and G were analysed individually in a DIP/EI/MS mode. The molecular ion ($M^{+\cdot}$) of P-1 had *m/z* = 414 (Figure 2A), consistent with the molecular formula of the di-TMS derivative of a monoalkyl adduct of guanine with mechlorethamine (di-2TMS-$C_{10}H_{13}N_6OCl$). Further fragmentations of the $M^{+\cdot}$ resulted in several prominent ions characteristic of the di-TMS derivative. The ion at *m/z* 352 appears to have arisen from the combined loss of neutral products (HCl) and (HC≡CH) or (H_2C=CClH) from the molecular ion. On the other hand, ions at *m/z* 248 and 246 appear to be fragmentation products of the $M^{+\cdot}$ of the di-TMS derivative of the monoalkyl aduct

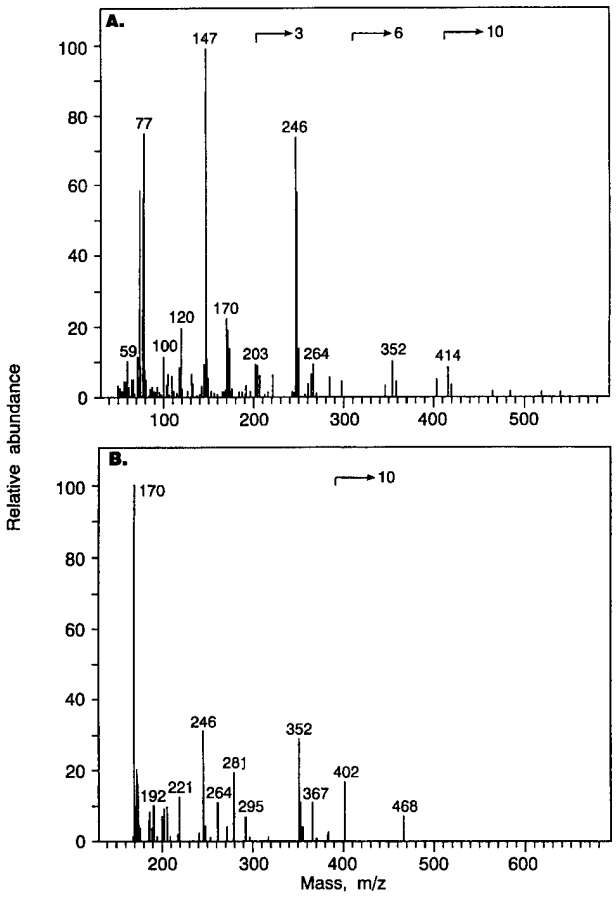

Figure 2. Electron impact mass spectra of the TMS derivatives: (A) P-1 and (B) P-2. P-1 and P-2 were isolated from the products of interaction in an aqueous solution of guanine with mechlorethamine by reverse-phase hplc, freeze dried and converted into their corresponding TMS derivatives; arrows denote the magnified relative intensity scale.

(P-1). Ions *m/z* 248 and 246 are attributed to combined losses of the following neutral fragments: [H_2 + CH_3–NH–CH_2–CH_2–Cl] and [2H_2 + CH_3–NH–CH_2–CH_2–Cl] respectively. The appearance of ions *m/z* 205 and 203 is attributed to the losses of the neutral fragment (HN=C=O) from the further fragmentations of ions *m/z* 248 and 246 respectively. The medium intensity ion *m/z* 170 is attributed to [(CH_3–Si=CH_2)–(N–TMS)–C≡N]$^+$. The high-intensity ion *m/z* 147, [(CH_3)$_3$–Si–O–Si–(CH_3)$_2$]$^+$, is characteristic and is diagnostic for the presence of oxygen in the base (McCloskey 1974). Scheme I explains the formation of all prominent daughter ions from the $M^{+\cdot}$ of the di-TMS derivative of P-1·

The DIP/EI/MS of the TMS preparation of the hplc-purified P-2 showed $M^{+\cdot}$ at *m/z* 468 (Figure 2B) to be consistent with the molecule 3TMS-$C_{10}H_{13}N_6O_2$. It appears from the spectrum that *m/z* 367 arises from silyl group migration from the sidechain alkyl group to the N-9 of the guanine moiety, resulting in the loss of a neutral fragment (~CH_2–CH_2–N(CH_3)–CH_2–CH_2–O~) from the $M^{+\cdot}$ (N-7 position of guanine moiety). Alternatively, the silyl group could migrate (McLafferty 1980) from the sidechain alkyl group to the -NH-TMS grouping at the C-3 atom of guanine, which subsequently expels ·CH_3, a loss of 15 (*m/z*) from the *m/z* 367 to give rise to a new ion, *m/z* 352. As described, loss of ·CH_3 is a characteristic of TMS compounds (McCloskey 1974). Also, the transfer of TMS groups from one to the other atom is not uncommon in TMS derivatives of heterocyclic organic compounds and specifically in nucleic acid components (McLafferty 1980). The low intensity ion at *m/z* 295 presumably arises from the *m/z* 367 as a result of loss of one of the silyl groups and subsequent protonation. Ions *m/z* 248 and 246 appear to be the consequences of combined losses of [HN(CH_3)–CH_2–CH_2–O–TMS + TMS] and [HN(CH_3)–CH_2–CH_2-OTMS + TMS + 2H·] respectively from the molecular ion (*m/z* 468). The intense ion *m/z* 170 is attributed to [(CH_3–Si=CH_2)–N(TMS)–C≡N]$^+$, which is not unusual in trimethylsilylated purine and pyrimidine bases as discussed (Scheme II). The low-intensity ion *m/z* 402 could not be identified from the available data. This ion could be due to the presence of a trace amount of contaminant in the sample.

The mass spectra of the TMS derivatives of the isolated sample (Figure 1, peak labelled G) and an authentic sample of guanine were identical (spectra not shown). Under the mass spectral conditions, no extensive fragmentation of the tri-TMS derivative was observed. The $M^{+\cdot}$ was observed at *m/z* 367, which corresponds to the tri-TMS derivative of guanine. The ion (*m/z* 352) represents ($M^{+\cdot}$–·CH_3). The ion (*m/z* 147) is attributed to [(CH_3)$_3$–Si–O–Si–(CH_3)$_2$]$^+$ as described earlier. In addition to these prominent ions, other low-intensity ions included *m/z* 294, 295, 281 and 221. These fragmentation patterns are identical to that previously reported (McCloskey *et al.* 1968) for the TMS derivative of guanine.

3.2. *pH-dependent formation of guanine–mechlorethamine adducts*

The interactions of guanine with nitrogen mustard were studied under a wide pH range in 100 mmol dm^{-3} ethanolamine hydrochloride buffer. Mixtures of guanine and mechlorethamine at

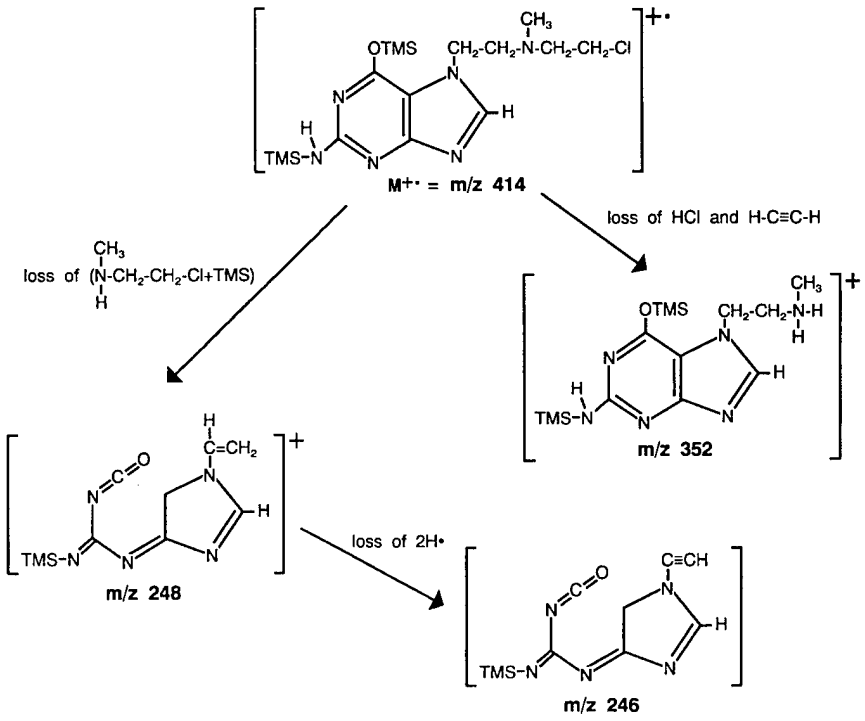

Scheme I. Plausible pathway of the mass spectral ion fragmentation pattern of the TMS derivative of P-1.

different pHs (between 3·0 and 12·0) were allowed to stand at room temperature for 3 h prior to analysis. At the end of the incubation period, each sample was analysed on a reverse-phase hplc. From the resulting chromatograms, the corresponding peak areas (p) for P-1 or P-2, and (g) of unaltered guanine (G) were determined for each pH. From the peak area values [$10^2 \times p/(p+g)$], the % product (P-1 or P-2) formed was derived for each sample and plotted as a function

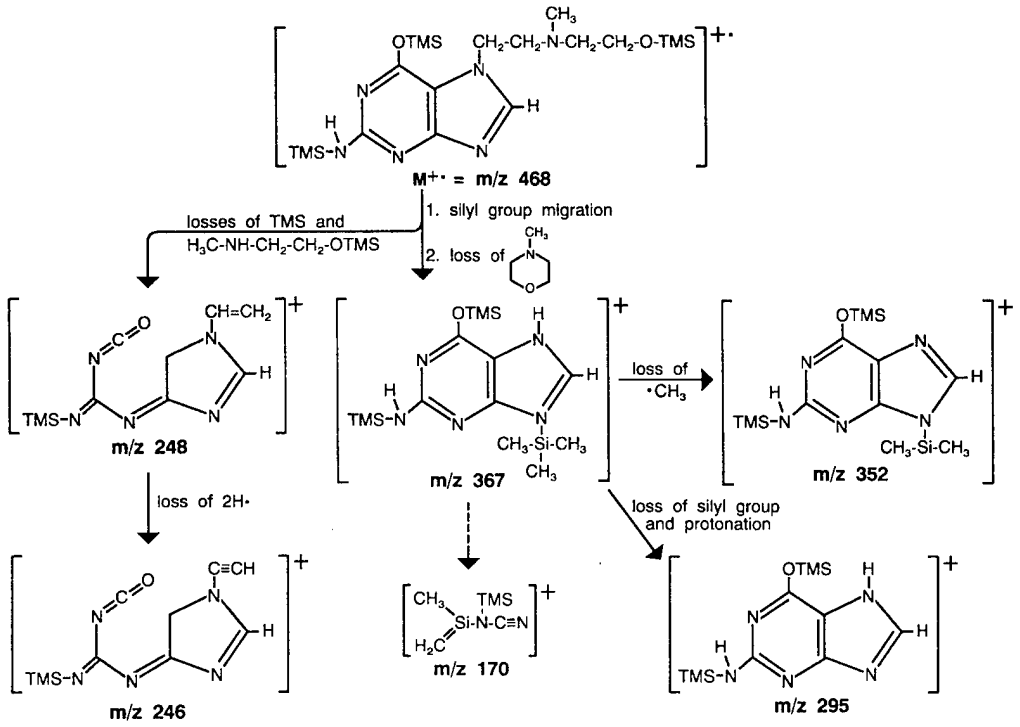

Scheme II. Plausible pathway of the mass spectral ion fragmentation pattern of the TMS derivative of P-2.

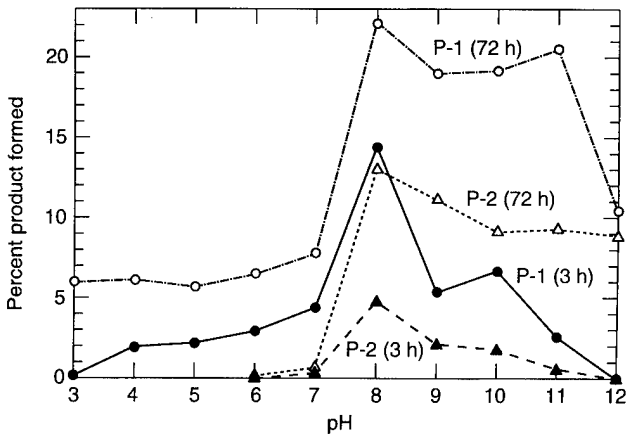

Figure 3. pH-dependent product formation: interaction of guanine with mechlorethamine. An equimolar solution of mechlorethamine and guanine was prepared in 100 mmol dm^{-3} triethanolamine hydrochloride, and samples (10 μl) from this solution were allowed to incubate at different pHs (3·0–12·0) at room temperature. Aliquots from these solutions were analysed by hplc at specific time intervals. From the hplc chromatograms, the formation of the product was determined by peak areas of product and intact guanine. As shown, the pH in the vicinity of 8·0 favours product formation to the greatest extent.

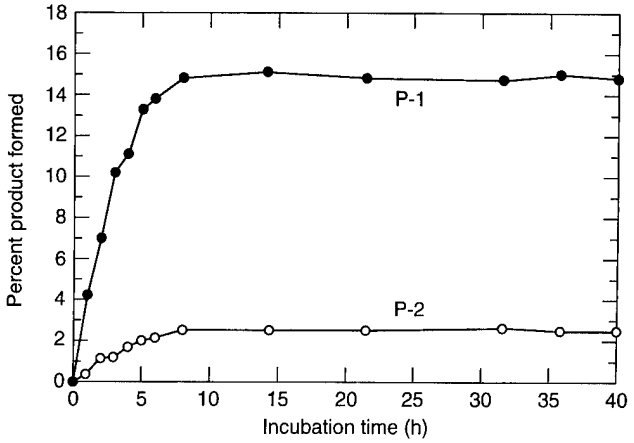

Figure 4. Time-course studies on interaction of guanine with mechlorethamine. Aliquots from the equimolar (0·5 mmol dm^{-3}) incubating solution of guanine with mechlorethamine in triethanolamine buffer (pH 8·0) were analysed on an hplc reverse-phase column at specific time intervals. The peak areas of P-1, P-2 and G were determined from the hplc chromatograms and from this P-1 and P-2 were quantified and plotted against time. At pH 8·0 the optimal time required for formation of P-1 and P-2 is between 8 and 10 h.

of pH. As evident in Figure 3 the maximum product formation occurred between pH 7·5 and 8·5. The samples were similarly analysed after 72 h, and from the peak area values were determined and plotted against the corresponding pHs. No significant qualitative differences were observed in the product formation for samples incubating for periods of 3 or 72 h although at pHs between 7·5 and 8·5 there were differences in the amounts of products formed when incubations were allowed to proceed for 72 as compared with 3 h. Figure 3 represents the means of three independent experimental observations.

3.3. *Time-dependent formation of guanine–mechloethamine adducts*

An equimolar (0·5 mmol dm^{-3}) mixture of guanine and mechlorethamine was allowed to incubate in either 100 mmol dm^{-3} triethanolamine or 100 mmol dm^{-3} sodium phosphate buffer at room temperature for 48 h. Progress of the reaction was monitored on an hplc by injecting 5 μl of the incubating mixture on a reverse-phase column. The formation of P-1 and P-2 in relation to the intact guanine was determined using peak areas from the corresponding chromatograms. From the peak areas p and g of products and intact guanine respectively for each sample, the peak area value was derived and plotted against time. As evident from data in Figure 4, which were recorded under optimal pH conditions and at room temperature, the plateau levels for formation of P-1 and P-2 were achieved after 8 h. When mechlorethamine–guanine interactions were studied in 100 mmol dm^{-3} sodium phosphate buffer (pH 7·4, room temperature or 37°C), P-1 and P-2 were observed but with lower yields (data not shown).

3.4. *Gamma-irradiation*

Irradiation of guanine in the presence and absence of nitrogen mustard was done as described in §2. Both sets of samples were analysed on a reverse-phase hplc column, and the resulting peak areas for each peak representing irradiation product (R) and unaltered guanine (G), r and g respectively, were determined (Figure 1). Under the described analytical conditions, the peak labelled R in the chromatogram was the only radiation product detected and was common to both sets of irradiated samples. From the hplc chromatogram values $[10^2 \times r/(r+g)]$, % guanine damage was determined for each sample and plotted as a function of radiation dose for both sets of experiments (Figure 5). Furthermore, eluents from the hplc peaks corresponding to product R were collected from both sets of

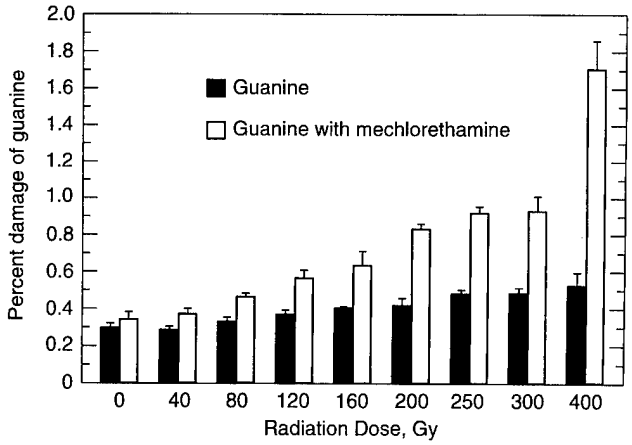

Figure 5. γ-Ray irradiation of guanine in the presence and absence of mechlorethamine. Samples of guanine and equimolar mixture of guanine with mechlorethamine were irradiated under optimal conditions as described in §2. The damage to guanine was determined from peak areas of the radiation product labelled R and intact guanine (G) in Figure 1c and d. Each column represents the means of three independent experiments ± SEM. As evidenced, the nitrogen mustard enhanced the radiation sensitivity of guanine.

irradiated samples, then combined and freeze-dried. A sample from the residue was reinjected into hplc to verify that the products R in both sets of experiments were identical. The remaining freeze-dried product R was converted into its corresponding TMS derivative, and this derivative was analysed on a mass spectrometer in a DIP/EI/MS mode. The mass spectrum of the TMS derivative (Figure 6) showed $M^{+\cdot}$ = *m/z* 455, being consistent with the molecular formula $C_5H_5O_2N_5$-$(TMS)_4$. The other prominent daughter ions

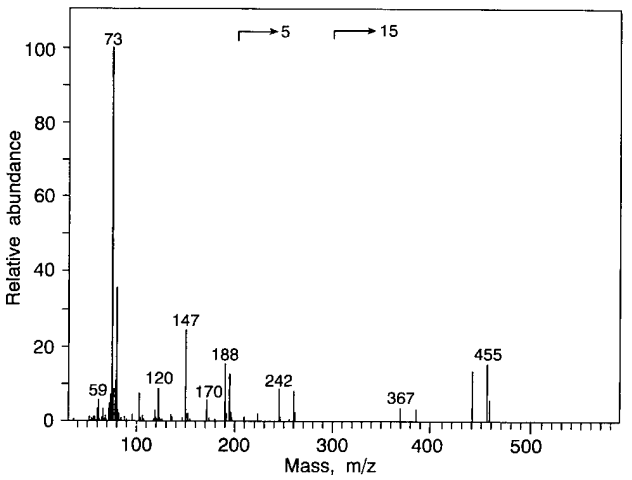

Figure 6. Electron impact mass spectrum of the radiation product of guanine: radiation product labelled R (Figure 1c and d) was purified as described §2. The product was converted into its TMS derivative and analysed on a DIP/EI/MS system.

were characterized as follows: the characteristic loss of CH_3, *m/z* 440 ($M^{+\cdot}-15$); *m/z* 367 (*m/z* 440 – TMS); and ions *m/z* 170 $[(CH_3-Si=CH_2)-N(TMS)-C\equiv N]^+$, *m/z* 147 $[(CH_3)_3-Si-O-Si-(CH_3)_2]^+$ and *m/z* 73 was attributed to $[Si-(CH_3)_3]^+$. On the basis of the fragmentation patterns of the TMS derivative of the product R and comparison of this pattern with that reported (Dizdaroglu 1985, Fuciarelli *et al.* 1989), we determined the chemical structure of product R to be 8-hydroxy-guanine (for the chemical structure, see Scheme III).

4. Discussion

To our knowledge very few reports have been published that adequately characterize the DNA adducts produced by alkylating chemotherapeutic agents, such as nitrogen mustards, in the presence of ionizing radiation, despite the fact that their primary effects are thought to be the results of their interactions with DNA. The nitrogen mustards present considerable challenges because their interaction products with DNA are likely to be labile and many undergo secondary reactions (Hemminki 1985). For example, alkylation of guanine-N-7 labilizes the guanine base, resulting in either an acid-catalysed depurination or an alkali-catalysed ring opening. Most of such studies have been performed at nucleoside levels. However, it has been reported (Hemminki *et al.* 1989) that the depurination is about 50 times faster in nucleosides than in double-stranded DNA (Brooks and Lawley 1961). Considering these reported observations and in order to get improved perspectives of these interactions at the DNA base level, we determined the optimal conditions (pH, buffer and time) governing the interactions of mechlorethamine with guanine. Our results suggest that these interactions produced two monoadduct derivatives P-1 and P-2. Both products of the alkylation reaction were purified and converted into their corresponding TMS derivatives to decrease polarity and increase volatility required for mass spectral analysis in DIP/EI/MS mode. From the mass spectral data, the chemical names assigned were *N*-(2-chloroethyl)-*N*-[2-(7-guanyl)ethyl]methylamine (P-1) and *N*-(2-hydroxyethyl)-*N*-[2-(7-guanyl)ethyl]methylamine (P-2) (for chemical structures, see Scheme III). The formation of these products can be rationalized by considerations of Scheme IV. Lowering the pH <7·5 results in a decrease in the reactivity of mechlorethamine towards nucleophilic reagents due to protonation of the nitrogen atom of the

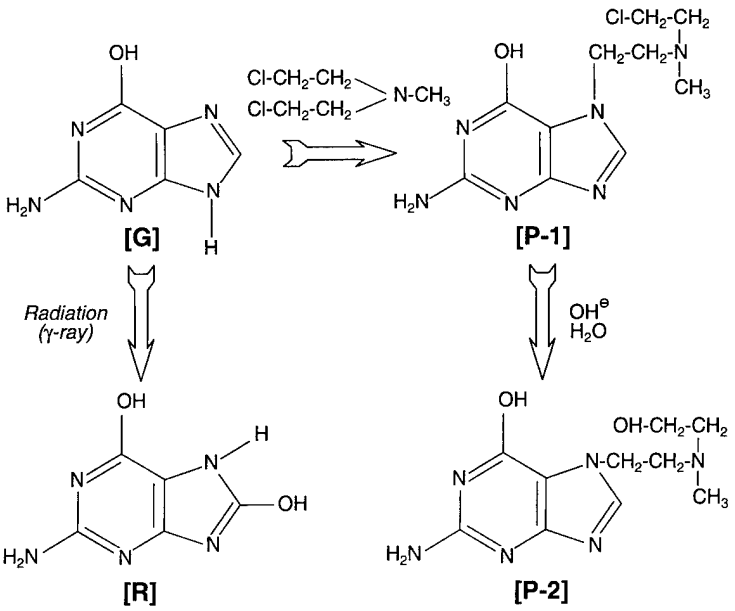

Scheme III. Chemical structures of P-1, P-2, G and R.

tertiary amine (*pKa* 4·95). At neutral or alkaline pH, by following the S_N1 reaction mechanism mechlorethamine initially forms a reactive carbonium ion (aziridinium ion) intermediate (Calabresi and Welch 1968); this in turn attacks guanine at its most nucleophilic site (N-7) to give a mono-adduct such as P-1. This mono-adduct, by similar S_N1 mechanisms, can either give rise to a di-adduct or can interact with the solvent and hydrolyze by following the S_N2-type reaction mechanisms to give products such as P-2. Kinetic model studies of Mattes (1992) on mechlorethamine reactions support these mechanistic pathways for production of the observed products. In the present studies, we did not detect formation of di-adduct from mechlorethamine and guanine. Interestingly, in cells, Larminant *et al.* (1993) observed that the mono- to di-adduct formation ratio is approximately 95 : 5. When these interactions were studied in a purely organic solvent system (trifluoroethanol) at high temperature, in addition to the major product as mono-adduct, some di-adduct was also isolated (Kallama and Hemminki 1986). This suggests that solvent and other environmental conditions can affect the quality and quantity of the adducts formed.

In order to optimize adduct formation at room temperature, interactions of mechlorethamine with guanine were studied at the stoichiometric ratio of 1 : 1. It was observed that adduct formation is largest for pHs between 7·5 and 8·5, and declines as pH is either raised or lowered. This could result from the hydrolysis reaction of mechlorethamine as well as the hydrolysis of the formed products. The relative percentage of the adduct(s) formed as determined from hplc analysis suggests that only a small amount of guanine interacts with the nitrogen mustard even under optimal pH conditions. Similarly, time-course studies for interaction of guanine with the nitrogen mustard in a 1 : 1 stoichiometric ratio were examined at the optimal pH (8·0). At this pH the relative percentage of the products formed remained constant after 8 h. Again, under optimal

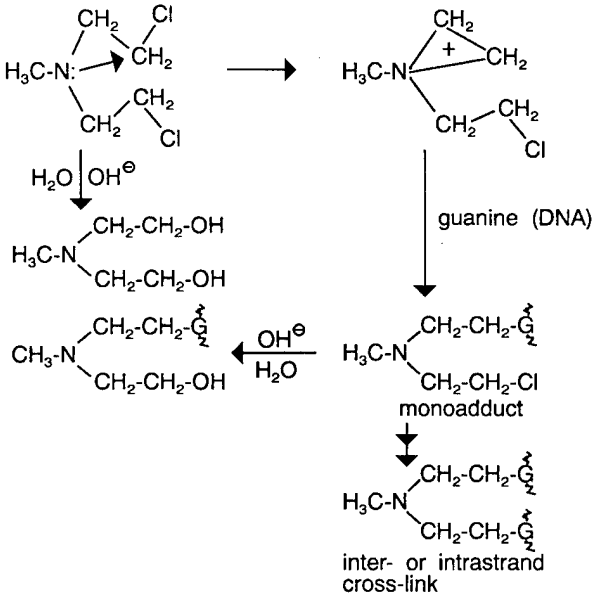

Scheme IV. Plausible mechanism: formation of various products.

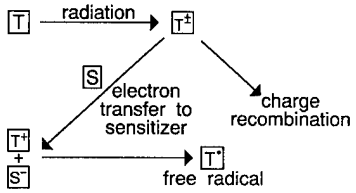

Scheme V. Plausible mechanism: electrophilic characteristic of the radiosensitizer and enhanced radiation sensitivity of the target molecule.

pH and time conditions no quantitative conversion of guanine to adduct formation was observed. This is perhaps due to the relatively short stability of mechlorethamine in aqueous solution (Cummings *et al.* 1993). No further attempts were made to gain quantitative conversions of guanine into alkylated guanine.

Gamma-radiolysis of guanine alone or in combination with mechlorethamine was examined under the described optimal alkylation conditions for radiation doses up to 400 Gy. On hplc analysis, both sets of experiments showed a new single common radiation product (labelled R in Figure 1). This new radiation product was isolated and its chemical structure determined to be 8-hydroxy-guanine by the mass spectrum of its TMS derivative. This radiation-induced formation of 8-hydroxy-guanine was previously reported by other investigators: for example, from DNA oligomer (Paul *et al.* 1987) and calf thymus DNA (Dizdaroglu 1985). Figure 1c and d compares the radiation-induced formation of 8-hydroxy-guanine when guanine was irradiated alone and when it was irradiated in the presence of mechlorethamine. As evidenced in Figure 5, mechlorethamine considerably enhances the radiation sensitivity of guanine. Since irradiations were performed under the optimal aqueous conditions for the formation of P-1 and P-2 and, considering the stability of mechlorethamine in aqueous solution and that it forms its two known hydrolysis products, chlorohydrine and *N*-methyl ethanolamine, these two along with P-1 and P-2 would be expected to be present during irradiation. Therefore, during the irradiation of guanine, in addition to mechlorethamine, at least four other compounds formed directly from mechlorethamine also influence the radiation sensitivity of guanine. The individual roles of these compounds in altering the radiation sensitivity are not known. Therefore, it seems very likely that mechlorethamine plays a direct and/or indirect role in enhancing the radiation sensitivity of guanine.

Several hypotheses have been proposed for the radiation sensitivity enhancement mechanisms of target molecules in the presence of a radiosensitizer. In this case, however, the observed enhancement of the radiation sensitivity of the guanine can be well-explained by considering of Adams' and Cook's hypothesis (Adams and Cook 1969, Adams 1970). According to this hypothesis, enhanced radiation sensitivity of the target molecule is due to differences between the electrophilic characteristics of the target molecules and the sensitizer. Radiation sensitizers are known to have higher electron affinity as verified experimentally by Greenstock *et al.* (1970). Scheme V illustrates the formation of free radicals from target molecules in the presence of sensitizer molecules: the direct or indirect effect of radiation results in charge separation in the target molecules, followed by electron transfer from the negatively charged site of the target molecule to a more electrophilic sensitizer. If, therefore, a molecule of higher electron affinity is present, either as a complex or as a free molecule in the immediate environment of the ionized target molecule, electron transfer from the ionized target molecule to the sensitizer could occur, rendering the target molecule positively charged. This process is expected to compete with the charge recombination, thereby rendering a 'self-healing' effect. Irreversible electron transfer to the sensitizer would lower the probability of self-healing and favour the decay of the highly reactive positive target ion by reacting with another neutral molecule, consequently transforming itself into a reactive free radical. Such electron transfer from negatively charged nucleotide radical anions to the sensitizers has been demonstrated by pulse radiolysis (Greenstock *et al.* 1970). Electron paramagnetic resonance spectroscopy experiments also demonstrated that the radical yields in the irradiated DNA increased in the presence of the sensitizer (Adams 1970). In the present case, in the absence of known rate-constants for electron transfer reactions between the target molecule and sensitizer, Adams' hypothesis of the higher electrophililic characteristic of the sensitizer appears to account for the nitrogen mustard-induced enhancement of radiation sensitivity of guanine.

Although the system studied here is a crude DNA model, it is still useful since the fundamental interaction pathways for the nitrogen mustard, ionizing radiation and guanine are expected to be similar to those pathways occurring in small DNA segments or native DNA. In the cell-free system in the absence of any repair processes, our data

demonstrate that under physiologically relevant conditions (pH, ionic strength and temperature) nitrogen mustard forms covalent adducts with guanine and also acts as a radiosensitizer, enhancing the radiosensitivity of guanine. In summary, the data presented here illustrate the importance of the chemical environment neighbouring a DNA moiety in altering the radiation sensitivity of the target.

Acknowledgements

We thank Dr Edward Clark for our discussions in the initial phase of this research, which was supported by the Armed Forces Radiobiology Research Institute under Project Work Unit WU09501.

References

ADAMS, G. E., 1970, Molecular mechanisms of cellular radiosensitization and protection. In *Radiation Protection and Sensitization*, edited by: H. L. Morson and M. Quintiliani (London: Taylor & Francis), pp. 1–12.

ADAMS, G. E. and COOKE, M. S., 1969, Electron-affinic sensitization. I. A structural basis for chemical radiosensitizers in bacteria. *International Journal of Radiation Biology*, **1,** 457–460.

BROOKES, P. and LAWLEY, P. D., 1961, The reaction of mono- and difunctional alkylating agents with nucleic acids. *Biochemical Journal*, **80,** 462–494.

CALABRESI, P. and WELCH, A. D., 1968, Cytotoxic drugs, hormones, and radioactive isotopes. In *The Pharmacological Basis of Therapeutics*, 3rd edn, edited by L. Goodman and A. Gilman (New York: McMillan), pp. 453–474.

CUMMINGS, J., MACLELLAN A., LONGDON S. J. and SMYTH, J. F., 1993, The long term stability of mechlorethamine (nitrogen mustard) ointment measured by HPLC. *Journal of Pharmacy and Pharmacology*, **45,** 6–9.

CURTIS, R. E., BOICE, J. D., STOVALL, M., BERNSTEIN, L., GREENBERG, R. S., FLANNERY, J. T., SCHWARTZ, A. G., WEYER, P., MOLONEY, W. C. and HOOVER, R. N., 1992, Risk of leukemia after chemotherapy and radiation treatment for breast cancer. *New England Journal of Medicine*, **326,** 1745–1751.

DIZDAROGLU, M., 1985, Application of capillary gas chromatography–mass spectrometry to chemical characterization of radiation-induced base damage of DNA: implications for assessing DNA repair processes. *Analytical Biochemistry*, **144,** 593–603.

EHRENBERG, L., 1961, Principles and methods of detection of chemical mutagenesis. In *Chemical Mutagenesis*, vol. 2, edited by A. Hollaeder (New York: Plenum), pp. 212–284.

EWIG, R. A. and KOHN, K. W., 1978, DNA–protein cross-linking and DNA interstrand cross-linking by haloethylnitrosourea in L1210 cells. *Cancer Research*, **38,** 3197–3202.

FUCIARELLI, A. F., WEGHER, B. J., GAJEWASKI, E., DIZDAROGLU, M. and BLAKELY, W. F., 1989, Quantitative measurement of radiation-induced base products in DNA using gas chromatography–mass spectrometry. *Radiation Research*, **119,** 219–231.

GREENSTOCK, C. L., ADAMS, G. E. and WILSON, R. L., 1970, Electron transfer studies of nucleic acid derivatives in solution containing radiosensitizers. In *Radiation Protection and Sensitization*, edited by H. L. Moroson and M. Quintiliani (London: Taylor & Francis), pp. 65–69.

GEACINTOV, N. E. and SWENBERG, C. E., 1993, Chemical, molecular biology, and genetic techniques for correlating DNA damage induced by ionizing radiation with biological endpoints. In *Physical and Chemical Mechanisms in Molecular Radiation Biology*, edited by W. A. Glass and N. M. Varma (New York: Plenum), pp. 453–474.

HARTLEY, J. A., BINGHAM, I. P. and SOUHAMI, R. L., 1992, DNA sequence selectivity of guanine N-7 alkylation by nitrogen mustards in intact cells. *Nucleic Acids Research*, **20,** 3175–3178.

HASKELL, C. M., 1990, Neoplasma therapy, In *Cancer Treatment*, 2nd edn (New York: W. B. Sanders) pp. 150–260.

HEMMINKI, K., 1985, Binding of metabolites of cyclophosphamide to DNA in a rat liver microsomal system and *in vivo* in mice. *Cancer Research*, **45,** 4237–4243.

HEMMINKI, K., PELTONEN, K. and VODIKA, P. ,1989, Depurination from DNA of 7-methylguanine, 7-(2-aminoethyl)-guanine and ring-opened 7-methylguanines. *Chemical and Biological Interactions*, **70,** 289–303.

KALLAMA, S. J. and HEMMINKI, K., 1986, Stabilities of 7-alkylguanosines and 7-deoxyguanosines formed by phosphoramide mustard and nitrogen mustard. *Chemical and Biological Interactions*, **70,** 289–303.

KOHN, K. W., SPEARS, C. L. and DOTY, P., 1966, Inter-strand cross-linking of DNA by nitrogen mustard. *Journal of Molecular Biology*, **19,** 266–280.

KOLLER, P. C., 1960, Comparison of the biological effects of X-rays and radiomimetic chemical agents. In *Proceedings of the 3rd Australasian Conference on Radiobiology*, edited by P. L. T. Ilberry (Sidney: Butterworth), pp. 281–286.

LARMINANT, F., ZHEN, W. and BOHR, V. A., 1993, Gene-specific DNA repair of interstrand cross-link induced by chemotherapeutic agents can be preferential. *Journal of Biological Chemistry*, **268,** 2649–2654.

MATTES, W. B., 1992, Use of 8-^{3}H-guanine-labeled deoxyribonucleic acid to study alkylating agent reagent kinetics and stability. *Analytical Biochemistry*, **206,** 161–167.

MATTES, W. B., HARTLEY, J. A. and KOHN, K. W., 1986, DNA sequence selectivity of guanine-N7 alkylation by nitrogen mustard. *Nucleic Acids Research*, **14,** 2971–2987.

MCCLOSKEY, J. A., 1974, Mass spectrometry. In *Basic Principles in Nucleic Acid Chemistry*, vol. 1, edited by P. O. P.TS'o (New York: Academic), pp. 209–308.

MCCLOSKEY, J. A., LOWSON, A. M., TSUBYAMA, K., KRUEGER, P. M. and STILLWELL, R. N., 1968, Mass spectrometry of nucleic acid components. Trimethylsilyl derivatives of nucleosides and bases. *Journal of the American Chemical Society*, **90,** 4182–4184.

MCLAFFERTY, F. W., 1980, Detailed mechanisms of ion fragmentations. In *Interpretation of Mass Spectra*, 3rd edn, edited by N. J. T. Turro (Mill Valley: University Science Books), pp. 170–172.

PAUL, C. R., ARAKALI, A. V., WALLACE, J. C., MCREYNOLDS, J. and BOX, H. C., 1987, Radiation chemistry of 2′-deoxycytidylyl-(3′-5′)-2′-deoxy-guanosine and its sequence

isomers in nitrous oxide and oxygen saturated solutions. *Radiation Research*, **112,** 464–478.

POVIRK, L. F. and SHUKER, D. E., 1994, DNA damage and mutagenesis induced by nitrogen mustards. *Mutation Research*, **318,** 205–226.

TOMAZ, M., 1969, Extreme lability of the C-8 proton: a consequence of 7-methylation of guanine residue in model compounds in DNA and its analytical applications. *Biochimica et Biophysica Acta*, **199,** 18–28.

VAISHNAV, Y. N. and SWENBERG, C. E., 1993, Radiolysis in aqueous solution of dinucleoside monophosphates by high-energy electrons and fission neutrons. *Radiation Research*, **133,** 12–19.

DISTRIBUTION LIST

DEPARTMENT OF DEFENSE

ARMED FORCES RADIOBIOLOGY RESEARCH INSTITUTE
ATTN: PUBLICATIONS BRANCH
ATTN: LIBRARY

ARMY/AIR FORCE JOINT MEDICAL LIBRARY
ATTN: DASG-AAFJML

ASSISTANT TO THE SECRETARY OF DEFENSE
ATTN: AE
ATTN: HA(IA)

DEFENSE SPECIAL WEAPONS AGENCY
ATTN: TITL
ATTN: DDIR
ATTN: RAEM
ATTN: MID

DEFENSE TECHNICAL INFORMATION CENTER
ATTN: ACQUISITION
ATTN: ADMINISTRATOR

FIELD COMMAND DEFENSE SPECIAL WEAPONS AGENCY
ATTN: DASIAC
ATTN: FCIEO

INTERSERVICE NUCLEAR WEAPONS SCHOOL
ATTN: DIRECTOR

LAWRENCE LIVERMORE NATIONAL LABORATORY
ATTN: LIBRARY

UNDER SECRETARY OF DEFENSE (ACQUISITION)
ATTN: OUSD(A)/R&E

UNIFORMED SERVICES UNIVERSITY OF THE HEALTH SCIENCES
ATTN: LIBRARY

DEPARTMENT OF THE ARMY

HARRY DIAMOND LABORATORIES
ATTN: SLCSM-SE

OFFICE OF THE SURGEON GENERAL
ATTN: MEDDH-N

U.S. ARMY AEROMEDICAL RESEARCH LABORATORY
ATTN: SCIENCE SUPPORT CENTER

U.S. ARMY CHEMICAL RESEARCH, DEVELOPMENT, & ENGINEERING CENTER
ATTN: SMCCR-RST

U.S. ARMY INSTITUTE OF SURGICAL RESEARCH
ATTN: COMMANDER

U.S. ARMY MEDICAL DEPARTMENT CENTER AND SCHOOL
ATTN: MCCS-FCM

U.S. ARMY MEDICAL RESEARCH AND MATERIEL COMMAND
ATTN: COMMANDER

U.S. ARMY MEDICAL RESEARCH INSTITUTE OF CHEMICAL DEFENSE
ATTN: MCMR-UV-R

U.S. ARMY NUCLEAR AND CHEMICAL AGENCY
ATTN: MONA-NU

U.S. ARMY RESEARCH INSTITUTE OF ENVIRONMENTAL MEDICINE
ATTN: DIRECTOR OF RESEARCH

U.S. ARMY RESEARCH LABORATORY
ATTN: DIRECTOR

WALTER REED ARMY INSTITUTE OF RESEARCH
ATTN: DIVISION OF EXPERIMENTAL THERAPEUTICS

DEPARTMENT OF THE NAVY

BUREAU OF MEDICINE & SURGERY
ATTN: CHIEF

NAVAL AEROSPACE MEDICAL RESEARCH LABORATORY
ATTN: COMMANDING OFFICER

NAVAL MEDICAL RESEARCH AND DEVELOPMENT COMMAND
ATTN: CODE 42

NAVAL MEDICAL RESEARCH INSTITUTE
ATTN: LIBRARY

NAVAL RESEARCH LABORATORY
ATTN: LIBRARY

OFFICE OF NAVAL RESEARCH
ATTN: BIOLOGICAL & BIOMEDICAL S&T

DEPARTMENT OF THE AIR FORCE

BROOKS AIR FORCE BASE
ATTN: AL/OEBZ
ATTN: OEHL/RZ
ATTN: USAFSAM/RZB

OFFICE OF AEROSPACE STUDIES
ATTN: OAS/XRS

OFFICE OF THE SURGEON GENERAL
ATTN: HQ AFMOA/SGPT
ATTN: HQ USAF/SGES

U.S. AIR FORCE ACADEMY
ATTN: HQ USAFA/DFBL

U.S. AIR FORCE OFFICE OF SCIENTIFIC RESEARCH
ATTN: DIRECTOR OF CHEMISTRY & LIFE SCIENCES

OTHER FEDERAL GOVERNMENT

ARGONNE NATIONAL LABORATORY
ATTN: ACQUISITIONS

BROOKHAVEN NATIONAL LABORATORY
ATTN: RESEARCH LIBRARY, REPORTS SECTION

CENTER FOR DEVICES AND RADIOLOGICAL HEALTH
ATTN: DIRECTOR

GOVERNMENT PRINTING OFFICE
ATTN: DEPOSITORY ADMINISTRATION BRANCH
ATTN: CONSIGNED BRANCH

LIBRARY OF CONGRESS
ATTN: UNIT X

LOS ALAMOS NATIONAL LABORATORY
ATTN: REPORT LIBRARY

NATIONAL AERONAUTICS AND SPACE ADMINISTRATION
ATTN: RADLAB

NATIONAL AERONAUTICS AND SPACE ADMINISTRATION
GODDARD SPACE FLIGHT CENTER
ATTN: LIBRARY

NATIONAL CANCER INSTITUTE
ATTN: RADIATION RESEARCH PROGRAM

NATIONAL DEFENSE UNIVERSITY
ATTN: LIBRARY TECHNICAL SERVICES

U.S. DEPARTMENT OF ENERGY
ATTN: LIBRARY

U.S. FOOD AND DRUG ADMINISTRATION
ATTN: WINCHESTER ENGINEERING AND ANALYTICAL CENTER

U.S. NUCLEAR REGULATORY COMMISSION
ATTN: LIBRARY

RESEARCH AND OTHER ORGANIZATIONS

AUSTRALIAN DEFENCE FORCE
ATTN: SURGEON GENERAL

AUTRE, INC.
ATTN: PRESIDENT

BRITISH LIBRARY
ATTN: ACQUISITIONS UNIT

CENTRE DE RECHERCHES DU SERVICE DE SANTE DES ARMEES
ATTN: DIRECTOR

FEDERAL ARMED FORCES DEFENSE SCIENCE AGENCY FOR NBC PROTECTION
ATTN: LIBRARY

FOA NBC DEFENCE
ATTN: LIBRARY

INHALATION TOXICOLOGY RESEARCH INSTITUTE
ATTN: LIBRARY

INSTITUTE OF NUCLEAR MEDICINE AND ALLIED SCIENCES
ATTN: DIRECTOR

INSTITUTE OF RADIOBIOLOGY, ARMED FORCES MEDICAL ACADEMY
ATTN: DIRECTOR

OAK RIDGE ASSOCIATED UNIVERSITIES
ATTN: MEDICAL LIBRARY

RESEARCH CENTER OF SPACECRAFT RADIATION SAFETY
ATTN: DIRECTOR

RUTGERS UNIVERSITY
ATTN: LIBRARY OF SCIENCE AND MEDICINE

UNIVERSITY OF CALIFORNIA
ATTN: DIRECTOR, INSTITUTE OF TOXICOLOGY & ENVIRONMENTAL HEALTH
ATTN: LIBRARY, LAWRENCE BERKELEY LABORATORY

UNIVERSITY OF CINCINNATI
ATTN: UNIVERSITY HOSPITAL, RADIOISOTOPE LABORATORY

XAVIER UNIVERSITY OF LOUISIANA
ATTN: COLLEGE OF PHARMACY

REPORT DOCUMENTATION PAGE

Form Approved
OMB No. 0704-0188

1. AGENCY USE ONLY *(Leave blank)*	2. REPORT DATE	3. REPORT TYPE AND DATES COVERED
	February 1997	Reprints

4. TITLE AND SUBTITLE

AFRRI Reports, Third - Fourth Quarters 1996

5. FUNDING NUMBERS

NWED QAXM

6. AUTHOR(S)

7. PERFORMING ORGANIZATION NAME(S) AND ADDRESS(ES)

Armed Forces Radiobiology Research Institute
8901 Wisconsin Avenue
Bethesda, MD 20889-5603

8. PERFORMING ORGANIZATION REPORT NUMBER

SR96-5 - SR96-11

9. SPONSORING/MONITORING AGENCY NAME(S) AND ADDRESS(ES)

Uniformed Services University of the Health Sciences
4301 Jones Bridge Road
Bethesda, MD 20814-4799

10. SPONSORING/MONITORING AGENCY REPORT NUMBER

11. SUPPLEMENTARY NOTES

12a. DISTRIBUTION/AVAILABILITY STATEMENT

Approved for public release; distribution unlimited.

12b. DISTRIBUTION CODE

13. ABSTRACT *(Maximum 200 words)*

This volume contains AFRRI Scientific Reports SR96-5 through SR96-11 for July-December 1996.

14. SUBJECT TERMS

15. NUMBER OF PAGES

64

16. PRICE CODE

17. SECURITY CLASSIFICATION OF REPORT	18. SECURITY CLASSIFICATION OF THIS PAGE	19. SECURITY CLASSIFICATION OF ABSTRACT	20. LIMITATION OF ABSTRACT
UNCLASSIFIED	UNCLASSIFIED	UNCLASSIFIED	UL

CLASSIFIED BY:

DECLASSIFY ON: